universität wien

MASTERARBEIT / MASTER'S THESIS

Titel der Masterarbeit / Title of the Master's Thesis

„Novel bromo-substituted 7*H*-indolo[2,3-*c*]quinoline-6(5*H*)-ones and their metal complexes as potential anticancer drugs“

verfasst von / submitted by

Christian Madejski, BSc

angestrebter akademischer Grad / in partial fulfilment of the requirements for the degree of

Master of Science (MSc)

Wien, 2021 / Vienna 2021

Studienkennzahl lt. Studienblatt / degree programme code as it appears on the student record sheet:	UA 066 862
Studienrichtung lt. Studienblatt / degree programme as it appears on the student record sheet:	Masterstudium Chemie
Betreut von / Supervisor:	ao. Univ.-Prof. Dr. Vladimir Arion

Acknowledgement

I want to thank all the people who helped me during my work on this master thesis:

Ao. Univ.-Prof. Dr. Vladimir Arion for the excellent supervision and patience during the work.

Dr. Felix Bacher for the supervision in the laboratory and for the constant exchange as well as for improvement of my theoretical and practical knowledge.

Ao. Univ.-Prof. Mag. Dr. Markus Galanski, Ass.-Prof. Mag. Dr. Hanspeter Kählig, Ing. Susanne Felsinger, Ricarda Bugl and Sabine Schneider for the measurements of one- and two-dimensional NMR spectra

Ing. Alexander Roller and his team

Mag. Johannes Theiner for performing the elemental analyses.

All friends and colleagues from the Institute of Chemistry at the Uiversity of Vienna, especially Gerhard Hagn BSc MSc., Njomza Isufaj, BSc, Antonio Kopic, BSc, Bojan Milic, Dr. Adriano Bauer, Dr. Felix Bacher, Mag. Dr. Miljan Milunovic, Rudi Eswein, BSc MSc, and Christopher Wittman, BSc MSc, for the excellent working atmosphere.

Abstract

In recent years, a significant increase in the preclinical development of organometallic compounds and classical metal complexes for therapeutic purposes against cancer is observed. With the appearance of cisplatin and other platinum(II)-based drugs a significant step in the treatment against cancer was achieved. However, these drugs show both, a series of severe side effects, as well as acquired resistance by malign cells.

Copper is an essential element in all living organisms, being involved in many biological and chemical processes. In humans it is available mainly in two oxidation states (Cu(I) and Cu(II)), where concentrations are highly regulated because copper(I) can disproportionate into copper(0) and copper(II). Redox cycling between Cu(II) and Cu(I) can generate a variety of reactive oxygen species (ROS). Numerous reports show that both the serum and tumour copper levels in a variety of cancer types are elevated, including solid tumour and blood cancer, respectively. Copper plays a vital role in angiogenesis. Due to copper's ability to form complexes with diverse ligands with different coordination numbers and oxidation states, numerous compounds have been prepared with the intent to treat cancer.

Indoloquinolines are natural, tetracyclic, aromatic products isolated from West African shrubs of the *Cryptolepis* species. They consist of fused indole and quinoline rings, which can intercalate into non-alternating GC base pairs of the DNA double helix, due to their polyaromatic character. Indoloquinolines and their metal complexes have been investigated for their anti-malarial and anti-cancer activity, the latter being the area of interest of this thesis.

The main aim of this thesis work was the synthesis and characterisation of copper(II) complexes of several novel bromo-substituted 7*H*-indolo[2,3-*c*]quinoline-6(5*H*)-ones. The characterisation of the designed and synthesised compounds was performed *via* one- and two-dimensional ^{1}H and ^{13}C NMR spectroscopy, elemental analysis and single crystal X-ray diffraction (SC-XRD). Cytotoxicity assays of the new compounds, which will be assessed in the nearest future, will determine their potential for further development as anticancer drugs.

Zusammenfassung

In den letzten Jahren wurde ein signifikanter Anstieg der präklinischen Entwicklung von metallorganischen Verbindungen und klassischen Metallkomplexen für therapeutische Zwecke gegen Krebs beobachtet. Mit dem Auftreten von Cisplatin und anderen auf Platin(II) basierenden Arzneimitteln wurde ein bedeutender Schritt bei der Behandlung von Krebs erreicht. Diese Medikamente zeigen jedoch sowohl eine Reihe schwerwiegender Nebenwirkungen als auch eine erworbene Resistenz durch maligne Zellen. Kupfer ist ein wesentliches Element in allen lebenden Organismen und an vielen biologischen und chemischen Prozessen beteiligt. Beim Menschen kommt Kupfer hauptsächlich in zwei Oxidationsstufen (Cu(I) und Cu(II)) vor, in denen die Konzentrationen stark reguliert sind, da Kupfer(I) in Kupfer(0) und Kupfer(II) disproportionieren kann. Aufgrund von „Redoxcycling“, zwischen Kupfer(I) und Kupfer(II), kann es zur Bildung von vielfältigen, reaktiven Sauerstoffspezies (ROS) kommen. Zahlreiche Berichte zeigen, dass sowohl der Serum- als auch der Tumorkupferspiegel bei einer Vielzahl von Krebsarten erhöht ist, einschließlich solide Tumore- bzw. Blutkrebs. Kupfer spielt eine wichtige Rolle bei der Angiogenese. Aufgrund der Fähigkeit von Kupfer, Komplexe mit verschiedenen Liganden mit unterschiedlichen Koordinationszahlen und Oxidationsstufen zu bilden, wurden zahlreiche Verbindungen mit der Absicht hergestellt, Krebs zu behandeln.

Indolochinoline sind natürliche, tetra-zyklische, aromatische Verbindungen, die aus westafrikanischen Sträuchern der *Cryptolepis*-Art isoliert werden. Sie bestehen aus kondensierten Indol- und Chinolinringen, die aufgrund ihres polyaromatischen Charakters in nicht alternierende GC-Basenpaare der DNA-Doppelhelix interkalieren können. Indolochinoline und ihre Metallkomplexe wurden auf ihre Anti-Malaria- und Anti-Krebs-Aktivitäten untersucht, wobei letztere im Bereich dieser Arbeit von Interesse sind.

Das Hauptziel dieser Arbeit war die Synthese und Charakterisierung von Kupfer(II)-Komplexen mehrerer neuer bromsubstituierter 7*H*-Indolo[2,3-*c*]chinolin-6 (5*H*) -one. Die Charakterisierung der synthetisierten Verbindungen erfolgte mittels ein- und zweidimensionaler ^{1}H- und ^{13}C-NMR-Spektroskopie, Elementaranalyse und Einkristall-Röntgenstrukturanalyse (SC-XRD). Zytotoxizitätstests der neuen Verbindungen, die in naher Zukunft bewertet werden, werden ihr Potenzial für die weitere Entwicklung als Krebsmedikamente bestimmen.

Table of Contents

1. Introduction

Cancer is a complex group of diseases with many possible causes, which span from chemicals in food and stimulants, sun light and other types of radiation, infections, to genetic defects in the cells of an organism. The patterns and trends in mortality vary between countries and specific cancer types. In 2017, every sixth death in the world was due to cancer, making it the second leading cause of death after cardiovascular diseases (see Figure 1). An estimated 9.6 million people have died from various forms of cancer in 2017, and 1 in 10 women and 1 in 8 men are likely to develop the disease during their lifetimes.[1] Especially in richer countries

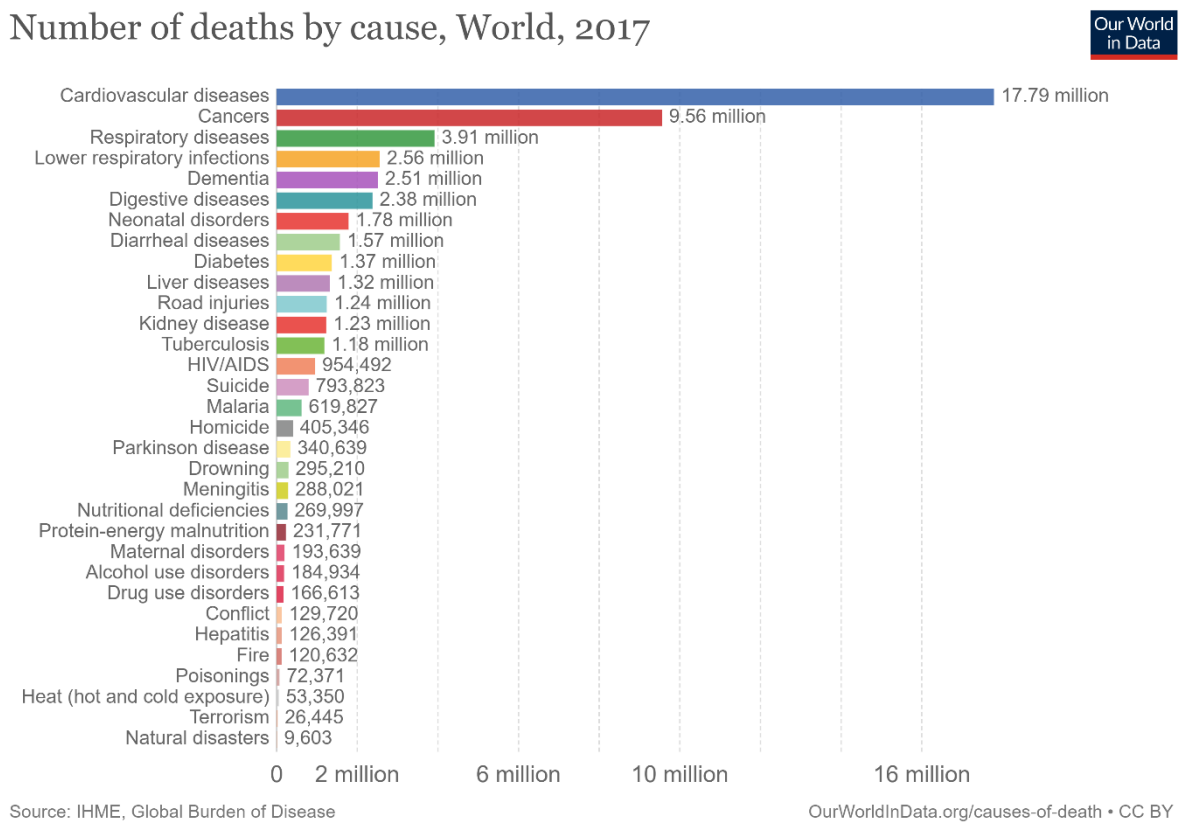

Figure 1. Overview of the number of deaths by cause worldwide in 2017.

where the life span is longer, the probability to develop cancer is much higher than in poor countries.[2] Coupled that with an estimated cost of US$ 1.16 trillion per year in combating this disease, makes cancer a public health priority, resulting in the worldwide recognition for the need to fight against cancer.[3]

In Austria the number of deaths caused by cancer increased by nearly 13% from 1990 to 2017. Of the total 41.389 documented diseases in 2017, 20.148 people have died in 2017. This number includes 9.215 women and 10.933 men.[4] Especially the number of bronchus, lung and tracheal cancer has visibly increased over the years, while the number of stomach cancer went down (see Figure 2). Advanced medical care, early detection measures for cancer at the primary care level, as well as improvement of drug quality are the main reasons for this development.

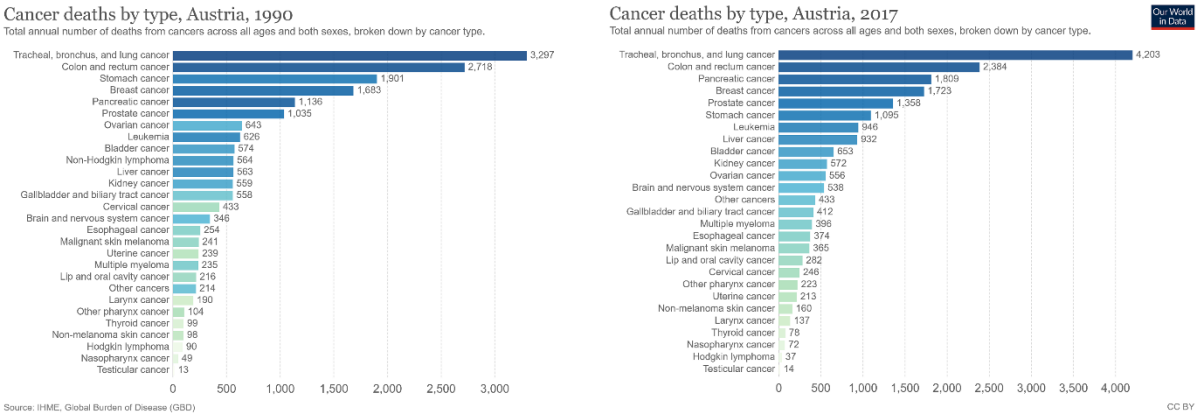

Figure 2. Mortality statistics caused by cancer types in 1990 and 2017.

Cancer risks increase significantly, as more people live longer and also due to the appearance of types of cancer as a result, of the changes in lifestyle.[5] To counteract this trend, the United Nations have set themself the goal of minimising premature mortality caused by non-communicable diseases (NCDs) by one third until 2030. An effective measure in preventing cancer and other NCDs is minimising the exposure to risk factors that contribute to these diseases, such as environmental factors (e.g., air pollution, solar radiation), unhealthy diet and physical inactivity, metabolic factors (e.g., overweight and obesity, high blood pressure, high cholesterol levels, etc.) and behavioural factors (e.g., tobacco use, excessive alcohol consumption).[6]

1.1 Oncogenesis

Oncogenesis is a complex, multi-step process by which normal cells transform into malign cells, resulting in the development of cancer, as an outcome of irreparable DNA damage. This uncontrolled cell growth is mainly the result of two processes occurring simultaneously [7]

- activation of oncogenes (e.g., RAF, RAS, MYC)
- deactivation of tumour suppressor genes (e.g., p53, APC, BRCA 1 & 2).

Experiments carried out on *drosophila melanogaster* in the 1920s have shown that cancer can arise from external influences, such as infections, ionising radiation or chemicals.[6] Only decades later it was discovered that spontaneous hydrolysis at 37 °C, reactive metabolites and coenzymes can damage the DNA. These exogenic and endogenic influences contribute to the change in the genetic material triggering mutations.[6] DNA repair is part of a wider DNA damage response, triggering signals to a checkpoint response that arrests cell-cycle progression, inhibits transcription and translation, and initiates DNA repair. If DNA damage is too severe, it initiates a programmed cell death, a mechanism known as apoptosis. Loss of function is a common feature in most human cancers.

1.2 Hallmarks of cancer

Neoplasm can occur anywhere in the body by deregulating growth promoting signals, typically containing intracellular tyrosine kinase domains, caused by defects in the DNA. [8] This allows for malign cells to inherit a series of biological abilities during their periodic growth. Therefore,

ten hallmarks of cancer that modulate cell physiology and improve their growth, were proposed by Hanahan and Weinberg.[6]

i. Sustaining proliferative signalling
ii. Evading growth suppressors
iii. Resisting apoptosis
iv. Enabling replicative immortality
v. Inducing angiogenesis
vi. Activating invasion and metastasis
vii. Tumour-promoting inflammation
viii. Evading immune destruction
ix. Reprogramming energy metabolism
x. Genome instability

Nowadays the focus is on the interactions between tumour cells and the potential involvement of additional distant factors. Together they form the tumour organismal environment (TOE).[9] Throughout oncogenesis, non-malign cells of the tumour microenvironment (TME) positively influence cancer growth.

I. Sustainment of proliferative signalling

Proto-oncogenes promote and regulate cell growth and mitosis.[7] A common representative in humans is the RAS-gene family (HRas, KRas and NRas), which codes for the RAS-protein, a GTPase in the inner cell membrane. This GTPase hydrolyse GTP to GPD and phosphate and is regulated by a growth factor receptor in the vicinity. When a cell enters the cell cycle, the growth factor is stimulated and activates the RAS-protein. This in turn causes a cascade of intracellular phosphorylation reactions of other proteins, followed by the activation of a transcription factor. The transcription factor transcribes the genes that contain the information for cell growth proteins (e.g., CDKs). CDKs are serine/threonine kinases and consist of two different sub-units; CDK itself and cyclin.[10] Hence, a mutation in the RAS-gene leads to an ongoing cascade of phosphorylation events that promote the building of cell growth proteins, and in addition, driving an overproduction of CDKs. This grants a cell to bypass the checkpoints of the cell cycle, allowing the cell to grow without any control. Malign cells acquire this trait of proliferative signalling by different ways[8]:

- Production of own growth signals
- Supply of growth factors by tumour microenvironment
- Elevating the level of receptor proteins
- Structural modifications of receptor proteins
- Downstream alterations

Malign cells attributes to activate cell membrane receptors are obscure, along with the crosstalk between the multiple pathways radiating from growth factor receptors. Non-malign cells can antagonise excessive signalling by inducing senescence and apoptosis. Malign cells are rich of morphological features of senescence (e.g., β-galactosidase enzyme), reflecting intracellular defence mechanisms.[11] Cancer cells either regulate the level of proliferative signalling to avoid these anti-proliferative defences or disable senescence/apoptosis-inducing circuitry.

II. Evading growth suppressor

Normally cells have a mechanism to stop abnormal cells from progressing the cell cycle, regulated by so called tumour suppressor genes (e.g., p53, PTEN, BRCA 1&2).[12] They check whether there is no progression of damaged cells during the cell cycle from extracellular and intracellular sources. The p53 protein communicates with stress and

abnormality sensors inside the intracellular operating systems. When information arrives that there is major damage to the genome or levels of metabolic and signalling molecules are suboptimal, p53 can intervene in the cell cycle until the conditions have been normalised or trigger apoptosis.[8] Somatic mutations in the p53 pathway prevent the production of proteins that act as inhibitors against CDKs, stimulate DNA repair and resist apoptosis. This complements the adolescence of abnormal cells.[13] Mutations in tumour suppressor genes can be inherited through the germline since their presence does not affect the embryonic development. The opposite is true for oncogenes, which are autosomal dominant.

III. Resisting apoptosis

Apoptosis is a fundamental ability of multicellular organisms, pre-programmed in telomers, the end region of chromosomes. These telomers consist of a series of TTAGGG sequences surrounded by the shelterin complex, a collection of proteins to protect the telomers.[14] Apoptosis must be highly regulated, once it is set in motion it cannot be stopped. Adjacent and professional phagocytic cells then consume the resulting bodies.

The apoptotic process consists of both, upstream regulators, and downstream effector components, whereby the regulators can be divided into the extrinsic (i.e., death receptor) and intrinsic program. In the intrinsic pathway (also known as mitochondrial pathway), the cell kills itself because it senses cell stress, while in the extrinsic pathway the cell kills itself because of signals from other cells. Weak external signals may also activate the intrinsic pathway of apoptosis, however each one of them leads to the activation of dormant proteases (e.g., caspases 8 and 9) [8] These then initiate a proteolytic cascade mobilising effector caspases that execute apoptosis, by progressive disassembly of a cell. Caspase activation is regulated by proteins of the Bcl-2 family (e.g., Bcl-2, Bcl-x_L, Bax, Bim). The activation is associated with p53, which can activate the transcription of genes that encode Bcl-2 proteins that promote the release of caspase activators like cytochrome *c* from mitochondria.

Malign cells develop several ways to limit or prevent apoptosis. A deciding factor is the deletion or inactivation of the p53-gene. Observations confirm that this occurs in more than 50% of human cancers.[8,15]Other possibilities are the overexpression of anti-apoptotic proteins (e.g., Bcl-2, Bcl-x_L), inactivation or downregulation of pro-apoptotic proteins (e.g., Bax, Bim)[16], increasing survival signals (PI_3K /AKT/mTOR pathway). All these factors increase the insensitivity to therapeutic methods (e.g., radiation, chemotherapy).

IV. Enabling replicative immortality

Healthy cells carry an implemented program that limits their augmentation and works autonomously. Only a limited number of cell cycles can be traversed by most cell lineage. This occurs due to shortening of the telomeres after each cell cycle (i.e., Hayflick limit) and is associated with senescence and end to end chromosome fusion (i.e., crisis).[8] While the expression of oncoproteins and inactivation of tumour suppressor proteins grant malign cells to proliferate, a mechanism of telomere stabilisation must occur in order to achieve cellular immortalisation. Telomerase, which is inactive in most adult somatic cells but functional in numerous immortalised cells as well as cancer cells, can counteract the persistent shortening of telomeres by lengthening telomeric DNA and therefore allowing cancer cells to prevent senescence and apoptosis. Revocation of *h*TERT mRNA repression permits the maintenance of telomers short enough to provide chromosome protection and prevent DNA damage response (DDR).[17] However, cell immortalisation by reactivating *h*TERT may only

account for up to 90% of tumour cases, making room for an alternative pathway to maintain telomeres.[18] This alternative lengthening of telomeres (ALT) occurs via homologous telomere recombination.[19] Recombination between homologous sequences can cause point mutations when the activity of mismatch repair proteins (MMR) are disrupted. This can lead to activation of ALT mechanisms to maintain telomere length when there is inhibition of telomerase functions. Reducing the amount of telomerase that malign cells can produce could allow the cells to age and die naturally, then again, deactivating telomerase completely could cause infertility and disturb healing processes. Although, reactivation of telomerase to maintain the length of telomeres is crucial for cellular immortalisation, pathological accumulation of chromosomal damages is required first for oncogenesis.

V. Inducing angiogenesis

Angiogenesis specifies a common process during the development and growth (e.g., embryogenesis) of new blood vessels from pre-existing ones. The constitution of new blood vessels also occurs in wound healing. Blood vessels bring oxygen and other nutrients via blood circulation into all tissues of the body. The blood also transports metabolic wastes, like carbon dioxide, away from these tissues. In adult's angiogenesis is inoperative, except during wound healing or menstruation. These angiogenetic regulator proteins either stimulate or inhibit cell-surface receptors located on endothelial cells. Endothelial growth factor-A (VEGF-A) and thrombospondin-1 (TSP-1) are two of the best-explored regulators of angiogenesis, while the former as an inducer of the latter is an inhibitor. Hypoxia and oncogene signalling can upregulate the expression of VEGF genes.[20] Cancer cells take over the bodies control of angiogenesis to recruit their own private blood supply. Characterisations of neovascularisation in tumours are disorganisation, abnormal morphology, and poor blood flow, resulting in them being "leaky". This stems from increased expression of VEGF-A and inhibition of vessel maturation. Because tumour derived VEGF-A acts directly on the growth of malign stem cells, suggestions for targeting VEGF-A in the tumour microenvironment were made, which could deteriorate further growth and inhibit metastasis.[21] However, treatments targeting the VEFG-A signalling lead to therapy induced resistance and the development of tumours that are robust against anti-angiogenic therapy.[22]

VI. Activating Invasion and Metastasis

Among the known hallmarks of cancer, metastasis is the biggest drawback for therapeutic treatments. For malign cells to initiate metastasis, an invasion is required, which enables the epithelial-mesenchymal transition (EMT)[23]. EMT is a developmental process that plays essential roles in embryogenesis, organ fibrosis, and wound healing. Oncogenic metabolism plays a key role in the induction of EMT by cancer cells.[8] The signalling pathways that regulate EMT programs include growth factors (e.g., TGF-β, EGF) and stress response signals in oncogenesis (e.g., PI3K/AKT/mTOR, ERK).[24] These signals activate EMT-inducing transcription factors (e.g., Snail/Slug) that regulate the expression of proteins that are involved in cell polarity, cell-cell contact and suppression of epithelial genes (e.g., CDH_1). The loss of cell-cell adhesion mediated by e-cadherin repression allows primary tumour cells to enter the bloodstream by break through basement membranes (i.e., intravasation). [25] After exiting the bloodstream these circulating tumour cells (CTCs) form micro-metastases, which causes the tumour cells to undergo mesenchymal-epithelial transition (MET), resulting in clonal outgrowth at these metastatic sites. Together, EMT and MET form the invasion-metastasis cascade that initiates and completes metastasis.[26] There are cancer types where the

primary tumour can liberate suppressor factors that can keep these micro-metastases calm. Observations of the removal of the primary tumour show an explosive growth of metastases. In others, like breast cancer and melanoma, the eruption of metastatic growth can occur decades after the resection or pharmacological destruction of a primary tumour.[8] In addition to playing pro-metastatic roles, these EMT-inducing transcription factors convolute tumour initiation and early tumour development, by being involved in inhibiting senescence and apoptosis. EMT may also be associated with the formation of cancer stem cells (CSCs) and the metabolic reprogramming of cancer cells.[23,27] Oncogenic metabolism can drive the EMT and CSC phenotypes, causing changes that can induce resistance to pharmacological therapy and promote tumour recurrence. Thus, targeting CSCs, EMT, and oncogenic metabolic pathways may reduce primary tumour recurrence, prevent invasion, and prevent distant metastasis.

VII. Tumour-promoting inflammation

Accumulated evidence shows that inflammation promotes the growth of many types of tumours. Inflammatory cells surround almost all tumours, regardless of the cause of their appearance. Under normal physiological conditions, inflammation is a tightly regulated process that can be very effectively turned on or off. The innate immune system predominantly mediates inflammation. It is essential for defence against infectious pathogens as well as for the removal of damaged and dead cells. Macrophages and neutrophils sense danger signals, such as bacteria or viruses, and react by engulfing dangerous elements plus producing molecules, such as nitric oxide, that kill infectious pathogens by increasing the level of local vascularisation and by stimulating the extravasation of myeloid and lymphoid cells.[28] If the acute inflammatory process fails to remove the insalubrious agents and restore tissue homeostasis, inflammation becomes chronic and might promote the expansion of the developing cancer. Acute inflammation can be treated therapeutically because it is primary a self-limiting process. Virchow *et al* assumed a connection between neoplasia and inflammation.[29] Nowadays, assumptions of around 15% of all cancer cases connect them to inflammation. [1] However, inflammation alone does not cause cancer, but further contributes to the promotion of oncogenesis by providing bioactive molecules (e.g., growth and survival factors) to the TME. In the event of acute inflammation, the immune system deploys white blood cells to the affected site to reduce it. Cases of chronic or severe inflammation show that these cells can account for the unduly amount of pro-inflammatory molecules (e.g., cytokines, chemokines, prostaglandins, nitric oxide, and leukotrienes) as well as the occurrence of tissue remodelling and angiogenesis, therefore playing key roles in cancer-related inflammation (CRI). Both, the intrinsic and the extrinsic circuit play a role in the emanation of pro-inflammatory molecules and cancer development. Especially transcription factors such as NF-κB, STAT3 and MAPK are endogenous promoters of inflammation and oncogenesis. In many malignancies, along with congenital immunities, an atypical regulation of NF-κB can be observed, which initiates the expression of inflammatory cytokines. Those cell adhesion molecules (CAMs) are subsets of key enzymes in several catalytic reactions like the prostaglandin synthase pathway (COX-2), inducing the expression of anti-apoptotic genes (e.g., Bcl2), as well as activating nitric oxide (NO) synthase and angiogenic factors. Inhibitors acting at different levels tightly control the NF-κB pathway. Maintaining the activation of NF-κB, STAT3 is vital. Another source for NF-κB activations could be epigenetic modifications (e.g., lysine acetylation and methylation, arginine methylation). Targeting NF-κB and STAT3 has become an attractive strategy, and various pharmacological inhibitors can modulate NF-κB and STAT3 activation in

tumour models. The use of non-steroidal anti-inflammatory drugs (e.g., aspirin, ibuprofen) protects against various malignancies. In addition, a few natural compounds have shown to inhibit inflammatory mediators involved in cancer progression (e.g., curcumin, ursolic acid, oleanolic acid, garcinol, zerumbone, resveratrol, thymoquinone, diosgenin, celastrol, butein, sulforaphane, and epigallocatechin gallate).[6,8,30,31]

VIII. Evading immune destruction

The immune system interacts with tumours throughout their entire process of disease development and progression to metastasis. This complex interplay between immunity and cancer cells can both inhibit and enhance tumour growth.[32] A healthy immune system normally scans and protects the body from abnormal and damaged cells, which could become cancerous. T cells and natural killer cells (NKs) precipitate the early omission of transformed cells and limit their progression, whereas inflammatory cells (e.g., macrophages M1 & M2) promote oncogenesis and tumour progression at different stages.[6] The evasion of immune destruction of malignant neoplasm is separated into three phases:[33]

i. Elimination
ii. Equilibrium
iii. Escape

Mutations or epigenetic alterations lead to the acquisition of protein-altering modifications that are either responsible for transformation or are a side effect of the genomic instability that accompanies cellular transformation, resulting in the expression of tumour specific antigens (TSAs). [34] Normally, expressions of these neo-antigens do not occur in healthy cells, making malign cells more immunogenic. Another class of antigens are tumour-associated antigens (TAAs). TAAs include proteins converted in the normal genome and may be either normal specialised antigens or abnormal expressed proteins. They usually have lower T cell receptor (TCR) affinity compared with TSAs or foreign antigens, hence, their attribute as an antigen depends on concentration levels or their environment to evade the destruction by the immune system. Once cancer cells have escaped elimination, they enter a phase of equilibrium where they balance cell growth and immune suppression. In this state, malign cells are neither able to proliferate uncontrollable nor can they be destroyed by the immune system, thus remain dormant in patients for many years. Consequently, the ceaseless interaction between cancer cells and the immune system may lead to the adaption of developing tumours, giving rise to selected tumours that are less immunogenic. Tumours that are pliable to immune attack progress into the third phase of the immunoediting process, termed escape. Tumours in the escape phase subvert the immune system through direct and/or indirect mechanisms alleviating their growth[35]. The ability of malignant neoplastic diseases to elude the destruction by a body's immune system is a sizeable drawback in scheming an efficient therapeutic strategy against cancer. [1]

IX. Reprogramming energy metabolism

For cells to develop and grow, they need sufficient energy. Likewise, to maintain homeostasis. The metabolic reactions responsible for energy production are known as cellular respiration.[36] These catabolic reactions provide energy by dividing large nutrients and storing them as small molecules (e.g., adenosine triphosphate, ATP). When energy is required, cells use respiration to assemble ATP or convert the stored ATP to fuel their metabolic reactions. The supply of ATP occurs in all tissues and

organs of the body Healthy cells use two types of respiration, aerobic and anaerobic respiration. Under normal conditions, they undergo aerobic respiration, which requires oxygen to form ATP. Here glucose is converted into pyruvate and carbon dioxide as a waste product.[37] During a lack of oxygen, cells switch to anaerobic respiration, whereby glucose is split into two molecules ATP and two molecules lactic acid respectively.[38] Furthermore, anaerobic respiration pays off far less than aerobic, which produces 32 molecules of ATP per molecule of glucose[39] Despite the presence of oxygen, most malignant cells meet their energy needs with turned up glycolysis (i.e. Warburg effect) rather than by oxidative phosphorylation. [39] The glutamine metabolism, pentose phosphate pathway (PPP), and synthesis of cholesterol and fatty acids are other possible enhanced oncogenic metabolic pathways that cover the increased demands of abnormal proliferation and the survival of cancer cells. by providing precursors for nucleic acids, lipids, and proteins. Additionally, the loss of tumour suppressors and the activation of oncogenes showed to drive tumour progression, especially the metabolic reprogramming. Transcription factors that contribute to the development of oncogenic metabolism, include HIF-1α, p53, and MYC.[37] Although, many research groups consider the Warburg effect to be a metabolic signature of tumour cells, latest results show that tumour cells exhibit high aerobic glycolysis and also mitochondrial metabolism.[23,37]

X. Genome instability

The tissue of a tumour consist a heterogeneous population of cancer cells surrounded by stromal cells, inheriting different genetic and epigenetic backgrounds. Their structural abnormalities localised in the genome result from genomic instabilities, which increases spontaneous mutations, chromosomal rearrangements, and the risk of aneuploidy. This enables the occurrence of oncogenesis. Furthermore, sustained modifications of tumour cell genomes foster the acquisition of more DNA alterations, clonal evolution, and tumour heterogeneity.[40] Almost all human cancers possess some form of genomic instability. However, the amount and type of genomic instability they experience vary considerably. Typically, the genomic instability can be subdivided into three categories based on the level of genetic disruption:

- Nucleotide instability (NIN)
- Microsatellite instability (MIN or MSI)
- Chromosomal instability (CIN)

NIN is characterised by an increased incidence of base substitutions, deletions and insertions of one or several nucleotides, which can affect gene structures and expression. Indeed, NIN is less common, it can cause dramatic phenotypes when it is present.

MSI are short nucleotide repeats and are the result of defects in mismatch repair genes, leading to their contraction and expansion.

CIN leads to changes in the structure and number of chromosomes. It is the most prominent instability in solid tumours. Human cancers exhibit roughly 90% of chromosomal abnormalities and aneuploidy. CIN develops early in oncogenesis and is associated with intrinsic multidrug resistance and poor prognosis, making its detection clinically relevant.[8,40]

1.3 Diagnosis and treatment of cancer

The earlier diagnosis of cancer, the higher is the possibility of finding the proper treatment that can raise the chances of a cure. Most detections of cancer cases happen after feeling a tumour or other symptoms developed. Cancer diagnosis begins with a systematic physical examination and a review of a patient's medical history. Laboratory tests of blood, urine and stool can detect anomalies that may indicate cancer. Imaging tests like X-rays, computed tomography (CT), magnetic resonance imaging (MRI), ultrasound, and fibre-optic endoscopy examinations can help visualising the size and location of a suspected tumour. Subsequently, for most cancers, performing a biopsy confirms the diagnosis. In doing so, a tissue sample from the suspected tumour is removed and studied under a microscope to check for malignant cells. When the diagnosis is positive, other tests are performed to provide specific information about the type and stage of cancer. During this staging phase, the appropriate treatment method is determined.

Four main cancer treatments used by modern medicine are:

- Surgery
- Radiation therapy
- Cancer immunotherapy
- Chemotherapy

1.3.1 Surgery

Surgery is the oldest and primary treatment for solid tumours. When the tumour has not metastasised, removing the tumour and the healthy surrounding tissue is the best chance of a cure. Surgeries allow to relieve symptoms and side effects caused by tumours that press on nerves, bones, or block intestines. If complete removal is not possible, the operation removes as much as possible; making another treatment method more effective.[41]

1.3.2 Radiation therapy

Radiotherapy uses ionising radiation to treat cancer. This is used in more than half of cancer treatments, either as a stand-alone method or in combination with surgery and/or chemotherapy. Nuclear DNA is the primary target of radiation therapy, causing double-strand breaks (DSBs), which damage and kill cancer cells very effectively. Irradiation can take place both directly and indirectly. It causes genotoxic stress by direct exposure; indirect radiation induces DNA damages by stimulating the formation of reactive oxygen species (ROS).[23] There are two main types of radiation therapy, external and internal beams. Which type of radiation therapy is used depends on the following factors:[42]

- The type of cancer
- The size of the tumour
- The tumour location in the body
- How close the tumour is to normal tissues that are sensitive to radiation
- General health and medical history
- Whether other types of cancer treatment may will be performed
- Other factors, such as age and other medical conditions

Radiation therapy not only kills or slows the growth of malign cells but can also affect nearby healthy cells. Damaging them can cause side effects.[43]

1.3.3 Cancer immunotherapy

Immunotherapy treats cancer by improving the natural ability of a patient's own immune system through artificial stimulation. Possible immunotherapies can be classified as active, passive

and/or hybrid therapies. Active therapy targets antigens of the tumour surface with modified antibodies that mark cancer cells so that antibodies of the immune system can inhibit and/or kill them. In passive immunotherapies, present anti-tumour responses are increased by using monoclonal antibodies, lymphocytes, and cytokines.[44]

1.3.4 Chemotherapy

Chemotherapy uses chemicals to treat cancer by reducing and/or prohibiting their cell growth. Chemicals can be used to kill tumours that cause pain and other issues as part of single agent therapy, as well as in combination with other treatments (e.g., surgery, radiotherapy). The first chemotherapy drugs applied were nitrogen mustards and antifolates (e.g., methotrexate) in the 1940's (see Figure 3). The mechanism of action of nitrogen mustard implies the formation of covalent bonds with DNA strands, which produce crosslinks that initiate apoptosis. [45] Over the last 80 years, discoveries of new drugs led to classification, based on their effect:

- Alkylation agents (e.g., nitrogen mustards, nitrosoureas, cisplatin and derivatives)
- Antimetabolites (e.g., methotrexate, 5-fluarouracil, 6-mercaptopurine)
- Anti-microtubule agents (e.g., *Vinca* alkaloids, taxanes)
- Topoisomerase inhibitors (e.g., irinotecan, topotecan, etoposide, doxorubicin)
- Cytotoxic inhibitors (e.g., anthracyclines)

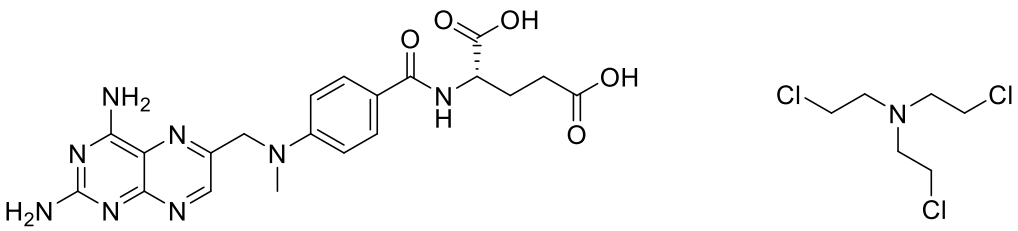

Methotrexate **Nitrogen mustard**

Figure 3. Chemical structures of methotrexate (MTX, left) and nitrogen mustard (tris(2-chloroethyl)amine, right).

In general, cytostatic drugs are infused, either through the vein (systemic), whereby they work in the whole body, or through the artery (non-systemic), where they work locally. Most cytostatic drugs cannot differentiate between pathological cancer cells and healthy cells in the body and attack cell groups with a high rate of division, causing side effects (e.g., hair loss, nausea, diarrhoea, reduced performance and fatigue).[46] From the very beginning of chemotherapy development, observations showed that cancer cells develop resistance against drugs over time.[45,47] These acquired resistances arise by mutations in drug targets, adaptions in drug transport and metabolism as well as in genetic rewiring that lead to vitiated apoptosis.[48] As early as the mid-nineteen sixties, cytostatic drugs were applied in combination with other chemotherapeutic agents on the assumption that an attack from different approaches could result in preventing drug-resistant cancer cells. Commonly, combination chemotherapy proved to be more effective than single agent therapy in patients who were at high risk of relapse after primary surgical treatment and metastatic cancer.[45] Thereby, establishing distinct chemotherapy regimens to medicate different types of cancer was important.

2. Transition metal based chemotherapeutic drugs

Nowadays, research focuses on the use of noble transition metal complexes as cytostatic drugs. Their coordination chemistry, photochemical and photophysical properties make them ideal candidates for diverse biological applications, with platinum-based compounds being the most successful.[49]

2.1 Platinum-based compounds

Cisplatin [*cis*-diamminedichlorido-platinum(II)] was the first worldwide-approved metal-based chemotherapeutic agent (see Figure 4).[50] First synthesised by Michele Peyrone in 1844, its biological activity was discovered by Barnett Rosenberg in 1965 during electrolysis experiments with *E. coli* bacteria. Cisplatin and its second and third-generation analogues carboplatin and oxaliplatin have become very lucrative substances, with incomes of US$ 1.1 Bn, in 2018.[51] Almost every second chemotherapy regimen contains platinum-based cytostatic drugs.[52] The use of cisplatin against certain cancers types, especially in testicular cancer, has high rates of success. The common mechanism of action of cisplatin and its analogues involves four key steps:[53]

i. Cellular uptake
ii. Aquation/activation
iii. DNA binding

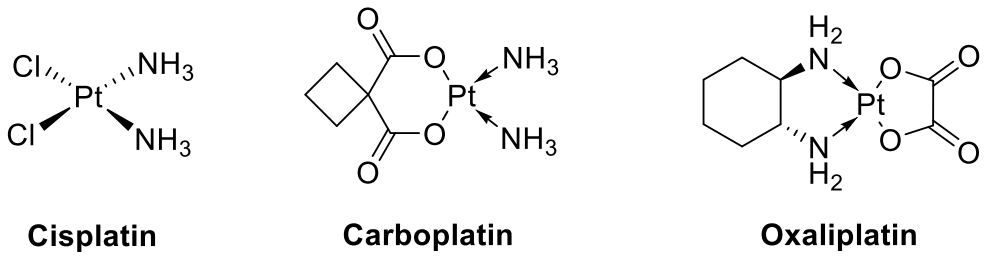

Figure 4. Chemical structures of cisplatin (cis-diamminedichloridoplatinum(II), left), carboplatin (diammino-cyclobutane-1,1-dicarboxylatoplatinum(II), middle) and oxaliplatin (1*R*, 2*R*-cyclohexane-1,2-diammine-oxalatoplatinum(II) right).

The cellular uptake of cisplatin most likely involves two pathways, passive diffusion, and active transport. The square planar geometry and small size of cisplatin derivatives favours entering the cells through passive diffusion and is proportional to the concentration of the supplied drug. The active transportation of platinum drugs is mediated through copper transporters, with high affinity to copper transporter 1.[46] Once entering the cell, the labile ligands (e.g., chlorides, carboxylates) leave the coordination sphere of platinum(II), because of low concentration of chlorine ions inside the cytoplasm (below 20 mM),[53] being substituted by aqua ligands. The resulting *cis*-$[Pt(NH_3)_2Cl(H_2O)]^+$ complex can enter the nucleus and bind the negatively charged DNA. The attack occurs predominantly on the *N*7 of guanine and/or adenine. Next, the second labile ligand is substituted by a second guanine base, leading to a crosslink, which can either be intra or intermolecular.[53] These crosslinks cause the DNA to unwind and bend, preventing transcription and replication, which activate apoptosis. Because platinum-based drugs are soft nucleophiles, they readily bind to proteins and peptides, that contain sulfur residues (e.g., cysteine, glutathione, methionine), as well as RNA.[46,53] However, platinum-based drugs encounter the same drug resistance and side effects as many other chemotherapeutics, simulating the continuous development of new and improved compounds.[46,54] Recently, the focus was set on the development of platinum(IV) compounds, which are generally non-toxic and can function as prodrugs. Their octahedral coordination sphere contains *cis*-dichlorido-diammine ligands in the equatorial plane and hemi labile O-donor ligands in axial position, making them very stable inside the bloodstream (see Figure 5). As soon as they enter malign cells, the hypoxic environment promotes intracellular reduction, leading to the formation of the cytotoxic square-planar platinum(II) species.

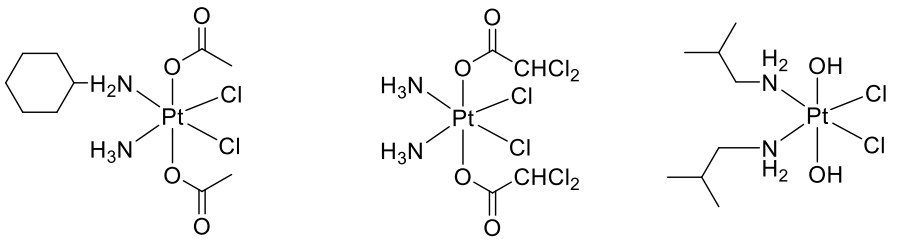

Figure 5.: Chemical structures of noble platinum (IV) compounds Satraplatin, Mitaplatin and Iproplatin.

Copper, gold, iridium, iron, osmium and ruthenium complexes and organometallic compounds have biological properties that raise expectations towards discovery of new potential anticancer drugs. Accumulated evidence indicates that using endogenous metals (e.g., iron, copper) in drug motifs could lead to chemotherapeutics with less side effects. Extensive research has led to the discovery of a series of non-platinum compounds which are currently in clinical trials.[55–57]

2.2 Iron

Iron is a trace element in the human body and active in many biological processes (e.g., iron- and haem-containing enzymes proliferation and growth of cells). Controlling iron levels is critical to the health of human body, as it is both essential and potentially toxic. Increased levels of iron in the human body correlate with magnified risks of developing malignancies. During cancer proliferation, the iron transport protein transferrin is overexpressed in accord, with an increased uptake of iron. The redox potential of iron enables generation of ROS that may damage lipids, proteins and oxidative damage to DNA, leading to oncogenesis.[58–60] Many organic compounds, which are studied as potential anticancer drugs are chelating agents or contain ferrocene, a sandwich molecule that carries an iron (II) between two cyclopentadienyl rings (see Figure 6). The functionalised rings can improve physical and chemical properties of this organometallic compound. Additionally, the iron(II) can be oxidised to iron(III), so that it can bind to iron(III) binding proteins (e.g., transferrin). Extensive studies of these ferrocene-containing compounds have shown a series of biological activities, including activities against many incurable types of cancer.[61] Especially ferrocene derivatives of tamoxifen (i.e., ferrocifens) containing cyclic imides, show strong antiproliferative effects by producing ROS at cancer cell sites as well as generating quinone methides that can target enzymes and induce apoptosis or senescence.[61–63]

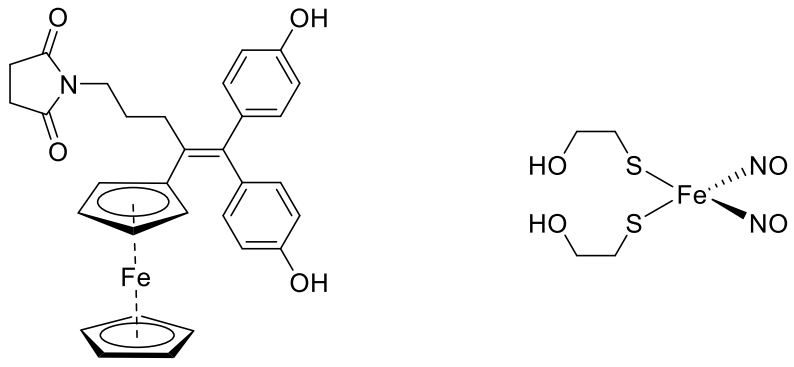

Figure 6. Chemical scaffolds of ferrocene- (left) and dinitrosyl based complex (right)-.

Other biologically active iron compounds are iron nitrosyl complexes (see Figure 8). As mentioned in the previous paragraph on the hallmarks of cancer (no. viii) nitric oxide is an important defence and signalling molecule that is deployed by macrophages against pathogens.[8,28] Naturally occurring dinitrosyl iron complex (DNIC) results from the degradation of iron-sulfur proteins by nitric oxide. Moreover, nitric oxide is very reactive under physiological conditions, making high dose delivery difficult. Attempts with a water-soluble DNIC that contains a cysteamine-2 mercaptoethanol ligand showed activation of apoptosis promoting proteins and in parallel the inhibition of survival-associated proteins, making DNICs interesting for further development as anticancer drugs.[62,64] Despite showing many positive attributes in cancer treatment, there are no approved iron-containing compounds currently in clinical trials.

2.3 Ruthenium

The most auspicious non-platinum-based anticancer agents belong to the class of ruthenium complexes, with three ruthenium (III) complexes, NAMI-A , KP1019 and NKP-1339, already in clinical trials.[50] Preclinical results showed anti-metastatic effects of NAMI-A, in particular, when added to human serum albumin (HAS). [62,65] Nevertheless, phase I studies of NAMI-A alone and phase I/II studies in combination with gemcitabine did not show any positive results for NAMI-A. Difficulties with the solubility hampered promising studies of KP1019 in Phase I on patients with solid tumours. Therefore, the indazolium counter cation in KP1019 was replaced with sodium (see Figure 7). This new compound NKP-1339 has a 30 times higher solubility than KP1019 and is currently undergoing Phase I/II clinical trials.[62,65,66]

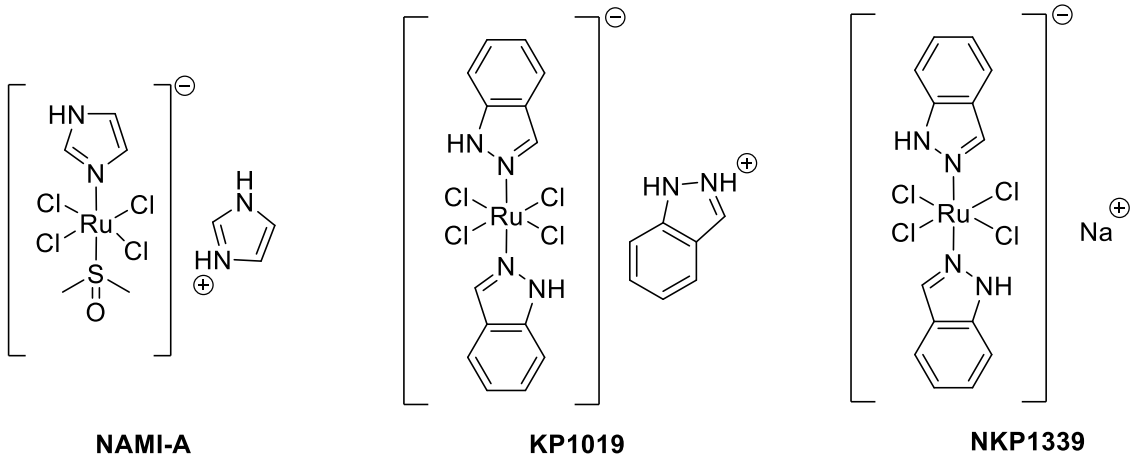

Figure 7. Chemical structures of NAMI-A (1*H*-imidazolium trans-[tetrachlorido-κN-imidazol-κS-dimethylsulfoxide-ruthenate(III)), KP1019 (1H-indazolium trans -[tetrachloridobis(1*H*-indazole)ruthenate(III)] and NKP1339 sodium trans-[tetrachloridobis (1*H*-indazole)ruthenate(III)].

The anticancer properties of ruthenium(III) complexes result from the *in vivo* reduction to ruthenium(II). Biological conditions (i.e., acidic pH, high glutathione levels, low oxygen concentrations) can facilitate the reduction of ruthenium(III) to ruthenium(II). This activation by reduction process led to the development of novel ruthenium (II) complexes (see Figure 8). These “half-sandwich piano-stool’’ compounds are activated by ligand exchange at the metal centre.[66] It is assumed that the activation of these complexes requires the dissociation of a halide, which facilitates the formation of an active Ru-OH_2 metabolite that preferably coordinates to *N*7 of guanine residues of DNA. Due to their hydrophilic PTA ligands RAPTA complexes are readily soluble in water. It is suggested that RAPTA complexes are activated *in vivo* by hydrolysis of chloride ligands. It is commonly believed that the activity of RAPTA compounds originates from their ability to interact with certain proteins rather than with DNA.

The cellular uptake of ruthenium complexes occurs through multiple mechanisms like passive diffusion, endocytosis and active transport.[58,65] One such mechanism is the endocytotic transferrin transport, where ruthenium instead of iron binds to the apotransferrin protein and is transported through a vesicle into the cell. Recent research engaged in the investigation ruthenium photosensitisers (PS) that activate oxygen radicals on site of the tumour, causing damages to the surrounding tissue. TLD1433 is a compound that shows promise in this respect, being currently tested in Phase Ib clinical trials.[65]

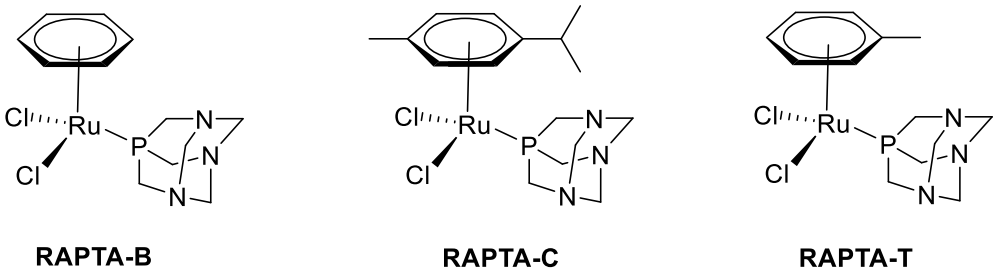

Figure 8. Chemical structures of ruthenium (II) "piano-stool" complexes RAPTA-B (left), RAPTA-C (middle) and RAPTA-T (right).

2.4 Osmium

Just like the other group-8 metals iron and ruthenium, osmium has shown to have biological applications despite its high toxicity. Osmium tetroxide is clinically used for synovectomy in arthritic patients, while osmium carbohydrate derivatives belong to potential antiarthritic agents.[67] In contrast to ruthenium, osmium prefers higher oxidation states, has slower ligand exchange kinetics, stronger π-backbonding from lower oxidation states and stronger spin-orbit couplings. As a result, osmium complexes are more stable under physiological conditions. Attempts to prepare osmium analogues of known ruthenium complexes with anticancer activity have resulted in a wide range of compounds (see Figure 9). Especially the osmium analogues of NAMI-A, KP1019 and NKP-1339 have shown equivalent or higher cytotoxicity.[68] Osmium(IV) analogues of KP1019 show an interesting structural phenomenon, because indazole binds to osmium either via the *N2* or the *N1*, while to Ru mainly via *N2*. Other potent anticancer agents are nitridoosmium(VI) complexes. These high-valent compounds have a nitrogen atom directly bound to the metal, displayed superior anticancer activity in *in vitro* studies against several human cancer cells lines.[68,69] The assumed mode of action of these complexes is the induced cell cycle arrest in the S phase and the premitotic G2 phase, which result from DNA damage.[68]

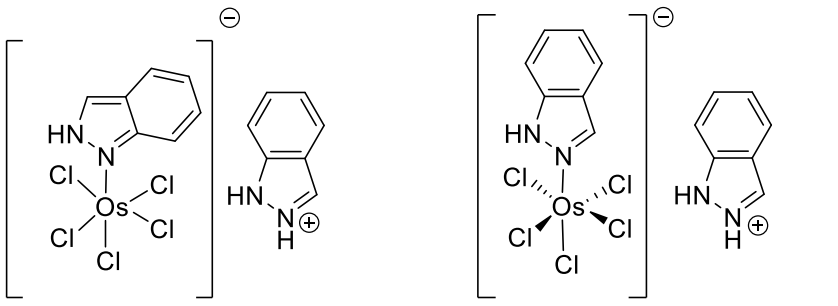

$[H_2Ind][Os(IV)Cl_5$(1*H-indazole*)] **$[H_2Ind][Os(IV)Cl_5$(2*H-indazole*)]**

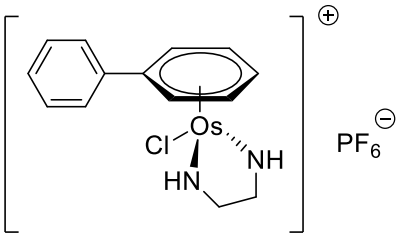

[Os(η^6-biphenyl)(*N*,*N'*-ethylendiamine)Cl][PF_6]

Figure 6. Chemical structures of osmium (IV) analogues of KP1019 and “piano-stool" compounds.

2.5 Copper

Copper is an essential trace element in all living organisms, being involved in many biological and chemical processes. In humans it is available in two oxidation states (Cu(I) and mainly Cu(II)), and is found primarily in the brain, liver, muscles and bones. Copper is a native metal and used by humankind for over 10.000 years. Archaeological data have shown that diseases were treated with copper compounds since 400 BC. As with many other metals in the body, copper concentrations are tightly regulated because copper(I) can disproportionate into copper(0) and copper(II), leading to the formation of ROS. Furthermore, coordination sites that are suitable for other metals are occupied by copper ions with increased concentrations of copper(I) and copper(II). This leads to alteration of the metal distribution in the body. Further, the elevated copper levels have been shown to be directly correlated to cancer progression.[62,67,70] The alternated metabolism of malign cells responds differently to copper and together with the natural antimicrobial and biostatic properties of copper compounds, it makes them potential anticancer agents. Due to copper ability to form complexes with a variety of ligands with different coordination numbers and oxidation states, numerous compounds have been prepared with the intent to treat cancer. Many of them target DNA by coordinating to nucleobases and phosphate groups as well as wedging between the aromatic moieties of nucleobases in double stranded DNA. Copper(II) cyclen compounds inhibit the synthesis of DNA/RNA by interfering with the polymerase mechanism due to intercalation, the stacking of π -electron systems with the purine and pyrimidine bases of adjacent base pairs in DNA. Their bulky side chains coordinate to the minor groove of DNA, inhibiting DNA transcription, leading to cytotoxicity.[62,71,72] Another area of application for copper(II) complexes is photodynamic therapy. Copper(II)-boron-dipyrromethene (BODIPY) is a photosensitiser with the ability to target mitochondria. When exposed to visible light BODIPY generates singlet oxygen that can create ROS in targeted mitochondria, inducing apoptosis. Currently a copper gluconate complex that works synergistically with disulfiram against recurrent glioblastoma is in Phase II clinical studies.[70,73]

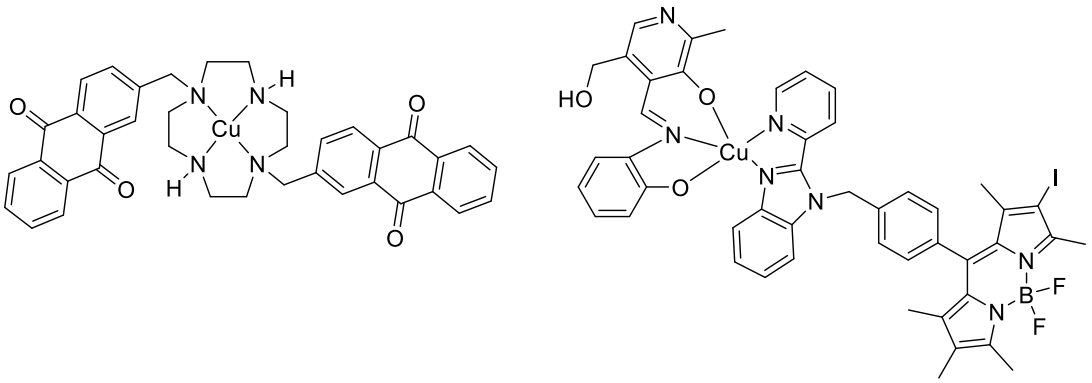

Figure 7. Chemical scaffolds of novel copper (II) cyclen (left) and copper (II)- boron-dipyrromethene (right) complexes.

3.0 Intercalators

Extensive studies on intercalators for their anticancer activities revealed their reversible binding to DNA. Planar polycyclic aromatic systems with positive charge can interact with polyanionic DNA. Lerman was the first to propose this mechanism in 1961.[74] Two broad classes of intercalators are known (i.e., parallel intercalators and perpendicular intercalators). While parallel intercalators have their aromatic system relatively parallel to the base pairs and do not possess additional bulky side groups perpendicular intercalators do have bulky functional side groups and their longitudinal axis is perpendicular to the base pairs. Examples for parallel and perpendicular intercalators are ethidium bromide and doxorubicin respectively (see Figure 11).[74]

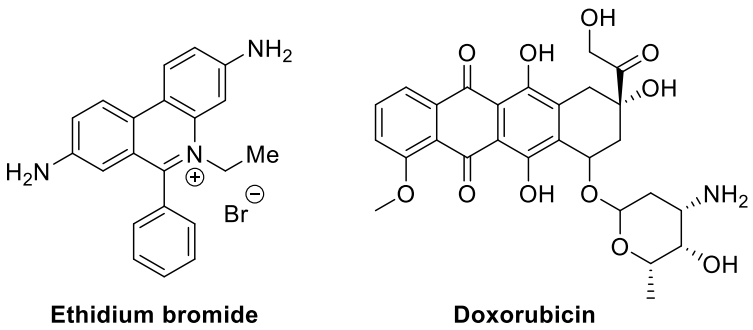

Figure 8. Chemical structures of ethidium bromide and doxorubicin.

When a ligand intercalates between base pairs, the helical structure of the DNA extends. Electrostatic and π-stacking interactions stabilise the DNA-intercalator-complex, leading to a shift of the binding site along the longitudinal axis of DNA (see Figure 12). Thereby, physiological enzymes (i.e., DNA topoisomerases) are no longer able to function accordingly, which induces apoptosis. Even though intercalators operate in healthy cells, malign cells are more affected.[74–76]

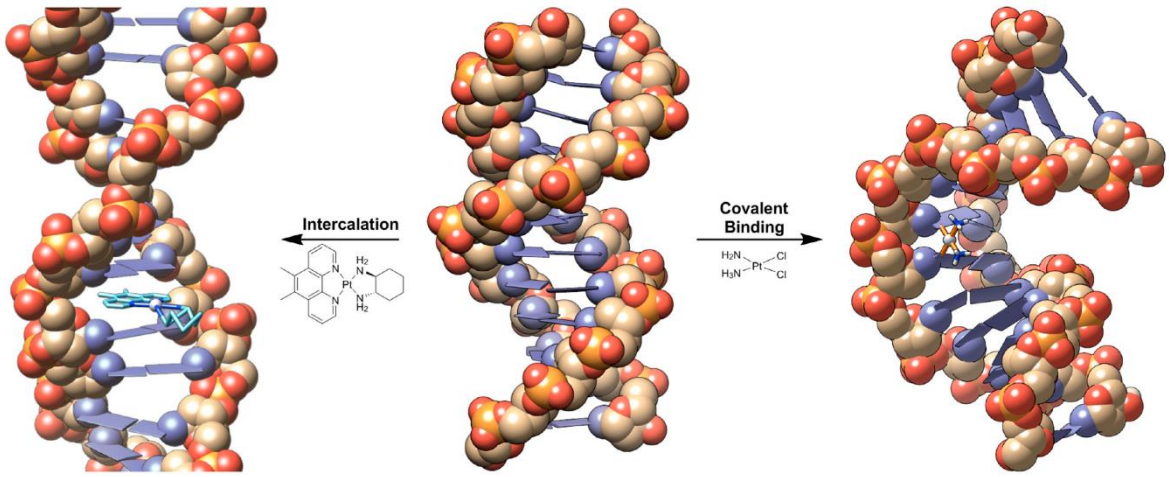

Figure 9. Schematic representation of metal complexes interacting with DNA. The figure is used with permission from Ref [76] © MDPI Basel, Switzerland.

To modify intercalating compounds many investigations on the structure-activity relationships (SAR) have been performed. Here, cryptolepines, a class of indoloquinolines, showed to be good intercalators by acting as topoisomerase II inhibitors. [77]

3.1 Topoismerase inhibitors as anticancer agents

DNA is a long molecule that is winded together to fit inside the cell. This DNA supercoil is not easily accessible for replication and transcription machineries. DNA topoisomerases regulate DNA supercoiling by winding and unwinding DNA strands through cleavage. They play an important role in DNA repair. Topoisomerases are divided into two groups based on the number of strands they trench (see Figure 13).

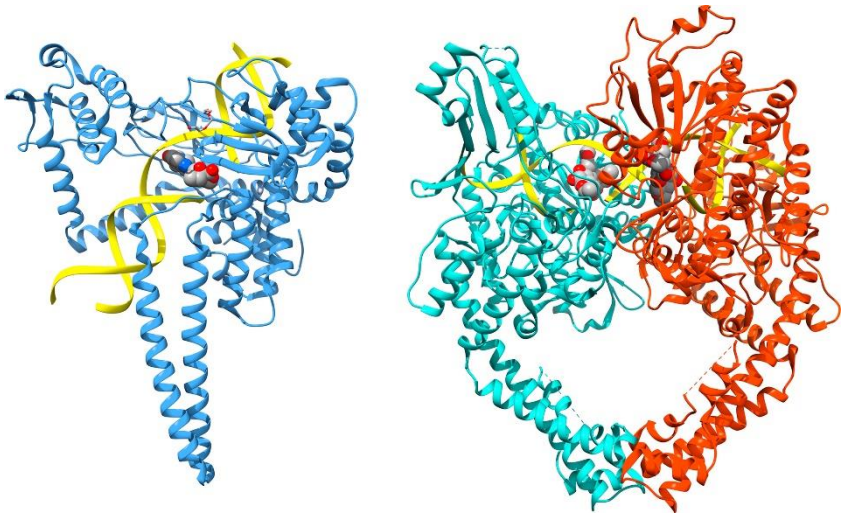

Figure 10. Structures of human topoisomerases I (left) and II (right). The figure is used with permission from Ref [77] © Elsevier B.V.

3.1.1 Topoisomerase type I

DNA topoisomerases of type I consist of two classes Iα and Iβ. These enzymes are important in the synthesis of DNA. They are monomeric enzymes that break only one strand of DNA helix. The mechanism involves the hydroxyl group of tyrosine 723, on topoisomerase I. Nucleophilic attack of the hydroxyl group onto one of the DNA strands produces a covalent

DNA-enzyme adduct (i.e., cleavable complex) that can be uncoiled. The double helix restores when a nucleotide attacks at the site of the cleavage complex (see Figure 14).[78,79]

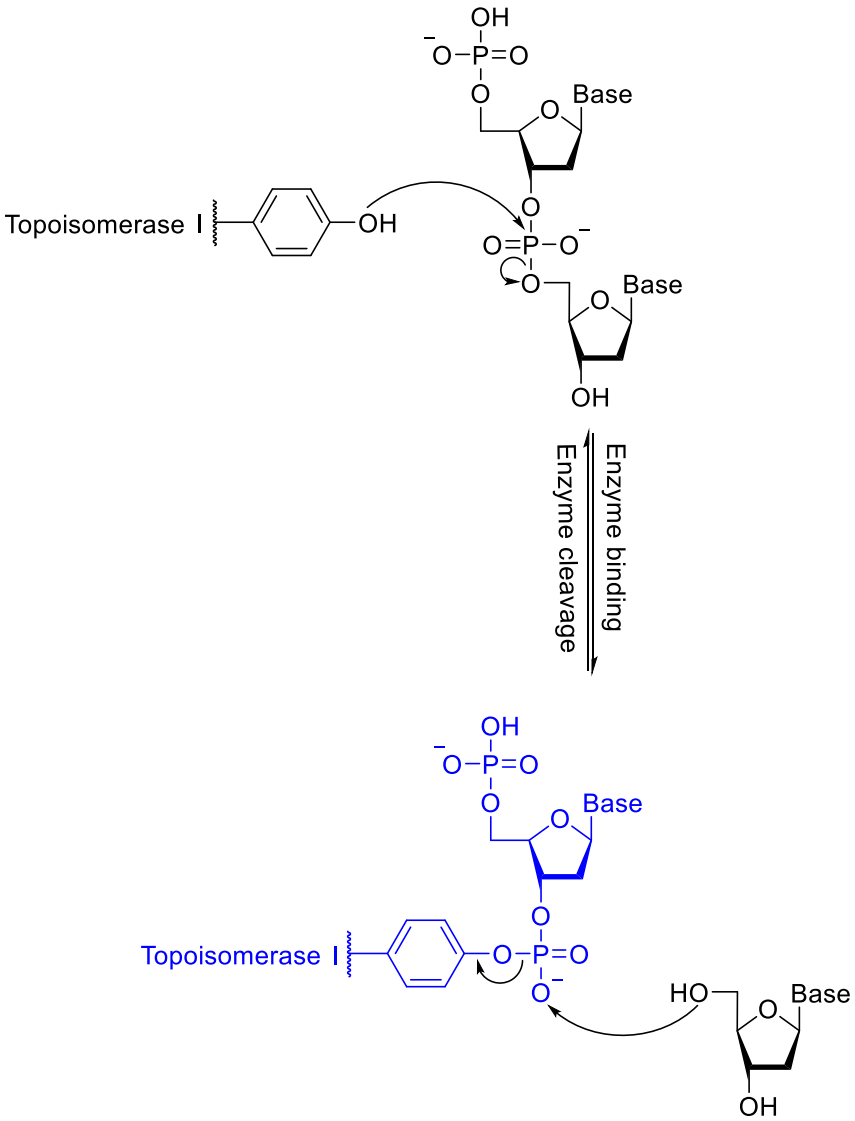

Figure 11. DNA cleavage by topoisomerase I. The cleavable complex is shown in blue.

3.1.2 Topoisomerase type II

DNA topoisomerases of type II also consist of two classes IIα and IIβ, but unlike topoisomerase I, topoisomerase II are multimeric enzymes and use ATP as fuel to cut both DNA strands of a helix. They attack through similar tyrosine residues at the active site, resulting in the separation of the cleaved strands. This mechanism also changes the linking number of circular DNA (i.e., plasmid) by ± 2. Topoisomerases type II are essential enzymes for the survival of all eukaryotic organisms.[78,80] Therefore, they have become targets for the development of anticancer agents. Many of the currently utilised chemotherapeutics against human cancer involve the inhibition of topoisomerase II.

3.2 Catalytic cycle of topoisomerase II

Topoismerase II is a homodimer that adopts two conformations, which are dependent on the presence of ATP. Together with two DNA segments, called gate and transport, topoisomerase II forms the pre-cleavable complex. When ATP binds to the enzyme, it changes its

conformation from open to closed clamp. During the conformation change, the enzyme cleaves the gate segment by nucleophilic attack of the tyrosine hydroxyl group. Allowing the transport segment pass through the gate, leading to the formation of the post-cleavage complex. Hydrolysis of ATP transforms the enzyme back to the open conformation and releasing the DNA products.

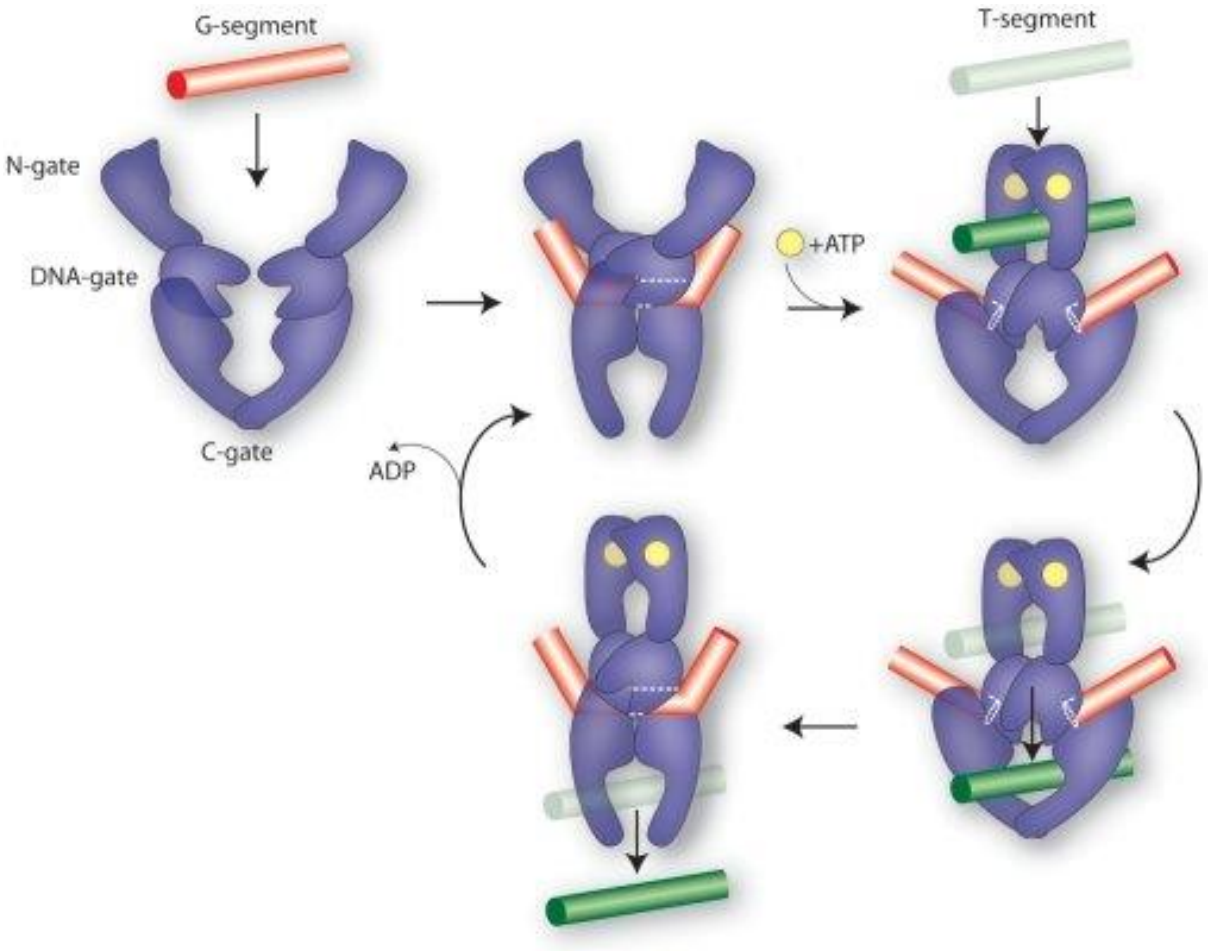

Figure 12. Catalytic cycle of topoisomerase II. The figure is used with permission from Oxford University Press ©.

Topoisomerase II inhibition is a major mechanism of several anticancer agents. Two established classes of drugs inhibit topoisomerase II:

- topoisomerase poisons
- catalytic inhibitors

3.3 Topoisomerase poisons

Topoisomerase poisons are ternary protein-DNA-drug complexes that stabilise the cleavable complex, which inhibits the re-ligation of DNA. This results in the accumulation of the cytotoxic cleavage complex. There are two mechanisms by which topoisomerase poisons work. The most common mechanism of action is through intercalation between the −1 and +1 DNA base pairs in the protein-DNA cleavage complex. The ternary complex is then stabilised by additional hydrophobic and electrostatic interactions, which hinder the re-ligation of double strand breaks. Another mechanism involves the formation of a redox-dependent, covalent drug-enzyme complex. Hereby, the compounds do not bind at the active site of the DNA but

lateral to it. This binding stabilises the enzyme-DNA cleavage complex, which again causes DNA strand breaks that lead to cell death. Examples for topoisomerase II poisons are amsacrine, doxorubicin and etopside (see Figure 16)[78,81]

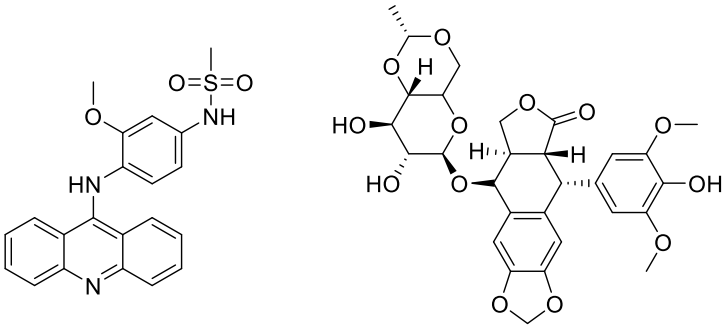

Figure 13. Chemical structures of amsacrine and etoposide.

3.4 Catalytic inhibitors

Based on their structure, catalytic inhibitors prevent the progression of the topoisomerase II catalytic cycle at different stages. The mode of action is competitive binding onto ATP binding site by small molecules, blocking the hydrolysis of ATP. This in turn hinders the transport segment from advancing through the gate of the DNA cleavage complex, preventing DNA replication and transcription, which results in cell death. Compounds including ICRF-193, merbarone, novobiocin and suramin belong to this class.[78,81]

4.0 Indoloquinolines

Since the beginning of mankind, natural products are used as therapeutics. Over the course of time natural products were developed further, resulting in saver and more potent derivatives. Their rich bioactivity is manifested by the impact they have on the pharmaceutical industry. Approximately 25% of available prescription drugs derive from plants.[82] One example is quindoline **1** (indolo[3,2-*b*]quinoline), a flat tetracyclic aromatic alkaloid isolated from the roots of the *Cryptolepis sanguinolenta* shrub, which is used as traditional medicine in Central and West Africa against malaria, inflammations and various other disorders.[83] Quindoline **1** belongs to the indoloquinolines, a small family of natural alkaloids. These heterocyclic compounds consist of an indole and a quinoline moiety, linked together by their pyrrole and pyridine rings, resulting in four isomeric ring systems, namely indolo[3,2-*b*]quinoline **1**, indolo[2,3-*b*]quinoline **2**, indolo[3,2-*c*]quinoline **3** and indolo[2,3-*c*]quinoline **4** (see Figure 17). Indoloquinolines may occur in two different tautomeric forms, 5*H* and 10*H* tautomers[77] Except for indolo[2,3-*c*]quinolines, all other classes of indoloquinolines have been found in nature.[84–86] Depending on the cell type, indoloquinolines inhibit the cell cycle in the S-phase or in the G2/M-phase (see Figure 18).[87] Furthermore, indoloquinolines have the typical framework of DNA intercalating agents, based on their planar structure and size as well as their shortage on flexibility; one could suggest that indoloquinolines would act as minor groove binding ligands.

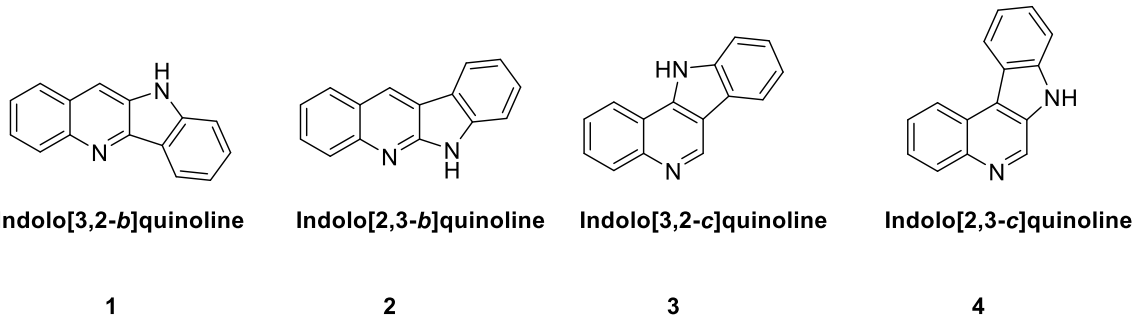

Figure 14. Chemical scaffolds of indoloquinoline isomers.

The indolo[3,2-*b*]quinoline scaffold overlays almost completely with the longitudinal axis of Watson-Crick AT and CG base pairs, where it is purely symmetric oriented (see Figure 19).

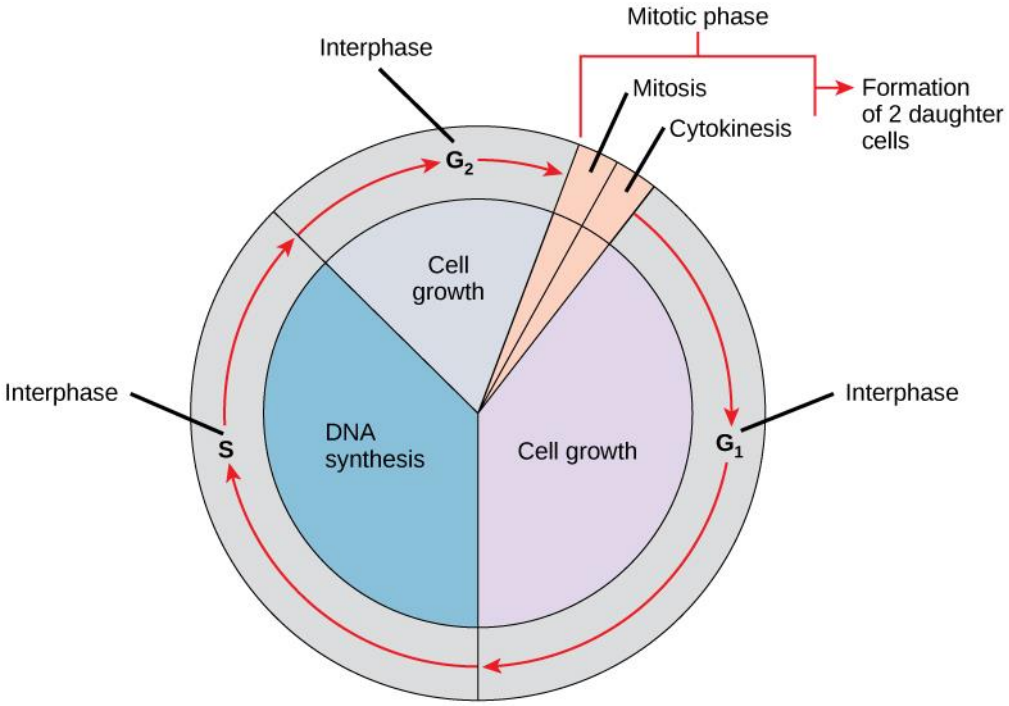

Figure 15. Illustration of the four cell cycle phases. The figure is used with permission from OpenStax College, Biology.

However, apart from the overall geometry, dipole-dipole interactions play a decisive role in the intercalation. Hence, the dipole moments for the four-isomer ring systems differ from each other, leading to the assumption that the stacking interactions differ too, without considering influences of substituents.[77]

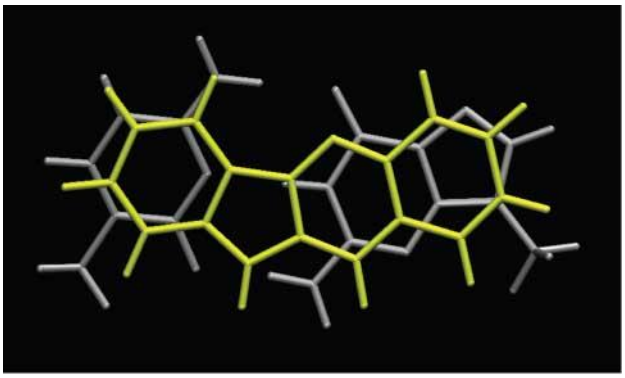

Figure 16. Superposition of indolo[3,2-*b*]quinoline (yellow) on a GC Watson-Crick base pair (grey).

4.1 Total synthesis of indoloquinoline alkaloids

Over the years a wide range of synthetic pathways for the preparation of indoloquinolines have been reported and reviewed. The synthetic methods utilised for the preparation of indoloquinoline alkaloids can be grouped into six categories, based on their ring formation reactions, namely palladium-catalysed coupling, aza-Wittig reaction, transition-metal mediated reductive cyclization, photochemical reactions, Graebe-Ullmann reaction and other miscellaneous transformations.[85]

i. Palladium-catalysed coupling reaction

Pd-catalysed coupling reactions established themselves as a potent way for the synthesis of natural and biologically active products, as well as various organic building blocks. Compared to first row transition metals (Fe, Ni, Cu, Zn) palladium catalysts feature higher activity, which allows the conversion of less active compounds at lower temperatures. The synthesis of Isocryptolepine **5** (an indolo[3,2-*c*]quinoline) and neocryptolepine **6** (an indolo[2,3-*b*]quinoline) were reported by Timari *et al.*, using Suzuki coupling (see Schemes 1 and 2).[85]

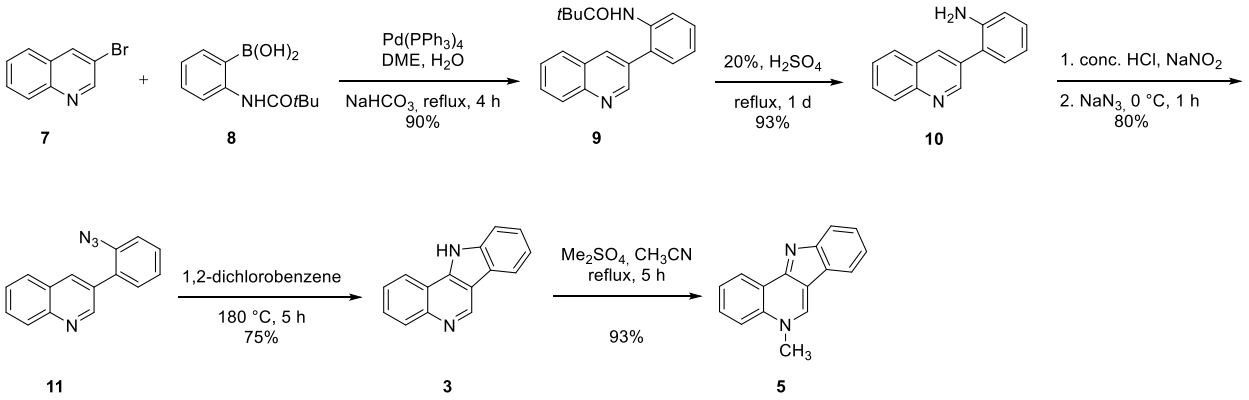

Scheme 1. The reaction of 3-bromoquinoline **7** with *N*-pivaloylaminophenyl boronic acid **8** in the presence of Pd(0) catalyst provided the desired biaryl compound **9** which, through hydrolysis with sulfuric acid gave amine **10**. The compound **10** was converted to azide **11** which, on nitrene insertion, gave exclusively the indolo[3,2-c]quinoline **3**. Regioselective methylation on quinoline nitrogen using dimethyl sulfate yielded the target molecule **5**.

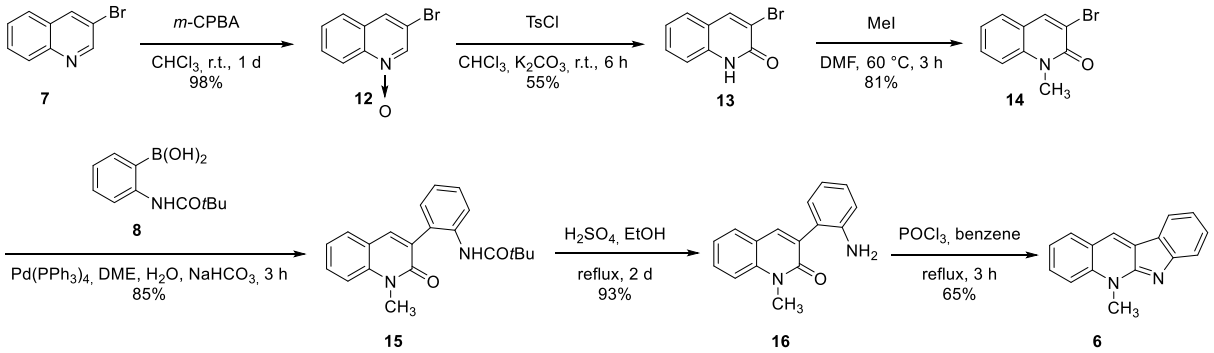

Scheme 2. 3-Bromo-1*H*-2-quinoline **13** was prepared from 3-bromo-quinoline **7** *via* its *N*-oxide **12** which, on treatment with methyl iodide, gave *N*-methyl compound **14**. Coupling reaction of **14** with **8** in the presence of Pd(0) catalyst afforded the biaryl compound **15**. Hydrolysis of **15** with sulfuric acid followed by cyclisation using $POCl_3$ resulted in **6**.

Quindoline **1** (10*H*-indolo[3,2-*b*]quinoline) is a rare example of a natural product that was first synthesised artificially before it was extracted from a natural source.[82] Fan and Ablordeppy presented the preparation of quindoline **1** by catalytic phenylation with

triphenylbismuth diacetate and metallic copper, followed by oxidative cyclisation (Scheme 3).[85]

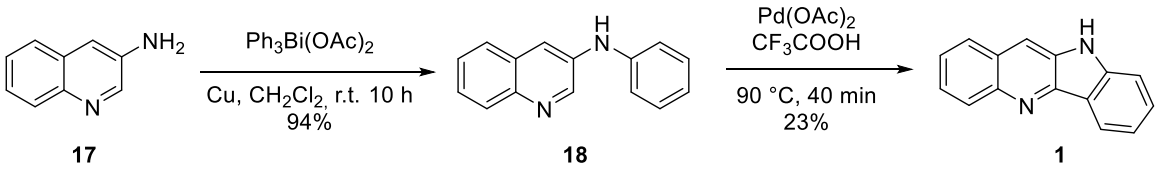

Scheme 3. *N*-arylation of 3-aminoquinoline **17** with triphenylbismuth diacetate and metallic copper yields the anilinoquinoline **18**, which cycles to quindoline **1**, using palladium acetate.

As mentioned previously, indolo[2,3-*c*]quinolines were not yet found in nature. However, a variety of syntheses have been developed to produce them. The preparation of isoneocryptolepine **25** uses a Suzuki coupling under Gronowitz conditions, which produces compound **4** as an intermediate (see Scheme 4).[85]

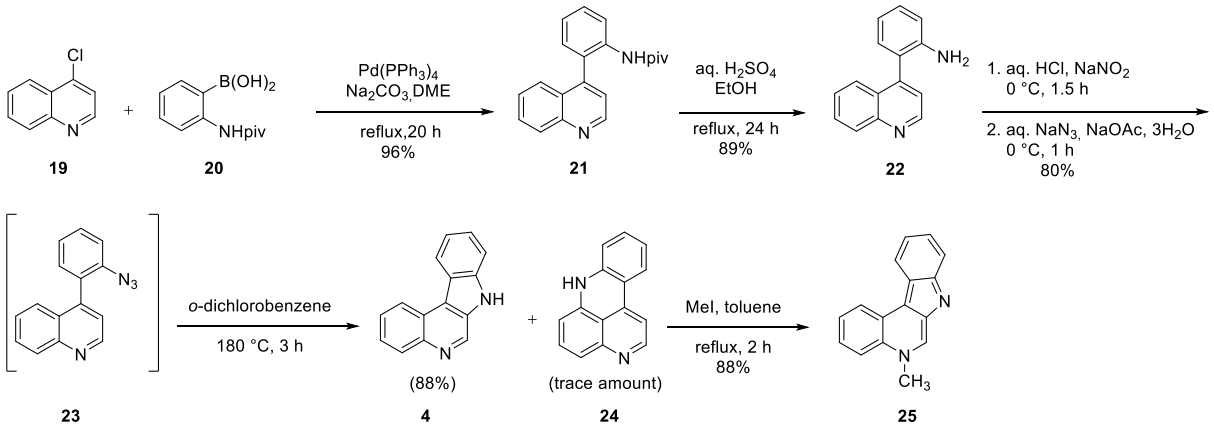

Scheme 4. Suzuki reaction of **19** with **20** under Gronowitz conditions yields compound **21**, and subsequent hydrolysis provides amine **22**. Diazotisation of the resulting amine **22** followed by introduction of azido group and then thermal decomposition of azide **23** in boiling *o*-dichlorobenzene yields species **4** in good yield and trace amount of **24**. Methylation of **4** affords the final product **25**.

ii. aza-Wittig reaction

Due to its mild conditions aza-Wittig reaction has become an important method in organic synthesis. Both cyclic and acyclic substances can be produced with good yields in neutral media without the presence of a catalyst. Various 6*H*-indolo[2,3-*b*]quinoline derivatives can be generated by using the methodology developed by Alajarin and co-workers (see Scheme 5).[85]

The poor yield can be improved by introducing a trimethylsilyl group at the acetylenic terminus. The trimethylsilyl group actively promotes the formation of **29**, where it acts as an alternative due to the absence of the hydrogen atom, leading to the formation of 6*H*-indolo[2,3-*b*]quinoline derivatives **2a-d**.[85]

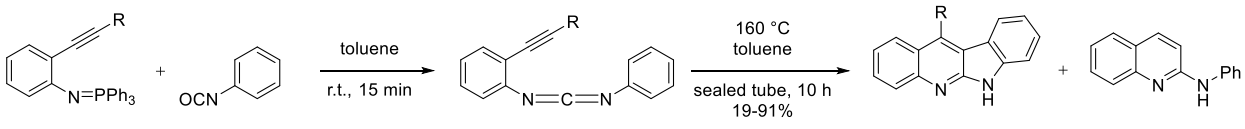

26a-d **27** **28** **2a-d** **29**

R = H, Me_3Si, *n*-Pr, *t*-Bu

Scheme 5. Aza-Wittig reaction of iminophosphane **26a-d** with phenyl isocyanate **27** yields carbodiimide **28** and triphenylphosphine oxide, followed by thermal treatment without purification, which results in **2a-d** in moderate to very good yield.

Important synthetic methods for the effective preparation of indoloquinolines using the aza-Wittig reaction, were cyclisation reactions of highly reactive nitrene intermediates. The cyclisation reaction was brought about by the thermal decomposition of an azide group (see Scheme 6).[88]

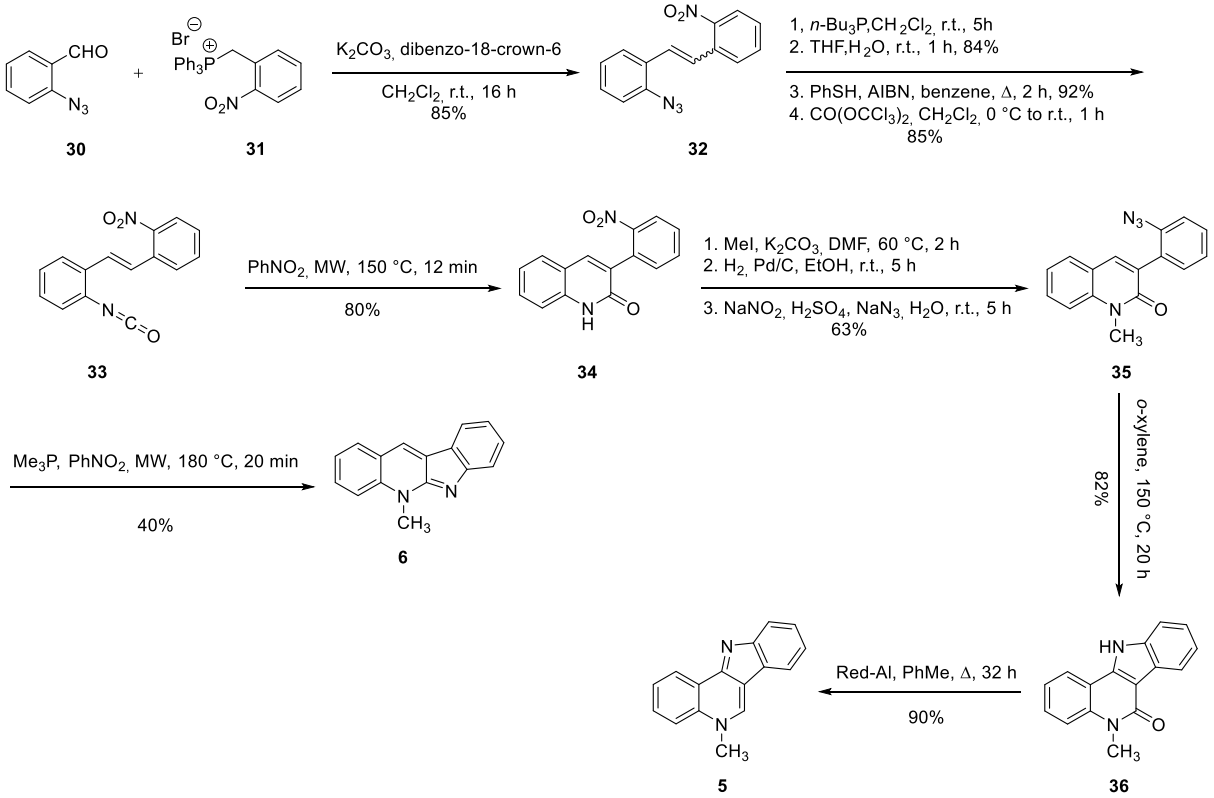

30 **31** **32** **33** **34** **35** **6** **5** **36**

Scheme 6. 2-Azidobenzaldehyde **30** reacts with Wittig reagent **31** to racemic species **32** which, on treatment with diphosgene, gives *o*-vinyl-substituted aryl isocyanate **33**. Addition of nitrobenzene leads to intramolecular cyclisation to quinoline **34**. Treatment with methyl iodide, followed by conversion to the azide gives compound **35**. **35** can either be converted with

trimethylphosphine into **6** *via* an intermediate iminophosphorane or cyclisation of nitrene formed upon thermal decomposition of azide gives **36** which finally yields **5**, by using red-Al as a reducing agent.

iii. Transition-metal mediated reductive cyclisation

Different research groups used reductive cyclisation provided by transition metals to synthesise quinoline ring bearing derivatives (e.g., indoloquinolines). Ho and co-workers reported the synthesis of neocryptolepine **6** and cryptolepine **40** from 1,3-bis(2-nitrophenyl)propan-2-one **38** (see Scheme 7).

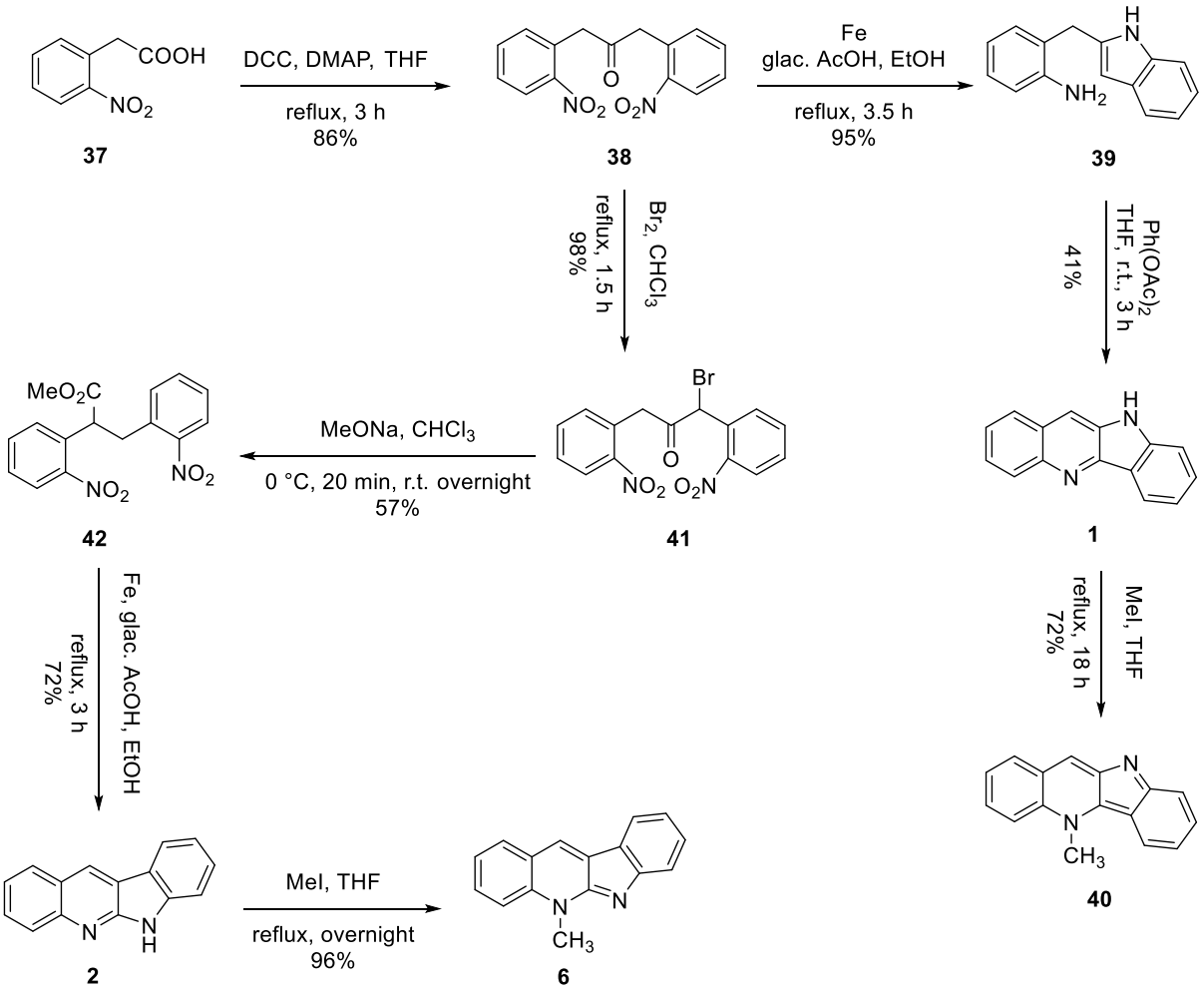

Scheme 7. The key constituent **38** is easily derived by reacting 2-nitrophenyl acetic acid with DCC in presence of DMAP. Reduction of nitro groups with Fe powder, followed by oxidative cyclisation produces **1**. Then *N*-methylation of **1** yields desired **40**. Compound **6** is acquired through bromination of **38**, followed by Favorskii rearrangement, reductive cyclisation, using Fe powder, and *N*-methylation with methyl iodide.

Neocryptolepine **6** can also be prepared b using the method reported by Parvatkar *et al.* They employed the Perkin reaction followed by two reductive cyclisation reactions as the main step (see Scheme 8).[85]

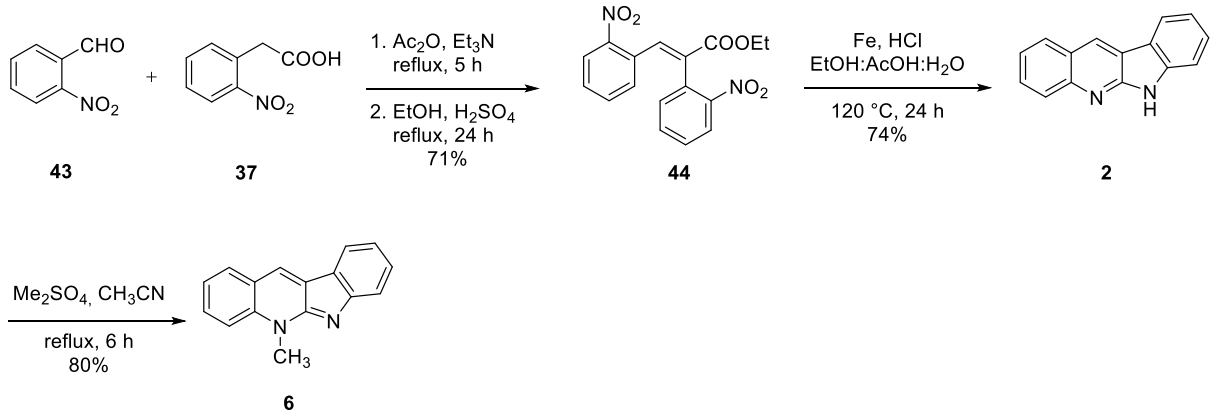

Scheme 8. Condensation of 2-nitrobenzaldehyde **43** with **37** in refluxing acetic anhydride in the presence of Et_3N gives α,β-unsaturated acid which on esterification affords the required ester **44** in good yield. Double reductive cyclisation with Fe powder furnishes **2** in one-pot transformation. Subsequent methylation with methyl iodide yields **6**.

iv. Photochemical reaction

Valuable methods in synthetic organic chemistry are photochemical reactions since they act in different way to thermal reactions by allowing for the formation of thermodynamically disfavoured products. This is achieved by overcoming high activation energies, which are not generated thermally. Another positive aspect of photochemical reactions is the lack of additional reagents, thereby avoiding the formation of by-products. Dhanabal *et al.* reported the synthesis of indoloquinoline derivatives *via* a photoannulation technique, directed at heteroatoms (see Schemes 9 and 10).[85]

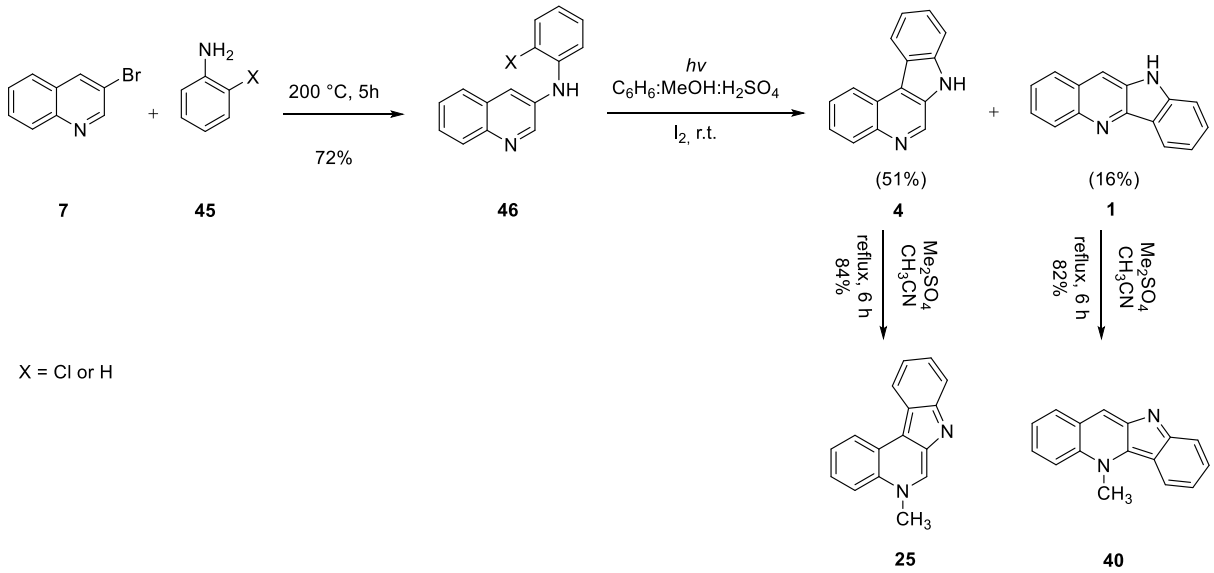

Scheme 9. Anilinoquinoline **46** is generated by nucleophilic substitution of 3-bromoquinoline 7 with aniline **45** at 200 °C. Photochemical cyclisation of **46** leads to both, angular- and linear-fused products, **4** and **1**. Following methylation yields cryptolepine **40** and isoneocryptolepine **25** respectively.

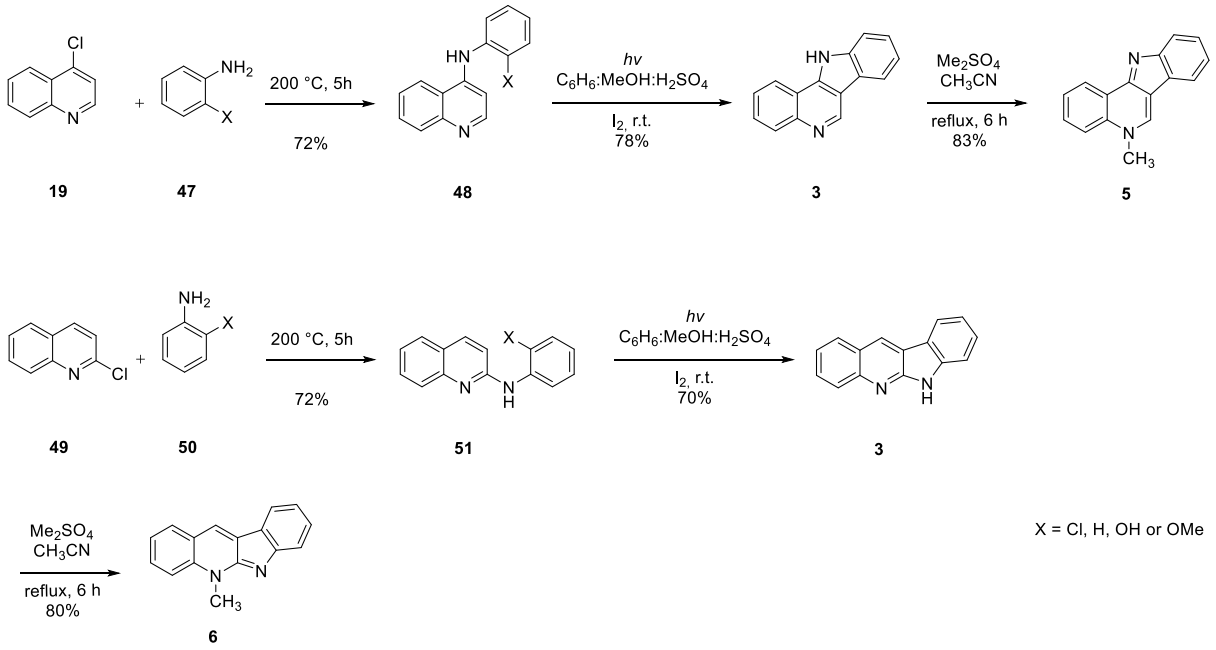

Scheme 10. Isocryptolepine **5** and neocryptolepine **6** are prepared by photocyclisation of the corresponding anilinoquinolines **48** and **51**, which in turn are obtained by nucleophilic substitution of chloroquinoline **19** and **49** with aniline **47** and **50**. Subsequent methylation with dimethyl sulfate leads to **5** and **6**, respectively.

v. Graebe-Ullman reaction

The synthesis of carbazoles by acid catalysed pyrolysis of phenyl benzotriazoles is known as the Graebe-Ullman reaction. The unstable phenyl benzotriazoles promptly undergo cyclisation from an unstable diradical intermediate to a 4a*H*-carbazole, which isomerises to carbazole *via* a [1,3] hydrogen shift. For the synthesis of indoloquinolines some research groups exploited haloquinolines as starting materials instead of halopyridines.[85] An example are the practices of Peczynska-Czoch and co-workers, where they prepare neocryptolepine derivatives by Graebe-Ullman reaction (see Scheme 11).

A common method to improve the yields of Graebe-Ullmann reaction is the use of microwaves. Vera-Luque *et al.* accomplished by microwaves assisted synthesis various 6*H*-indolo[2,3-*b*]quinolines (see Scheme 12).[85]

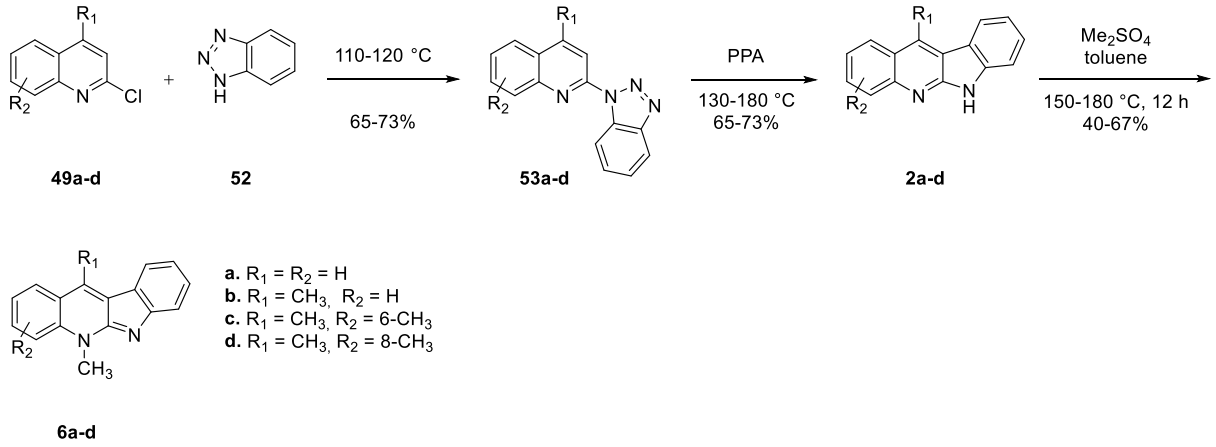

Scheme 11. 2-Chloroquinolines **49a-d** are heated with benzotriazole **52** to give triazoles **53a-d**, which decompose into indoloquinolines when heated at **130-180 °C** in the presence of PPA. Subsequent methylation with DMS yields neocreptolepines **6a-d.**

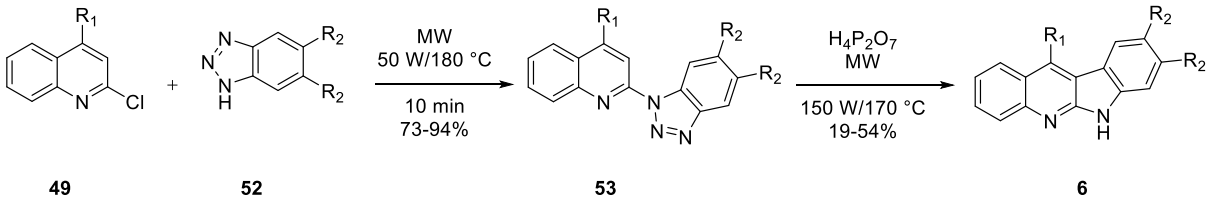

Scheme 12. Triazole **53** is prepared by microwave irradiation of benzotriazoles **52** and 2-chloroquinoline **49** in good to very good yields. Subsequent microwave irradiation in the presence of pyrophosphoric acid yielded 6*H*-indolo[2,3-*b*]quinolines **6.**

vi. Other miscellaneous methods

Several research groups developed different synthetic pathways for the preparation of indoloquinoline alkaloids. A few of them are mentioned in this section. Bierer and co-workers reported the preparation of various cryptolepine derivatives to assay their antimalarial activities (see Scheme 13).[85]

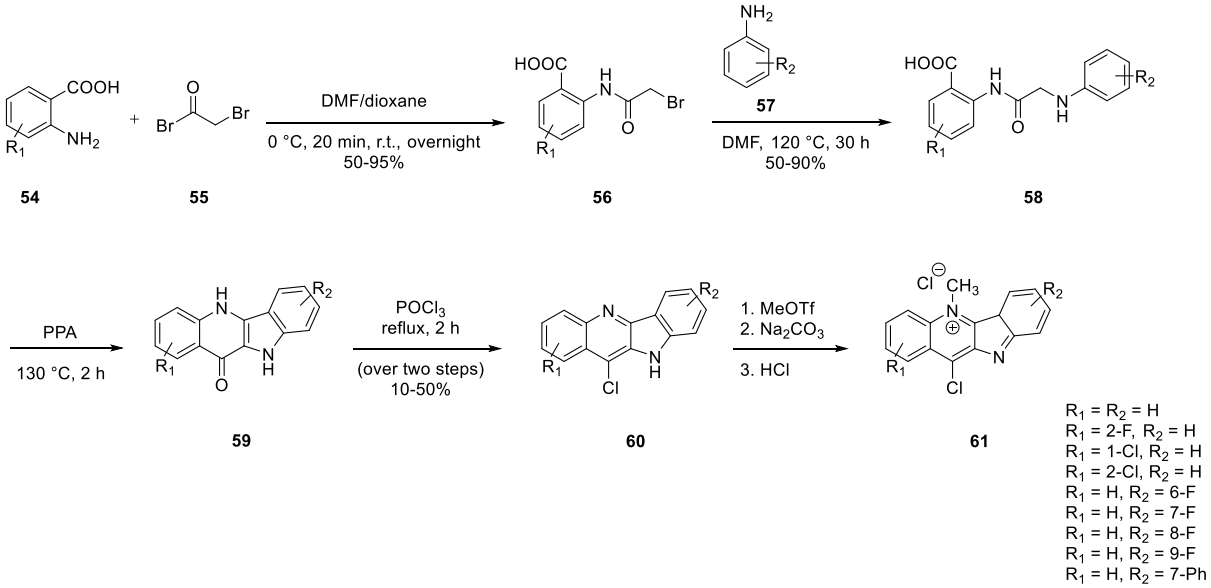

Scheme 13. Nucleophilic acetylation of anthranilic acid derivatives **54** with bromoacetyl bromide **55** gives compounds **56**. Treatment with aniline **57** results in amides **58,** which by acid-catalysed cyclisation with PPA are conerted into quindolone **59**. Reflux in $POCl_3$ leads to the corresponding 11-chloroquinolines **60.** Finally, *N*-methylation provides the 11-chlorocryptolepine hydrochloride salts **61**.

Radl and co-workers synthesised quindoline **1** *via* a nucleophilic denitrocyclisation reaction (see Scheme 14)**.**

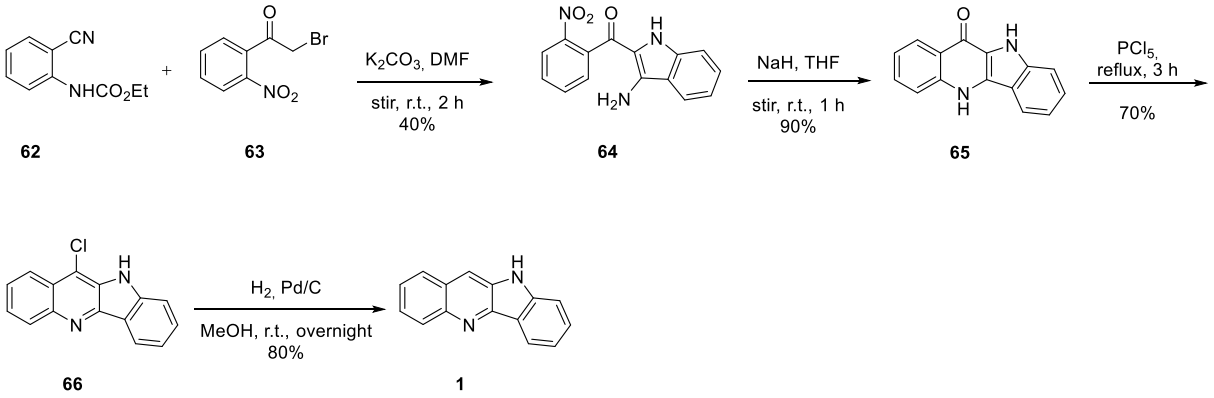

Scheme 14. Anthranilonitrilo derivative **62** and phenacyl bromide **63** give the intermediate **64** in the presence of potassium carbonate. Addition of sodium hydride leads to nucleophilic denitrocyclisation of **64** to tetracyclic compound **65**. Subsequent treatment with PCl_5 and work-up yielded **1**.

A simple method by Engqvist and Bergman was used for the synthesis of neocryptolepine **6** shown below (see Scheme 15).[85]

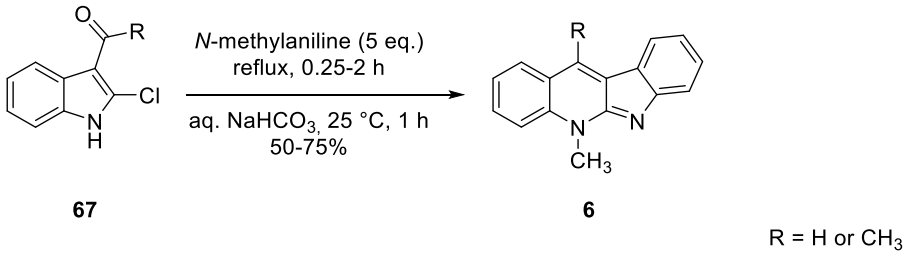

Scheme 15. Chloroindole derivatives **67** are refluxed with *N*-methylaniline in excess for up to 2 h. Ensuing addition of aqueous sodium hydrogen carbonate yield **6**.

4.2 Anti-neoplastic activity of indoloquinoline-derivatives

Indoloquinolines intercalate with DNA double helices, changing their conformation, leading to the inhibition of DNA replication and transcription (e.g., topoisomerases I and II). Indoloquinolines analysed in biophysical studies have shown to have a high affinity to bind triple-helical or quadruplex targets, opening the possibilities for indoloquinolines as potential target therapies. Cryptolepine, a *N*5-methyl-substituted derivative of quindoline, was first synthesised in 1906 by Boehringer and Fichter, whilst investigating novel dyes, showed anti-inflammatory activity and cytotoxicity by interfering with topoisomerase II. It is believed that cryptolepine interacts with DNA due to its structural similarity to 9-aminocridine, which intercalates into DNA.[88] It has an asymmetric planar structure, which allows it to slide between base pairs, especially at CG rich regions and non-alternating CC sites. Compared with other topoisomerase II inhibitors, cryptolepine and its analogues show lower mutagenicity, suggesting that topoisomerase II inhibition may not fully account for the cytotoxicity. Cell culture trials with cryptolepine showed increases in p53 protein, causing cellular responses in the G1 phase of the cell cycle, when present at all concentrations. DNA stand breaks promote the increase of p53 protein concentrations, which stimulate p53-mediated signalling pathways.[8,12,89] Affinity studies have shown that the biological activity strongly depends on the methylation of the *N*5.[77]

Neocryptolepine **6**, the [2,3-*b*]-isomer of cryptolepine has shown to be less cytotoxic than cryptolepine due to its structure. Because both nitrogen atoms are on the same side of the ring, the binding affinity to the intercalation pocket slightly declines. Like with cryptolepine analogues, missing the *N*5-methylation affects its DNA binding abilities of neocryptolepine and

its analogues. However, extensive studies on neocryptolepine has shown that it possesses high antiplasmodial activity, becoming a lead development compound for antimalarial agents.[77] Indolo[3,2-*c*]quinoline, indolo[2,3-*c*]quinolines and their derivates were much less investigated than the other two isomers. A human tumour cell line screen study, organised by the US National Cancer Institute, displayed that indolo-[3,2-*c*]quinolin-2(1*H*)-one possesses an inhibitory activity with GI_{50} value of 19.0 µM.[87] Further human DNA interactions studies of isocryptolepine and isoneocryptolepine showed that they bind through intercalation onto duplex DNA. Recent studies have shown that indoloquinolines possess high affinities to interact with DNA triplexes as well as G-quadruplexes.[77,88] Especially G-quadruplexes attract researches, due to their high occurrence in eukaryotic telomers. G-quadruplexes are guanine rich DNA sequences capable to fold into four-stranded structures, which prohibit telomere elongation. The 3' end terminus of telomerase, a ribonucleoprotein that preserves telomers, has G-rich sequences that fold themselves into G-quadruplexes. Telomeres are crucial for the survival of cancer cells, stabilisation of the G-quadruplexes inhibits the telomerase activity, which can prevent cancer proliferation.[77] To improve the pharmacological profile of these compounds, metal-complexes were synthesised. Ruthenium- and osmium-based indolo[3,2-*c*]quinolines with chelating iminopyridine moieties showed high cytotoxicity *in vitro*.[87,90]

4.3 Indoloquinoline-based metal complexes

The indoloquinoline backbone is a planar, four-membered, conjugated heteroatomic ring system. Despite the development of indoloquinolines with increased DNA binding affinity, the selectivity for tumour cells is comparatively low. Furthermore, insufficient aqueous solubility and bioavailability restricts their further development as anticancer agents. Like many other organometallic complexes, the metal complexes of indoloquinoline derivatives show medical potential in the treatment against cancer. Since naturally occurring indoloquinolines do not possess suitable binding sites for metal ions, they must be introduced artificially. Filak *et al.* synthesised the ruthenium(II)- and osmium(II)-arene complexes of indolo[3,2-*c*]quinolines by introducing an ethane-1,2-diamine moiety as a binding site (see Scheme 16). However, these novel indoloquinoline complexes dissociate in aqueous media by releasing the ligands.[85]

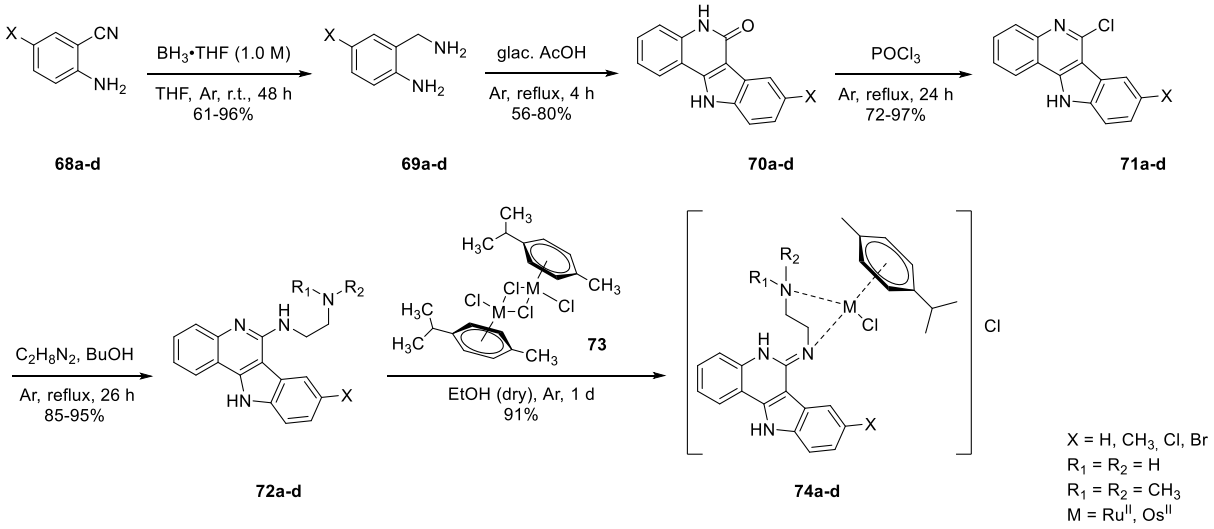

Scheme 16. Substituted benzylamines **69a-d** were obtained by reduction of compounds **68a-d** with borane in dry THF. Addition of glacial acetic acid give the respective 8-substituted 5,11-dihydroindolo[3,2-*c*]quinolin-6-ones **70a-d**. The following addition of $POCl_3$ leads to 8-substituted 6-chloro-11*H*-indolo[3,2-*c*]quinolines **71a-d**, which were reached with ethane-1,2-diamine in butanol to give *N*-(11*H*-Indolo[3,2-*c*]quinolin-6-yl)-ethane-1,2-diamine **72a-d**. Complexes **74a-d** were obtained by the addition of dichloro(*p*-cymene)ruthenium(II) dimer **73** in dry ethanol.

To retain the *in vitro* antiproliferative activities of those compounds, modifications at the sp^2-hybridised N-donor atoms were performed by Primik *et al*. Hereby, a Schiff' base is introduced by the condensation reaction of an indoloquinoline hydrazine with a 2-formyl- or 2-acetylpyridine, which binds to ruthenium(II)- or osmium(II)-arene complexes as well as copper(II) ions. (see Scheme 17). This led to an increase in thermodynamic and kinetic stability of the ensuing indolo[3,2-*c*]quinoline metal complexes.[85]

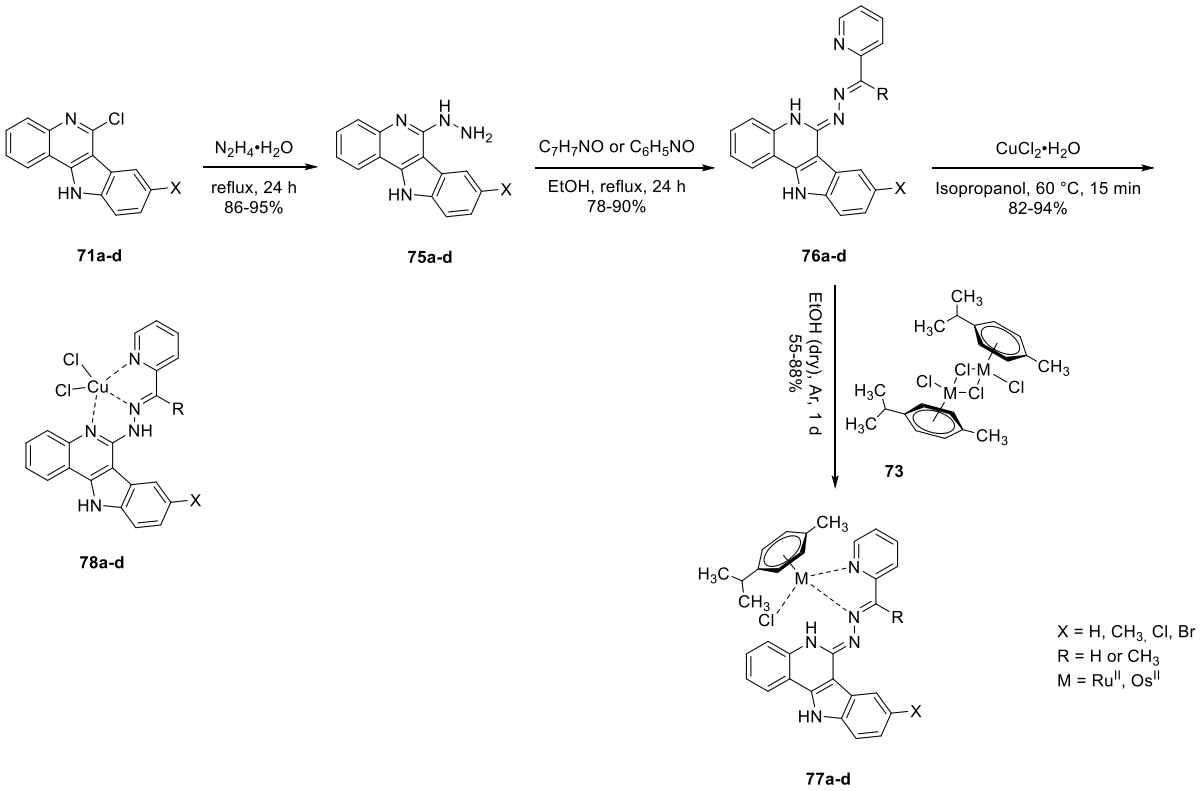

71a-d **75a-d** **76a-d** **73** **78a-d** **77a-d**

Scheme 17. Hydrazine hydrate is added to 8-substituted 6-chloro-11*H*-indolo[3,2-*c*]quinolines **71a-d** and stirred at 115 °C. The resulting 8-substituted 5,11-dihydroindolo[3,2-*c*]quinolin6-ylhydrazines **75a-d** are suspended in ethanol and mixed with either 2-formylpyridine or 2-acetylpyridine at 50 °C, leading to the corresponding ligands **76a-d**. Following addition of **73** or copper(II) chloride dihydrate yielded complexes **77a-d** and **78a-d** respectively.

5.0 Experimental part

5.1 General

Chemicals

All commercially available reagents were obtained from Sigma-Aldrich, Acros Organics, Alfa Aesar, Brenntag, Donau Chemie, Iris-Biotech, Merck, TCI, Thermo Fisher Scientific or VWR and used without further purification.

Chromatography

- Flash column chromatography

Preparative flash column chromatography was performed by using Merck silica gel (230-400 mesh).

- Thin layer chromatography

All reactions were monitored using coated aluminium plates. TLC was carried out on 0.20 mm thick silica gel 60, F_{254} Merck plates. Spots were detected by UV light.

NMR spectroscopy

^{1}H and ^{13}C (*J* modulated) NMR spectra were measured on Bruker Avance II 600 (^{1}H at 600 MHz, ^{13}C at 151 MHz) at 300 K, unless otherwise specified. 2D NMR spectra were measured on Bruker Avance III 700 (^{1}H at 700 MHz, ^{13}C 175 MHz). Chemical shifts were referenced either to residual DMSO-d_6 (δH = 2.50)/H_2O (δH = 4.80) or DMF-d_7 (δH = 2.74, 2.91, 8.02)/H_2O (δH = 3.50) All chemical shifts (δ) are given in ppm and *J* values in Hz. The following abbreviations were used to describe spin multiplicities: s = singlet, d = doublet, t = triplet, q = quartet, sept = septet, m = multiplet, dd = doublet of doublet, dt = doublet of triplet, dsept = doublet of septet etc.

Mass spectroscopy

Mass spectra were recorded on Bruker spectrometers

Crystallographic Structure Determination

The measurements were performed mainly on a Bruker D8 Venture and Bruker X8 APEX-II CCD diffractometers. The data were processed using SAINT software.

5.2 Synthesis of 8-, 9-, and 10-bromo-5,7-dihydro-6*H*-indolo[2,3-*c*]quinoline-6-ones

For the synthesis of the desired bromo-substituted *7H*-indolo[2,3-*c*]quinoline-6(5*H*)-ones the method reported by J.B. Petersen and K. H. Lakowitz was utilised (see Scheme 18).[91]

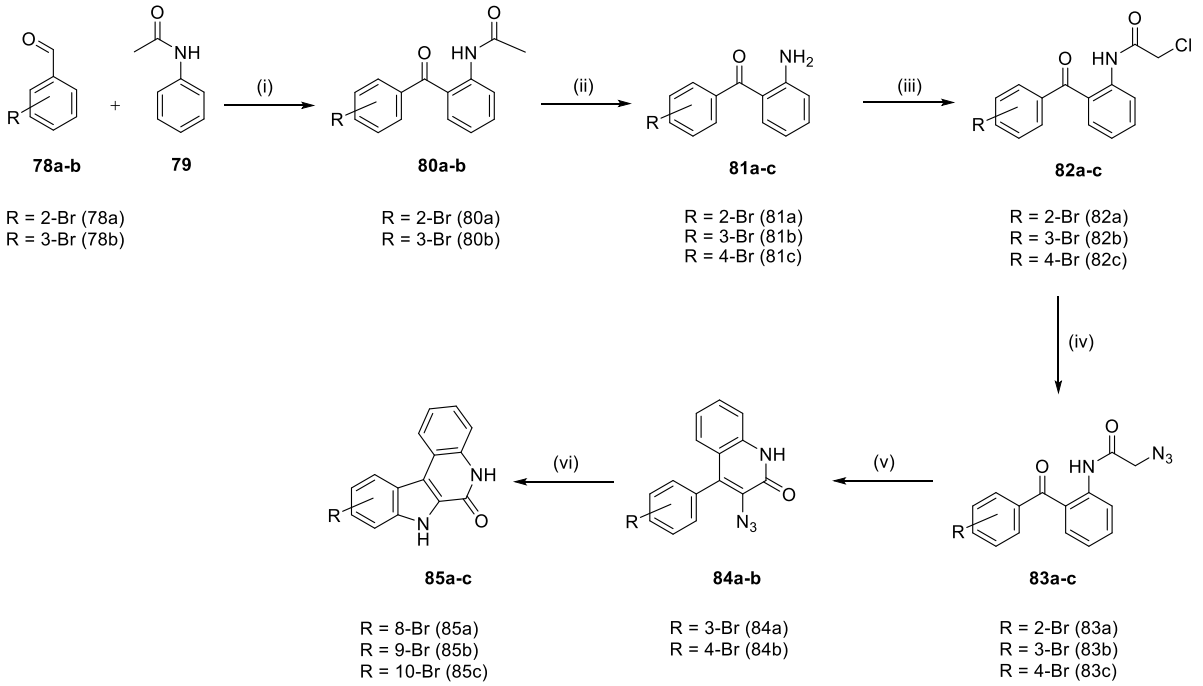

Scheme 18 Synthetic pathway to generate bromo-substituted 7*H*-indolo[2,3-*c*]quinoline-6(5*H*)-ones. (i) palladium(II) acetate, sodium dodecyl sulfate, acetanilide, water, trifluoroacetic acid, 2- or 3-bromo-benzaldehyde and *tert*-butyl hydroperoxide room temperature, 25 h. (ii) Acetone, hydrochloric acid, 70 °C, 3 – 5 h. (iii) chloroacetyl chloride, chloroform, 71 °C, reflux, 30 min; (iv) Sodium azide, dimethyl formamide, water, 60 °C, 30 min. (v) Ethanol, aq. sodium hydroxide (40%), 60 °C, 5 h. (vi) toluene, 130 °C, reflux. 2 h.

N-(2-(2-bromobenzoyl)phenyl)acetamide 80a

To palladium(II) acetate (407 mg, 1.85 mmol), sodium dodecyl sulfate (533 mg, 1.85 mmol), acetanilide **79** (5.00 g, 36.99 mmol) in water (37.0 mL) in a 100 mL round-bottom flask a mixture of trifluoroacetic acid (740 µL, 9.62 mmol), 2-bromobenzaldehyde **78a** (8.60 mL, 73.9 mmol) and *tert*-butyl hydroperoxide (70% solution in water) (9.30 mL, 2.00 mmol) was added under stirring. Thereafter, the reaction mixture was stirred at room temperature for 25 h. The resulting suspension was extracted with ethyl acetate (3 × 75 mL) and the combined organic layers were dried over magnesium sulfate. The solvent was removed under reduced pressure. The product was obtained as a yellow oil. Yield: 5.73 g, 49%. ^{1}H NMR (500 MHz, DMSO-d_6) δ 10.96 (s, 1H, N*H*), 8.29 (dd, *J* = 8.4, 1.1 Hz, 1H, $H_{(Ar)}$), 7.75 (dd, *J* = 7.9, 1.1 Hz, 1H, $H_{(Ar)}$), 7.65 (ddd, *J* = 8.6, 7.2, 1.7 Hz, 1H, $H_{(Ar)}$), 7.56 – 7.44 (m, 3H, $H_{(Ar)}$), 7.31 (dd, *J* = 7.9, 1.6 Hz, 1H, $H_{(Ar)}$), 7.16 (ddd, *J* = 8.2, 7.4, 1.2 Hz, 1H, $H_{(Ar)}$), 2.09 (s, 1H, CH_3).

N-(2-(3-Bromobenzoyl)phenyl)acetamide 80b

To palladium(II) acetate (407 mg, 1.85 mmol), sodium dodecyl sulfate (533 mg, 1.85 mmol), acetanilide **79** (5.00 g, 36.99 mmol) in water (37.0 mL) in a 100 mL round-bottom flask a mixture of trifluoroacetic acid (740 µL, 9.62 mmol), 3-bromobenzaldehyde **78b** (8.60 mL, 73.9 mmol) and *tert*-butyl hydroperoxide (70% solution in water), (9.30 mL, 2.00 mmol) was added under stirring. Then, the reaction mixture was stirred at room temperature for 24 h. The resulting suspension was extracted with ethyl acetate (3 × 75 mL) and the combined organic layers were dried over magnesium sulfate. The solvent was removed under reduced pressure and the crude product was purified on silica using a mixture of hexane:ethyl acetate 80 : 20 as eluent. The product was obtained as a yellow oil. Yield: 12.0 g, quantitative. ^{1}H NMR (500 MHz, DMSO-d_6) δ 10.12 (s, N*H*), 7.82 (dd, *J* = 7.9, 0.9 Hz, $H_{(Ar)}$), 7.75 (s, $H_{(Ar)}$), 7.63 (d, *J* = 7.8 Hz, $H_{(Ar)}$), 7.60 – 7.54 (m, $H_{(Ar)}$), 7.49 – 7.40 (m, 2H, $H_{(Ar)}$), 7.37 (dd, *J* = 7.6, 1.2 Hz, $H_{(Ar)}$), 7.27 (t, *J* = 7.2 Hz, $H_{(Ar)}$), 1.76 (s, CH_3).

(2-Aminophenyl)(2-bromophenyl)methanone 81a
To *N*-(2-(2-bromobenzoyl)phenyl)acetamide **80a** (3.50 g, 11.0 mmol) in acetone (73.5 mL) in a 250 mL round-bottom flask. hydrochloric acid (6 M) (73.5 mL) was added and the reaction mixture was stirred at 70 °C for 5 hours. The resulting solution was transferred into a 500 mL separating funnel and the pH was adjusted to 10 using saturated aq. potassium carbonate solution. The aqueous phase was extracted with dichloromethane (3 × 75 mL) and the combined organic layers were washed with brine (100 mL) and dried over magnesium sulfate. The solvent was removed under reduced pressure and the product was crystallised from ethanol (7.00 mL). Yield: 3.01 g, 99%. 1H NMR (500 MHz, DMSO-d_6) δ 7.70 (d, J = 8.0 Hz, 1H, $H_{(Ar)}$), 7.55 – 7.44 (m, 3H, $H_{(Ar)}$), 7.41 (td, J = 7.9, 1.6 Hz, 1H, $H_{(Ar)}$), 7.35 (dt, J = 15.2, 7.6 Hz, 1H, $H_{(Ar)}$), 7.31 – 7.22 (m, 1H, $H_{(Ar)}$), 6.92 (dt, J = 11.9, 5.9 Hz, 1H, $H_{(Ar)}$), 6.85 (t, J = 10.6 Hz, 1H, N*H*), 6.42 (t, J = 7.5 Hz, 1H, N*H*). ESI-MS (acetonitrile/ methanol + 1% water), positive: *m/z* 298.14 $[M + Na]^+$.

(2-Aminophenyl)(3-bromophenyl)methanone 81b
To *N*-(2-(3-bromobenzoyl)phenyl)acetamid **80b** (11.8 g, 37.0 mmol) in acetone (247 mL) in a 1000 mL round-bottom flask. hydrochloric acid (6 M, 247 mL) was added and reaction mixture was stirred at 70 °C for 3 h. The resulting solution was transferred into a 2 L separating funnel and the pH was adjusted to 11 using saturated aq. potassium carbonate solution. The aqueous phase was extracted with dichloromethane (2 × 200 mL) and the combined organic layers were washed with brine (200 mL) and then dried over magnesium sulfate. The solvent was removed under reduced pressure and the product was crystallised from ethanol (20.0 mL). Yield: 5.91 g, 58%. ^{1}H NMR (500 MHz, DMSO-d_6) δ 7.77 (ddd, J = 7.8, 1.9, 1.2 Hz, 1H, $H_{(Ar)}$), 7.68 (t, J = 1.7 Hz, 1H, $H_{(Ar)}$), 7.52 (dt, J = 7.6, 1.3 Hz, 1H, $H_{(Ar)}$), 7.46 (t, J = 7.8 Hz, 1H, $H_{(Ar)}$), 7.30 (ddd, J = 8.4, 7.0, 1.5 Hz, 1H, $H_{(Ar)}$), 7.24 – 7.17 (m, 3H, $H_{(Ar)}$), 6.86 (dd, J = 8.4, 0.8 Hz, 1H, N*H*), 6.53 – 6.47 (m, N*H*). The obtained crystals were of X-ray diffraction quality.

***N*-(2-(2-bromobenzoyl)phenyl)-2-chloroacetamide 82a**.
To (2-aminophenyl)(2-bromophenyl)-methanone **81a** (3.00 g, 11.00 mmol) in chloroform (12.0 mL) a solution of 2-chloroacetyl chloride (1.28 mL, 16.1 mmol) in chloroform (2.00 mL) was added in one portion. The resulting mixture was refluxed for 30 min. After cooling to room temperature, the solvent was removed under reduced pressure. The crude product was recrystallised from ethanol (11.0 mL) affording yellow crystals. Yield: 2.63 g, 68%. ^{1}H NMR (500 MHz, DMSO-d_6) δ 11.76 (s, 1H, N*H*), 8.50 (dd, J = 8.4, 0.7 Hz, 1H, $H_{(Ar)}$), 7.77 (d, J = 7.9 Hz, 1H, $H_{(Ar)}$), 7.75 – 7.69 (m, 1H, $H_{(Ar)}$), 7.58 – 7.48 (m, 3H, $H_{(Ar)}$), 7.35 (dd, J = 7.9, 1.5 Hz, 1H, $H_{(Ar)}$), 7.25 – 7.19 (m, 1H, $H_{(Ar)}$), 4.48 (s, 2H, CH_2). ESI-MS (acetonitrile/methanol + 1% water), positive: *m/z* 376.08 $[M + Na]^+$.

***N*-(2-(3-bromobenzoyl)phenyl)-2-chloroacetamide 82b**
(2-Aminophenyl)(3-bromophenyl)methanone **81b** (5.89 g, 21.3 mmol) was dissolved in chloroform (21.0 mL) and a solution of chloroacetyl chloride (2.52 mL, 31.7 mmol) in chloroform (5.65 mL) was added in one portion. The reaction mixture was stirred under reflux for 30 minutes. The solvent was removed under reduced pressure and the product was crystallised from ethanol (21.0 mL). The pale-yellow crystals were filtered off and dried *in vacuo*. Yield: 6.49 g, 86%. ^{1}H NMR (500 MHz, DMSO-d_6) δ 10.62 (s, 1H, N*H*), 7.85 (ddd, J = 8.0, 2.0, 1.0 Hz, 1H, $H_{(Ar)}$), 7.78 (t, J = 1.7 Hz, 1H, $H_{(Ar)}$), 7.67 – 7.62 (m, 3H, $H_{(Ar)}$), 7.50 – 7.42 (m, 2H, $H_{(Ar)}$), 7.36 – 7.31 (m, 1H, $H_{(Ar)}$), 4.10 (s, CH_2). ESI-MS (acetonitrile/ methanol + 1% water), positive: *m/z* 373.95 $[M + Na]^+$. The obtained crystals were of X-ray diffraction quality.

***N*-(2-(4-bromobenzoyl)phenyl)-2-chloroacetamide 82c**
To 2-amino-4'-bromo-benzophenone **81c** (5.15 g, 18.7 mmol) in chloroform (18.5 mL) a solution of chloroacetyl chloride (2.20 mL, 27.7 mmol) in chloroform (5.70 mL) was added in one portion. The reaction mixture was stirred under reflux for 30 min. After cooling to room

temperature, the solvent was removed under reduced pressure and the product was crystallised from ethanol (18.5 mL). The next day the product was filtered off and dried *in vacuo*. The product was obtained as light-yellow crystals. Yield: 5.95 g, 91%. ^{1}H NMR (500 MHz, DMSO-d_6) δ 10.58 (s, 1H, N*H*), 7.76 – 7.67 (m, 3H, $H_{(Ar)}$), 7.62 (ddt, J = 11.0, 9.0, 2.0 Hz, 3H, $H_{(Ar)}$), 7.44 (dd, J = 7.7, 1.5 Hz, 1H, $H_{(Ar)}$), 7.31 (td, J = 7.6, 1.2 Hz, 1H, $H_{(Ar)}$), 4.11 (s, 2H, $H_{(Ar)}$). ESI-MS *(acetonitrile/methanol + 1% water), positive: m/z* 374.08 $[M + Na]^+$.

2-azido-*N*-(2-(2-bromobenzoylphenyl)acetamide 83a

To *N*-(2-(2-bromobenzoyl)phenyl)-2- chloroacetamide **82a** (2.60 g, 7.38 mmol) in a 250 mL round-bottom flask in dimethylformamide (8.60 mL) sodium azide (530 mg, 8.18 mmol) was added and the mixture was heated to 60 °C. Then water (75.0 mL) was added dropwise and the reaction mixture stirred for 30 min. The resulting suspension was cooled to room temperature and stored at 4 °C for 1 h. Then the product was dissolved in boiling ethanol (3.60 mL) cooled to room temperature and stored at 4 °C overnight. The product (white flakes) was filtered off and dried *in vacuo*. Yield: 2.12 g, 80%. ^{1}H NMR (500 MHz, DMSO-d_6) δ 11.48 (s, 1H, N*H*), 8.43 (t, J = 14.1 Hz, 1H, $H_{(Ar)}$), 7.77 (d, J = 7.7 Hz, 1H, $H_{(Ar)}$), 7.71 (t, J = 7.5 Hz, 1H, $H_{(Ar)}$), 7.58 – 7.47 (m, 3H, $H_{(Ar)}$), 7.34 (d, J = 7.6 Hz, 1H, $H_{(Ar)}$), 7.22 (t, J = 7.5 Hz, 1H, $H_{(Ar)}$), 4.26 (s, 2H, CH_2). ESI-MS *(acetonitrile/methanol + 1% water), positive: m/z* 358.95 $[M + H]^+$.

2-Azido-*N*-(2-(3-bromobenzoyl)phenyl)acetamide 83b

To *N*-(2-(3-bromobenzoyl)phenyl)-2-chloroacetamide **82b** (6.45 g, 18.3 mmol) in dimethylformamide (21.0 mL) in a 250 mL round-bottom flask, sodium azide (1.31 g, 20.5 mmol) was added and the resulting mixture was stirred at 60 °C for 30 min. Then water (146 mL) was added dropwise while maintaining the temperature at 60 °C. Upon complete addition the reaction mixture was cooled to room temperature and allowed to stand at 4 °C overnight. The next day the precipitate was filtered off and recrystallised from ethanol (9.00 mL). The yellow precipitate was filtered off and dried *in vacuo*. Yield: 3.83 g, 78%. ^{1}H NMR (500 MHz, DMSO-d_6) δ 10.42 (s, N*H*), 7.87 – 7.82 (m, $H_{(Ar)}$), 7.78 (s, $H_{(Ar)}$), 7.69 – 7.59 (m, 3H, $H_{(Ar)}$), 7.52 – 7.41 (m, 2H, $H_{(Ar)}$), 7.37 – 7.28 (m, $H_{(Ar)}$), 3.84 (s, 2H, CH_2). ESI-MS (acetonitrile/ methanol + 1% water), positive: *m/z* 381.01 $[M + Na]^+$.

2-Azido-*N*-(2-(4-bromobenzoyl)phenyl)acetamide 83c

To *N*-(2-(4-bromobenzoyl)phenyl)-2-chloroacetamide **82c** (5.94 g, 16.8 mmol) in dimethylformamide (19.5 mL) in a 250 mL round-bottom flask, sodium azide (1.22 g, 18.8 mmol) was added and the mixture was heated to 60 °C. Then water (171 mL) was added dropwise and the resulting mixture was stirred at 60 °C for 30 min. The resulting suspension was cooled to room temperature and stored at 4 °C for 1 h. Next the product was recrystallised from ethanol (8.30 mL), cooled to room temperature and allowed to stand at 4 °C overnight. The next day the product (white flakes) was filtered off and dried *in vacuo*. Yield: 5.35 g. 89%. ^{1}H NMR (500 MHz, DMSO-d_6) δ 10.38 (s, 1H, N*H*), 7.76 – 7.70 (m, 2H, $H_{(Ar)}$), 7.66 – 7.57 (m, 4H, $H_{(Ar)}$), 7.45 – 7.41 (m, 1H, $H_{(Ar)}$), 7.31 (ddd, J = 7.8, 6.6, 2.0 Hz, 1H, $H_{(Ar)}$), 3.85 (s, 2H, CH_2). ESI-MS (acetonitrile/ methanol + 1% water), positive: *m/z* 381.13 $[M + Na]^+$.

3-Azido-4-(3-bromophenyl)quinolin-2(1*H*)-one 84a

To 2-azido-*N*-(2-(3-bromobenzoyl) phenyl)acetamide **83a** (5.16 g, 14.4 mmol) in ethanol (165 mL) at 60 °C and two drops of 40% aqueous sodium hydroxide solution were added. The resulting mixture was stirred at 60 °C for 5 h. After cooling to room temperature, the reaction mixture was allowed to stand at -20 °C overnight. The next day the product was filtered off, washed with cold ethanol (-20 °C) and dried *in vacuo*. The product was obtained as a white powder. Yield: 4.08 g, 83%. ^{1}H NMR (500 MHz, DMSO-d_6) δ 12.46 (s, 1H, N*H*), 7.70 (d, J = 8.1 Hz, 1H, $H_{(Ar)}$), 7.58 (s, 1H, $H_{(Ar)}$), 7.54 – 7.44 (m, 2H, $H_{(Ar)}$), 7.37 (dd, J = 26.7, 7.8 Hz, 2H, $H_{(Ar)}$),

7.14 (t, *J* = 7.5 Hz, 1H, $H_{(Ar)}$), 6.96 (d, *J* = 8.0 Hz, 1H, $H_{(Ar)}$). ESI-MS (acetonitrile/ methanol + 1% water), positive: *m/z* 340.96 $[M + H]^+$.

3-Azido-4-(4-bromophenyl)quinolin-2(1*H*)-one 84b
2-Azido-*N*-(2-(4-bromobenzoyl)phenyl) acetamide **83b** (5.35 g, 14.9 mmol) was dissolved in ethanol (171 mL) and heated to 60 °C. Then one drop of 40% aqueous sodium hydroxide was added. The resulting mixture was stirred at 60 °C for 6 h. After cooling to room temperature, the reaction mixture was stored at -20 °C overnight. The following day the product was filtered off, washed with cold ethanol (-20 °C) and dried *in vacuo*. The product was obtained as a white powder. Yield: 4.36 g, 86%. 1H NMR (500 MHz, DMSO-d_6) δ 12.45 (s, 1H, N*H*), 7.78 – 7.68 (m, 2H, $H_{(Ar)}$), 7.51 – 7.43 (m, 1H, $H_{(Ar)}$), 7.40 (d, *J* = 7.6 Hz, 1H, $H_{(Ar)}$), 7.34 – 7.26 (m, 2H, $H_{(Ar)}$), 7.17 – 7.09 (m, 1H, $H_{(Ar)}$), 7.02 – 6.9 7 (m, 1H, $H_{(Ar)}$). ESI-*MS (acetonitrile/ methanol + 1% water), positive: m/z* 329.12 $[M – N + H]^+$.

8- and 10-Bromo-5,7-dihydro-(6*H*)-indolo[2,3-*c*]quinolin-6-one 85a and 85c
3-Azido-4-(3- bromophenyl)quinolin-2(1*H*)-one **84a** (3.44 g, 10.0 mmol) was dissolved in hot toluene (200 mL) and refluxed for 2 h. Then the reaction mixture was cooled to room temperature and stored at 4 °C overnight. The next day the white product was filtered off and washed with toluene. The white powder was filtered off and dried *in vacuo*. The raw NMR showed two isomers in 0.7 : 1 (**85a** : **85c**) ratio. Yield: 3.09 g, 99%. Separation of this isomeric mixture has proven to be difficult due to the low solubility of the product in commonly used solvents for chromatography. However, a small fraction has been separated and NMR spectra were measured. **85a**: ^{1}H NMR (500 MHz, DMSO-d_6) δ 12.50 (s, 1H, N*H*), 11.98 (s, 1H, N*H*), 8.55 (d, *J* = 7.8 Hz, 1H, $H_{(Ar)}$), 8.47 (d, *J* = 7.6 Hz, 1H, $H_{(Ar)}$), 7.72 (d, *J* = 7.1 Hz, 1H, $H_{(Ar)}$), 7.52 – 7.48 (m, 1H, $H_{(Ar)}$), 7.47 – 7.42 (m, 1H, $H_{(Ar)}$), 7.37 – 7.32 (m, 1H, $H_{(Ar)}$), 7.27 (t, *J* = 7.8 Hz, 1H, $H_{(Ar)}$). **85c**: ^{1}H NMR (500 MHz, DMSO-d_6) δ 12.58 (s, 1H, N*H*), 11.96 (d, *J* = 19.3 Hz, 1H, N*H*), 8.67 (s, 1H, $H_{(Ar)}$), 8.45 (d, *J* = 7.7 Hz, 1H, $H_{(Ar)}$), 7.59 (d, *J* = 0.8 Hz, 2H, $H_{(Ar)}$), 7.50 (d, *J* = 7.5 Hz, 1H, $H_{(Ar)}$), 7.45 – 7.39 (m, 1H, $H_{(Ar)}$), 7.36 – 7.30 (m, 1H, $H_{(Ar)}$). ESI-MS (acetonitrile/ methanol + 1% water), positive: *m/z* 334.98 $[M + Na]^+$. X-ray diffraction quality crystals of **85a** were obtained by slow diffusion of diethyl ether into a dimethylformamide solution of the compound (c ≈ 10 mg/mL).

9-Bromo-5,7-dihydro-6*H*-indolo[2,3-*c*]quinolin-6-one 85b.
3-Azido-4-(4-bromophenyl) quinolin-2(1*H*)-one **84b** (100 mg, 0.29 mmol) was dissolved in hot toluene (7.00 mL) and refluxed for 2 h Then the solution was cooled to room temperature and stored at 4 °C for 90 min. Afterwards the product was filtered off, washed with toluene and dried *in vacuo*. The product was obtained as a white powder. Yield: 98 mg, 98%. ^{1}H NMR (500 MHz, DMSO-d_6) δ 12.51 (s, 1H, N*H*), 11.94 (s, 1H, N*H*), 8.46 (d, *J* = 8.7 Hz, 1H, $H_{(Ar)}$), 8.42 (d, *J* = 7.5 Hz, 1H, $H_{(Ar)}$), 7.78 (d, *J* = 1.7 Hz, 1H, $H_{(Ar)}$), 7.51 (d, *J* = 7.7 Hz, 1H, $H_{(Ar)}$), 7.44 (dt, *J* = 15.5, 5.0 Hz, 2H, $H_{(Ar)}$), 7.34 (t, *J* = 7.1 Hz, 1H, $H_{(Ar)}$). ESI-MS (acetonitrile/ methanol + 1% water), positive: *m/z* 649.00 $[(M)_2 + Na]^+$.

5.3 Synthesis of indolo[2,3-c]quinoline proligands

The compounds were prepared as reported by Filak et al. and Primik et al.. [92–94]

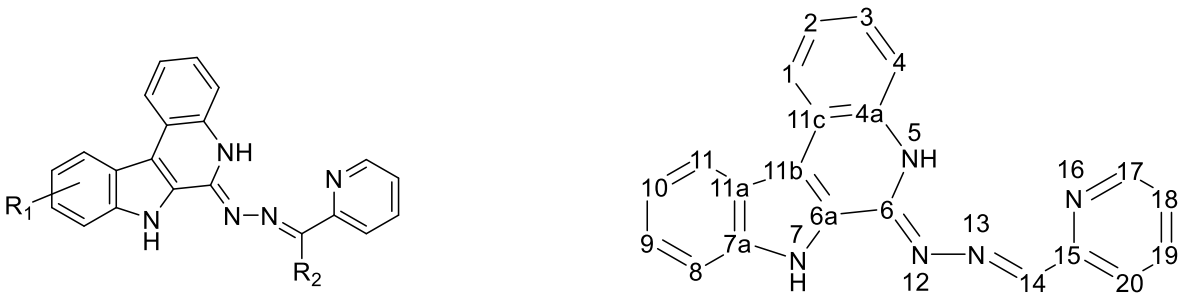

HL$^{1-4}$

R_1 = 8-Br or 9-Br
R_2 = H or CH_3

Figure 17 Structures and atom numbering of the desired ligands, for NMR resonance assignement.

Scheme 19 shows the synthetic pathway. 2-Formylpyridine and 2-acetylpyridine were used to obtain two sets of Schiff bases.

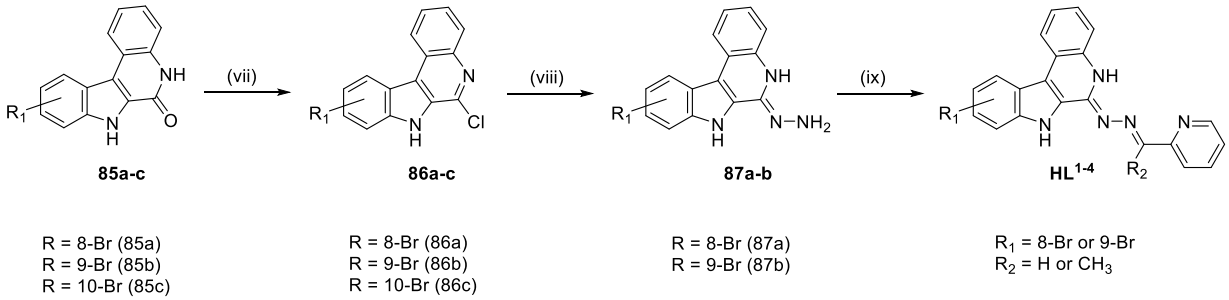

85a-c R = 8-Br (85a), R = 9-Br (85b), R = 10-Br (85c)

86a-c R = 8-Br (86a), R = 9-Br (86b), R = 10-Br (86c)

87a-b R = 8-Br (87a), R = 9-Br (87b)

HL$^{1-4}$ R_1 = 8-Br or 9-Br, R_2 = H or CH_3

Scheme 19 Synthetic pathway for the desired ligands. (vii) Phosphorus oxychloride, 130 °C, reflux, overnight. (viii) Hydrazine hydrate, 131 °C, reflux, overnight. (ix) Ethanol, 2-formyl- or 2-acetylpyridine, 85 °C, overnight.

8- and 10-bromo-6-chloro-7*H*-indolo[2,3-*c*]quinoline 86a and 86c

An isomeric mixture of 8- and 10-bromo-5,7-dihydro-6*H*-indolo[2,3-*c*]quinolin-6-one (**85a** : **85c**, 0.7 : 1) (2.29 g, 7.30 mmol) and phosphorus oxychloride (35 mL) were mixed in a 100 mL nitrogen flask under argon atmosphere. The mixture was refluxed overnight. The next day the solution was cooled to room temperature and poured on ice water (600 mL). Then pH adjusted to 12, using sodium hydroxide. The mixture was extracted with dichloromethane (3 × 300 mL). The organic phase was washed with brine (1 x 300 mL) and dried over magnesium sulfate. The solvent was removed under reduced pressure and the crude product was purified on silica using a mixture of hexane/ethyl acetate (first 90 : 10, then 80 : 20, then 70 : 30) as eluent. The product was obtained as a white powder. Yield: 0.98 g, 40% **86a**; 1.27 g 52% **86c**. **86a** ^{1}H NMR (500 MHz, DMSO-d_6) δ 12.35 (s, 1H, N*H*), 8.86 (dd, *J* = 8.2, 1.4 Hz, 1H, $H_{(Ar)}$), 8.77 (dd, *J* = 8.2, 1.0 Hz, 1H, $H_{(Ar)}$), 8.13 (dd, *J* = 8.2, 1.3 Hz, 1H, $H_{(Ar)}$), 7.90 (dd, *J* = 7.7, 0.9 Hz, 1H, $H_{(Ar)}$), 7.82 – 7.79 (m, 1H, $H_{(Ar)}$), 8 7.76 – 7.73 (m, 1H, $H_{(Ar)}$), 7.39 (t, *J* = 7.9 Hz, 1H, $H_{(Ar)}$). **86c** ^{1}H NMR (500 MHz, DMSO-d_6) δ 12.67 (s, 1H, N*H*), 8.90 (d, *J* = 1.7 Hz, 1H, $H_{(Ar)}$), 8.85 (dd, *J* = 8.2, 1.4 Hz, 1H, $H_{(Ar)}$), 8.11 (dd, *J* = 8.3, 1.3 Hz, 1H, $H_{(Ar)}$), 7.83 – 7.69 (m, 4H, $H_{(Ar)}$). ESI-MS (acetonitrile/ methanol + 1% water), positive: *m/z* 333.06 $[M + H]^+$.

9-Bromo-6-chloro-7*H*-indolo[2,3-*c*]quinoline 86b

9-Bromo-5,7-dihydro-6*H*-indolo[2,3- *c*]quinoline-6-one **85b** (1.00 g, 3.20 mmol) was placed in a 50 mL round bottom flask and dissolved in phosphorus oxychloride (15.5 mL, 169 mmol) under argon atmosphere. The solution was refluxed at 130 °C overnight. The next day the solution was cooled to room temperature and then poured on 270 mL of ice water. The pH was adjusted to 12, using sodium hydroxide. The mixture was extracted with dichloromethane (3 x 100 mL). The organic layers were combined, washed with brine (1 x 300 mL), and dried over magnesium sulfate. The solvent was removed under reduced pressure. The product was

obtained as a white powder. Yield: 770 mg, 73%. ^{1}H NMR (500 MHz, DMSO-*d*$_6$) δ 12.62 (s, 1H, N*H*), 8.81 (d, *J* = 7.5 Hz, 1H, *H*$_{(Ar)}$), 8.69 (d, *J* = 8.6 Hz, 1H, *H*$_{(Ar)}$), 8.17 – 8.08 (m, 1H, *H*$_{(Ar)}$), 7.93 (d, *J* = 1.7 Hz, 1H, *H*$_{(Ar)}$), 7.84 – 7.78 (m, 1H, *H*$_{(Ar)}$), 7.76 – 7.70 (m, 1H, *H*$_{(Ar)}$), 7.57 (dd, *J* = 8.6, 1.8 Hz, 1H).

8-bromo-6-hydrazineyl-7*H*-indolo[2,3-*c*]quinoline 87a

8-bromo-6-chloro-7*H*-indolo[2,3-*c*]quinoline **86a** (160 mg, 0.47 mmol) was mixed with hydrazine monohydrate (8.00 mL) in a 50 mL nitrogen flask under argon atmosphere. The reaction mixture was refluxed overnight. The next day it was cooled to room temperature and stored at 4 °C overnight. The following day the product was filtered off, washed with water and dried *in vacuo*. The product was obtained as a light-yellow powder. Yield: 150 mg, 98%. ^{1}H NMR (500 MHz, DMSO-*d6*) δ 11.56 (s, 1H, N*H*), 8.58 (s, 3H, *H*$_{(Ar)}$), 7.77 (s, 2H, *H*$_{(Ar)}$), 7.58 – 7.16 (m, 3H, N*H*, *H*$_{(Ar)}$), 4.65 (s, 2H, N*H*$_2$). ESI-MS (acetonitrile/methanol + 1% water), positive: *m/z* 327.14 $[M + H]^+$.

9-bromo-6-hydrazineyl-7*H*-indolo[2,3-*c*]quinoline 87b

9-Bromo-5,7-dihydro-6*H*-indolo[2,3-*c*]quinolin-6-one **86b** (300 mg, 0.91 mmol) was mixed with hydrazine hydrate (11.6 mL) and refluxed overnight. The next day, the mixture was cooled to room temperature and stored at 4 °C for 24 hours. Then the product was filtered off, washed with water and dried *in vacuo*. The product was obtained as a light-yellow powder. Yield: 290 mg, 99%. ^{1}H NMR (500 MHz, DMSO) δ 11.57 (s, 1H, N*H*), 8.55 (dd, *J* = 32.1, 7.4 Hz, 3H, N*H*, *H*$_{(Ar)}$), 7.87 – 7.64 (m, 2H, *H*$_{(Ar)}$), 7.51 – 7.44 (m, 1H, *H*$_{(Ar)}$), 7.42 – 7.21 (m, 2H, *H*$_{(Ar)}$), 4.65 (s, 2H, N*H*). ESI-MS (acetonitrile/methanol + 1% water), positive: *m/z* 329.13 $[M + H]^+$.

HL^1·0.1H$_2$O

8-Bromo-6-hydrazineyl-7*H*-indolo[2,3-*c*]quinoline **87a** (330 mg, 1.01 mmol) was suspended in ethanol (7.00 mL) in a 25 mL Schlenk tube. The mixture was degassed by bubbling a stream of argon through the solvent, for 10 min. 2-Formylpyridine (140 µL, 1.46 mmol) was then added and the reaction mixture was stirred at 86 °C overnight. The next day the reaction mixture was cooled to room temperature and stored at +4 °C overnight. The following day the product was filtered off, washed with cold ethanol and dried *in vacuo*. Yield 320 mg, 93%. Anal. Calcd for $C_{21}H_{14}BrN_5 \cdot 0.1H_2O$ (M 418.07 g mol^{-1}): C, 60.33; H, 3.42; N, 16.75. Found: C, 60.19; H, 3.32; N, 16.51. ^{1}H NMR (600 MHz, DMF-d$_7$) δ 12.13 (s, broad, 1H, *H*^{7}), 11.65 (s, broad, 1H, *H*^{12}), 8.83 (d, *J* = 4.1 Hz, 1H, *H*^{17}), 8.76 (d, *J* = 8.0 Hz, 1H, *H*^{11}), 8.72 (d, *J* = 6.5 Hz, 1H, *H*^{1}), 8.44 (s, 1H, *H*^{14}), 8.06 – 8.03 (m, 1H, *H*^{19} (overlapped DMF peak)), 8.01 – 7.98 (m, 1H, *H*^{20} (overlapped DMF peak)), 7.92 – 7.86 (m, 2H, *H*9 , *H*^{4}), 7.60 (t, *J* = 7.4 Hz, 1H, *H*^{3}), 7.57 – 7.52 (m,1H, *H*^{2}), 7.47 – 7.42 (m, 2H, *H*^{18}, *H*^{10}). ^{13}C NMR (151 MHz, DMF) δ 154.73 (Cq, *C*^{15}), 153.92 (CH, *C*^{14}), 151.41 (CH, *C*^{17}), 147.96 (Cq, *C*^{6}), 138.34 (Cq, *C*^{7a}), 138.10 (CH, *C*^{19}), 136.71 (Cq, *C*^{4a}), 129.87 (CH, *C*^{9}), 128.97 (Cq, *C*^{6a}), 127.47 (CH, *C*^{3}), 124.84 (CH, *C*^{2}), 124.57 (CH, *C*^{18}), 124.48 (Cq, *C*^{11a}), 123.99 (CH, *C*^{1}), 123.24 (CH, *C*^{11}), 123.17 (CH, *C*^{11}), 122.34 (CH, *C*^{20}), 119.70 (Cq, *C*^{11c}), 118.78 (Cq, *C*^{11b}), 117.56 (CH, *C*^{4}), 106.40 (Cq, *C*^{8}). ESI-MS (acetonitrile/methanol + 1% water), positive: *m/z* 418.04 $[M + H]^+$.

HL^2·0.5H$_2$O

8-Bromo-6-hydrazineyl-7*H*-indolo[2,3-*c*]quinoline **87a** (225 mg, 0.69 mmol) was suspended in ethanol (5.00 mL) in a 25 mL Schlenk tube. The mixture was degassed by bubbling a stream of argon through the solution for 10 min. 2-Acetylpyridine (85 µL, 0.76 mmol) was added and the resulting mixture was stirred at 86 °C overnight. Then it was cooled to room temperature and stored at 4 °C overnight. The next day the yellow precipitate was filtered off, washed with cold ethanol and dried *in vacuo*. Yield: 256 mg, 86%. Anal. Calcd for $C_{22}H_{16}BrN_5 \cdot 0.5H_2O$ (M 438.06 g mol^{-1}): C, 60.14; H, 3.90; N, 15.94. Found: C, 59.90; H, 3.78; N, 15.58. ^{1}H NMR

(600 MHz, DMF-d_7) δ 11.83 (s, broad, 1H, H^7), 11.07 (s, 1H, H^5), 8.69 – 8.62 (m, 1H, H^{17}), 8.60 (d, J = 8.0 Hz, 1H, H^{20}), 8.55 (d, J = 8.0 Hz, 1H, H^{11}), 8.45 (d, J = 7.8 Hz, 1H, H^1), 7.92 (t, J = 7.1 Hz, 1H, H^4), 7.87 – 7.82 (m, 1H, H^{19}), 7.73 (d, J = 7.6 Hz, 1H, H^9), 7.43 – 7.37 (m, 2H, H3 , H^{18}), 7.35 – 7.28 (m, 2H, H2 , H^{10}), 2.70 – 2.66 (m, 3H, H^{21}). ^{13}C NMR (151 MHz, DMF-d_7) δ 159.57, (Cq, C^{14},) 156.97 (Cq, C^{15}), 148.70 (CH, C^{17}), 145.19 (Cq, C^6), 138.09 (Cq, C^{7a}), 137.12 (CH, C^{19}), 135.95 (Cq, C^{4a}), 129.01 (Cq, C^{6a}), 128.38 (CH, C^9), 126.62 (CH, C^3), 125.02 (Cq, C^{11a}), 123.42 (CH, C^{18}), 123.12 (CH,C^1), 122.19 (CH, C^{10}), 122.08 (CH, C^2), 121.28 (CH, C^{20}, C^{11} (overlapped siganls)), 118.68 (Cq, C^{11c}), 117.12 (Cq, C^{11b}), 116.54 (CH, C^4), 105.32 (Cq, C^8), 12.91, (CH3, C^{21}). ESI-MS (acetonitrile/methanol + 1% water), positive: *m/z* 430.18 $[M + H]^+$.

$HL^3 \cdot 0.2H_2O$

9-Bromo-6-hydrazine-yl-7*H*-indolo[2,3-*c*]quinoline **87b** (290 mg, 1.01 mmol) was suspended in ethanol (6.10 mL) in a 25 mL Schlenk tube. The resulting mixture was degassed by bubbling a stream of argon through the suspension for 10 min. 2-Formylpyridine (120 µL, 1.72 mmol) was then added and the reaction mixture was stirred at 86°C overnight. The next day the reaction mixture was cooled to room temperature and stored at +4 °C overnight. The following day the product was filtered off, washed with cold ethanol and dried *in vacuo*. Yield: 350 mg, 96%. Anal. Calcd for $C_{21}H_{14}BrN_5 \cdot 0.2H_2O$ (M 419.88 g mol^{-1}): C, 60.07; H, 3.46; N, 16.68. Found: C, 60.11; H, 3.33; N, 16.43. ^{1}H NMR (600 MHz, DMSO-d_6) δ 12.31 (s, 1H, H^7), 11.10 (s, 1H, H^5), 8.64 – 8.59 (m, 2H, H17, H^{20}), 8.53 (s, 1H, H^{14}), 8.39 (d, J = 8.5 Hz, 1H, H^{11}), 8.34 (d, J = 7.7 Hz, 1H, H^1), 7.95 – 7.88 (m, 2H, H^4, H^{19}), 7.80 (s, 1H, H^8), 7.44 – 7.37 (m, 3H, H^{18}, H^3, H^{10}), 7.30 (t, J = 7.3 Hz, 1H, H^2). ^{13}C NMR (151 MHz, DMSO-d_6) δ 154.45 (Cq, C^{15}), 152.26 (CH, C^{14}), 149.29 (CH, C^{17}), 146.40 (Cq, C^6), 140.05 (Cq, C^{7a}), 136.26 (CH, C^{19}), 134.88 (Cq, C^{4a}), 127.28 (Cq, C^{6a}), 126.34 (CH, C^3), 123.79 (CH, C^{11}), 123.52 (CH, C^{18}), 123.48 (CH, C^{10}), 122.94 (CH, C^1), 122.29 (CH, C^2), 121.32 (Cq, C^{11a}), 121.21 (CH, C^{20}), 118.27 (Cq, C^{11c}), 118.13 (Cq, C^9), 116.57 11 (CH, C^4), 116.10 (Cq, C^{11b}), 115.30 (CH, C^8). ESI-MS (acetonitrile/methanol + 1% water), positive: *m/z* 416.06 $[M + H]^+$.

$HL^4 \cdot 0.5H_2O$

9-Bromo-6-hydrazin-yl-7*H*-indolo[2,3-*c*]quinoline **87b** (300 mg, 0.92 mmol) was suspended in ethanol (11.5 mL) in a 25 mL Schlenk tube. The resulting mixture was degassed by bubbling an argon stream through the solvent for 10 min. 2-Acetylpyridine (110 µL, 1.18 mmol) was then added and the reaction mixture was stirred overnight at 86°C. The next day it was cooled to room temperature and stored at +4 °C overnight. The following day the product was filtered off, washed with cold ethanol and dried *in vacuo*. Yield: 320 mg, 80%. Anal. Calcd for $C_{22}H_{16}BrN_5 \cdot 0.5H_2O$ (M 439.31 g mol^{-1}): C, 60.15; H, 3.90; N, 15.94. Found: C, 60.50; H, 3.68; N, 15.82. ^{1}H NMR (600 MHz, DMSO-d_6) δ 12.06 (s, 1H, H^7), 10.79 (s, 1H, H^5), 8.72 (d, J = 8.0 Hz, 1H, H^{20}), 8.63 (d, J = 4.6 Hz, 1H, H^{17}), 8.37 (d, J = 8.6 Hz, 1H, H^{11}), 8.31 (d, J = 7.8 Hz, 1H, H^1), 7.90 – 7.82 (m, 3H, H4, H^{19}, H^8), 7.44 – 7.34 (m, 3H, H^{18}, H^{10}, H^3), 7.26 (t, J = 7.5 Hz, 1H, H^2), 2.68 (s, 3H, H^{21}). 13C NMR (151 MHz, DMSO-d_6) δ 158.64 (Cq, C^{14}), 156.34 (Cq, C^{15}), 148.47 (CH, C^{17}), 144.49 (Cq, C^6), 139.93 (Cq, C^{7a}), 135.89 (CH, C^{19}), 135.05 (Cq, C^{4a}), 128.04 (Cq, C^{6a}), 126.19 (CH, C^3), 123.47 (CH, C^{18}), 123.46 (CH, C^{10}), 123.36 (CH, C^{11}), 122.84 (CH, C^1), 122.01 (CH, C^2), 121.53 (Cq, C^{11a}), 121.33 (CH, C^{20}), 118.22 (Cq, C^{11c}), 117.87 (Cq, C^9), 116.55 (CH, C^4), 115.43 (Cq, C^{11b}), 115.28 (CH, C^8), 13.21 (CH3, C^{21}). ESI-MS (acetonitrile/methanol + 1% water), positive: *m/z* 430.1 $[M + H]^+$.

5.4 Synthesis of metal complexes

The structures of the newly designed complexes are shown below (see Figure 18).

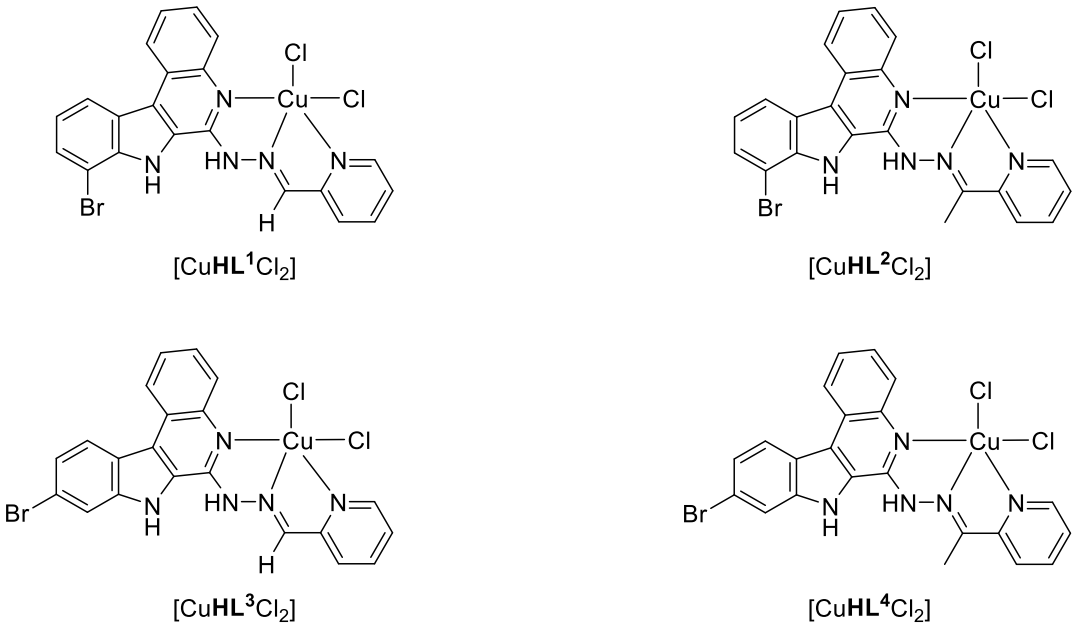

Figure 18 Structures of four newly prepared copper(II) complexes.

The reaction of the proligands with copper(II) dichloride dihydrate lead to the desired complexes of the $[CuHLCl_2]$ type (see Scheme 20). For this synthesis the method of Primik et al. was utilised.[95]

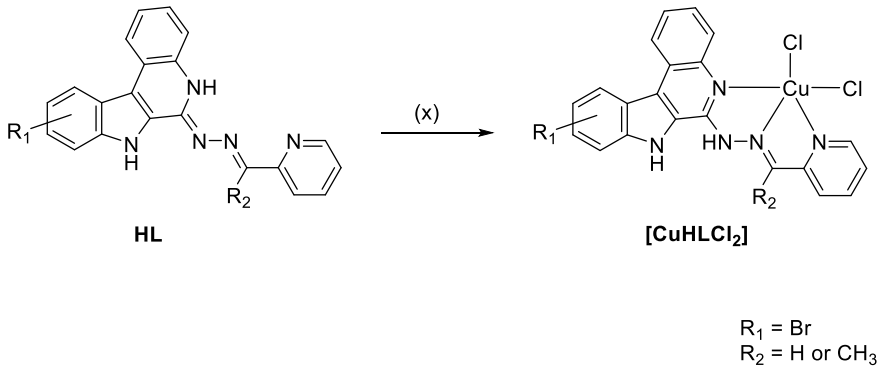

Scheme 20 Synthetic pathway for the desired copper(II) complexes. (x) Isopropyl alcohol or methanol or dimethylformamide, copper(II) chloride dihydrate, reflux, 15 min. (xi) Isopropyl alcohol or methanol or dimethylformamide, triethylamine, copper(II) chloride dihydrate, reflux or 80 °C, 15 min.

$[CuHL^1Cl_2]\cdot H_2O$

To **HL^1** (150 mg, 0.36 mmol) in boiling methanol (35.0 mL), copper(II) chloride dihydrate (70 mg, 0.43 mmol) in methanol (1 mL) was added. The colour of the solution changed from yellow to dark-red and the mixture was refluxed for 15 min. Then the mixture was cooled to room temperature and stored at +4 °C overnight. The next day, the product was filtered off and dried *in vacuo*. Yield 180 mg, 90%. Anal. Calcd for $C_{21}H_{14}BrCl_2CuN_5\cdot H_2O$ (M 568.74 g mol^{-1}): C, 44.35; H, 2.84; N, 12.31. Found: C, 44.51; H, 2.60; N, 12.07. ESI-MS (acetonitrile/methanol + 1% water), positive: *m/z* 514.94 $[M - Cl]^+$, 479.15 $[M - Cl - HCl]^+$.

$[CuHL^2Cl_2]\cdot MeOH$

To **HL^2** (130 mg, 0.36 mmol) in boiling methanol (30.0 mL), copper(II) chloride dihydrate (60 mg; 0.37 mmol) in methanol (1.00 mL) was added. The colour changed from yellow to dark-red, and the mixture was refluxed for 15 min. Then the mixture was cooled to room temperature and stored at 4 °C overnight. The next day, the product was filtered off and dried in vacuo for 3 days. The product was obtained as dark red powder. Yield 190 mg, 92%. Anal. Calcd for $C_{22}H_{16}BrCl_2CuN_5\cdot CH_3OH$ (M 596.79 g mol^{-1}): C, 46.29; H, 3.38; N, 11.74. Found: C,

46.39; H, 3.40; N, 11.50. ESI-MS (acetonitrile/methanol + 1% water), positive: *m/z* 493.11 $[M - Cl - HCl]^+$.

$[CuHL^3Cl_2]$
To **HL^3** (150 mg, 0.36 mmol) in boiling methanol (60 mL), copper(II) chloride dihydrate (70 mg, 0.43 mmol) in methanol (1 mL) was addedThe colour changed from yellow to dark-red, and the mixture was refluxed for 25 min. Then the mixture was cooled to room temperature and stored at 4 °C overnight. The next day, the product was filtered off and dried *in vacuo*. Yield 190 mg, 93%. Anal. Calcd for $C_{21}H_{14}BrCl_2CuN_5$ (M 550.72 g mol^{-1}): C, 45.80; H, 2.56; N, 12.72. Found: C, 45.60; H, 2.51; N, 12.45. ESI-*MS (acetonitrile/methanol + 1% water), positive: m/z* 515.06 [M – Cl], 479.10 $[M - Cl - HCl]^+$.

$[CuHL^4Cl_2]\cdot 0.8H_2O$
To **HL^4** (150 mg, 0.35 mmol) in boiling methanol (60 mL), copper(II) chloride dihydrate (70 mg, 0.43 mmol) in methanol (1 mL) was added. The colour changed from yellow to dark-red, and the mixture was refluxed for 15 min. Then the mixture was cooled to room temperature and stored at +4 °C overnight. The next day, the product was filtered off, washed with cold methanol and dried *in vacuo*. Yield 190 mg, 94%. Anal. Calcd for $C_{22}H_{16}BrCl_2CuN_5\cdot 0.8H_2O$ (M 579.16 g mol^{-1}): C, 45.62; H, 3.06; N, 12.09. Found: C, 45.91; H, 2.72; N, 11.82. ESI-MS (acetonitrile/methanol + 1% water), positive: *m/z* 542.11 [M – Cl], 493.15 $[M - Cl - HCl]^+$.

6.0 Results and Discussion

The synthesis of the indolo[2,3-*c*]quinolinone backbones was performed starting from the respective aminobenzophenones **81a - c** using a synthetic path developed by Petersen and Lakowitz.[91] The final ligands and complexes were prepared by following previously reported protocols.[95] Since 2- and 3-bromo-aminobenzophenone (**81a** and **b**) are not commercially available they were synthesised in two steps by known methods.[96,97]. The aminobenzophenones **81a – b** were converted with chloroacetyl chloride to give acetylated compounds **82a – c** in 58 – 91% yields. In the next step, the chloro substituent was replaced by an azido functional group giving **83a – c** in 80 – 89% yields. Base catalysed cyclisation led to azidophenylquinolinones **84a – b** in 83 – 86% yields. The presence of a bromo-substituent in position 3 and 4 slows the reaction speed down. Therefore, prolongation of the reaction time from 1 to 6 h for a complete conversion is required. The desired cyclisation of **83a** did not occur. Attempts to prolong reaction time, enhance temperature or ad more base only led to undesired side reactions. Most likely the bulky bromo substituent in ortho position prevents nucleophilic attack at the carbonyl carbon, preventing the reaction. Therefore desired 11-bromo-5,7-dihydro-6*H*-indolo[2,3-*c*]quinolin-6-one was not accessible by this synthetic path. However, the synthesis of precursors is still described herein as these are new compounds that might be useful for other syntheses. The obtained azidophenylquinolinones **84a – c** are not stable at high temperature and can be converted into desired indolo[2,3-*c*]quinolinones in a second cyclisation step, accompanied by loss of nitrogen gas, simply by refluxing them in toluene, giving indoloquinolines **85b**, as well as **85a** and **85c** (as isomeric mixture) in excellent yields (98 – 99%). 3-Azido-4-(3-bromophenyl)quinolin2(1*H*)-one, 6b gave rise to two isomers (8- and 10-bromo-5,7-dihydro-(6*H*)-indolo[2,3-*c*]quinolin-6-one, **85a** and **85c**) in a ratio of approximately 0.7 : 1 respectively. This is due to the rotation of the bromo substituted phenyl ring in **84a**. The isomers proved to be difficult to separate, due to their low solubility in solvents commonly used in column chromatography. However, separation was possible after the next step in which the indolo[2,3-c]quinolinones **85a – c** were reacted with phosphorous oxychloride to give 6-chloro substituded indolo[2,3- *c*]quinolines **86a – c** in good yields (40 - 73%). Consequently 6-chloro derivatives **86a – c** were reacted with hydrazine monohydrate to give 6-hydrazin-yl derivatives 9a – d in excellent yields (95 – 99%). Finally, the hydrazine-yl

derivatives **87a – b** were reacted with 2-formyl- or 2-acetylpyridine in a Schiff base reaction, giving proligands **HL $^{1-4}$** in 93, 86, 96, and 80% yields, respectively. In the NMR spectra of proligands **HL$^{1-4}$** two sets of signals were observed. However, the signals were only assigned for the predominant species, containing an exocyclic double bond in each case, low signal intensity combined with signal overlapping made signal assignment for the minor species impossible. The ratios between major and minor species in DMSO-d_6 are approximately 1 : 0.25 and 1 : 0.10 for **HL^3** and **HL^4**, as well as 1 : 0.5, 1 : 1 for **HL^1** , **HL^2** in DMF-d_7.

The proligands **HL$^{1-4}$** were treated with copper(II) chloride in isopropyl alcohol, methanol or DMF to give complexes **[CuHL$^{1-4}$Cl$_2$]** in 90, 92, 93 and 94% yields respectively. The use of different solvents was necessary due to differences in the solubility between the different isomers. These complexes adopt a distorted square-pyramidal geometry with the ligands acting as tridentate ones, binding via three *N*-atoms. The remaining two coordination sites are occupied by chlorido ligands, leading to an overall charge of zero.

It is worth noting, that apart from the separation of **86a** and **86c** no chromatographic purification was needed to obtain the reported compounds. This means that in theory this synthesis could be upscaled to an industrial scale.

7.0 Conclusion

A new class of potential metal-based antitumour drugs were synthesised and characterised. The primary organic scaffold was synthesised in six steps and the introduction of the metal binding sites via three additional steps. The Schiff base reactions with 2-formylpyridine and 2-acetylpyridine yielded proligands **HL$^{1-4}$**. The synthesis of 11-bromo-5,7-dihydro-(6*H*)-indolo[2,3-*c*]quinolin-6-one did not work because the bromo substitutent in the ortho position may hinder a nucleophilic attack at the carbonyl carbon. Another strategy is needed here to achieve the desired proligand.

Four copper(II) complexes of the type **[CuHL$^{1-4}$Cl$_2$]** were synthesised and isolated as brown - dark red powders. Crystals of X-ray diffraction quality for the two compounds prepared were obtained by diethyl ether vapour diffusion into dimethylformamide solutions of the copper(II) complexes.

References

(1) Bray, F.; Ferlay, J.; Soerjomataram, I.; Siegel, R. L.; Torre, L. A.; Jemal, A. Global Cancer Statistics 2018: GLOBOCAN Estimates of Incidence and Mortality Worldwide for 36 Cancers in 185 Countries. *CA: A Cancer Journal for Clinicians* **2018**, *68* (6), 394–424. https://doi.org/10.3322/caac.21492.

(2) Roser, M.; Ritchie, H. Cancer https://ourworldindata.org/cancer (accessed Mar 21, 2020).

(3) Griego, F. *Cancer Prevention and Control in the Context of an Integrated Approach*; 2017.

(4) Prammer-Waldhör, M.; Hackl, M.; Ihle, P.; Klimont, J.; Leitner, B. *Jahrbuch Der Gesundheitsstatistik*; STATISTIK AUSTRIA, 2018.

(5) Hackl, M. M.; Ihle, P. *Krebserkrankungen in Österrreich 2018*; 2018.

(6) Wild, C. P.; Weiderpass, E.; Stewart, B. W. *Cancer Research for Cancer Prevention World Cancer Report*; 2020.

(7) Belikov, A. v. The Number of Key Carcinogenic Events Can Be Predicted from Cancer Incidence. *Scientific Reports* **2017**, *7* (1), 12170. https://doi.org/10.1038/s41598-017-12448-7.

(8) Hanahan, D.; Weinberg, R. A. Hallmarks of Cancer: The next Generation. *Cell*. March 4, 2011, pp 646–674. https://doi.org/10.1016/j.cell.2011.02.013.

(9) Laplane, L.; Duluc, D.; Bikfalvi, A.; Larmonier, N.; Pradeu, T. Beyond the Tumour Microenvironment. *International Journal of Cancer* **2019**, *145* (10), 2611–2618. https://doi.org/10.1002/ijc.32343.

(10) Ajit Kumar Saxena, G. C. Targetting Cdks in Cancer: An Overview and New Insights. *Journal of Cancer Science & Therapy* **2014**, *6* (12). https://doi.org/10.4172/1948-5956.1000313.

(11) Milanovic, M.; Fan, D. N. Y.; Belenki, D.; Däbritz, J. H. M.; Zhao, Z.; Yu, Y.; Dörr, J. R.; Dimitrova, L.; Lenze, D.; Monteiro Barbosa, I. A.; Mendoza-Parra, M. A.; Kanashova, T.; Metzner, M.; Pardon, K.; Reimann, M.; Trumpp, A.; Dörken, B.; Zuber, J.; Gronemeyer, H.; Hummel, M.; Dittmar, G.; Lee, S.; Schmitt, C. A. Senescence-Associated Reprogramming Promotes Cancer Stemness. *Nature* **2018**, *553* (7686), 96–100. https://doi.org/10.1038/nature25167.

(12) Fitzgerald, L. The Roles of P53, BRCA1, and PTEN in Hereditary Cancers http://blogs.shu.edu/cancer/2016/05/18/the-roles-of-p53-brca1-and-pten-in-hereditary-cancers-lauren-fitzgerald-contributor/ (accessed Mar 30, 2020).

(13) Muller, P. A. J.; Vousden, K. H. P53 Mutations in Cancer. *Nature Cell Biology* **2013**, *15* (1), 2–8. https://doi.org/10.1038/ncb2641.

(14) de Lange, T. Shelterin: The Protein Complex That Shapes and Safeguards Human Telomeres. *Genes and Development*. September 15, 2005, pp 2100–2110. https://doi.org/10.1101/gad.1346005.

(15) Portt, L.; Norman, G.; Clapp, C.; Greenwood, M.; Greenwood, M. T. Anti-Apoptosis and Cell Survival: A Review. *Biochimica et Biophysica Acta (BBA) - Molecular Cell Research* **2011**, *1813* (1), 238–259. https://doi.org/https://doi.org/10.1016/j.bbamcr.2010.10.010.

(16) Fulda, S. Tumor Resistance to Apoptosis. *International Journal of Cancer* **2009**, *124* (3), 511–515. https://doi.org/10.1002/ijc.24064.

(17) Greenberg, R. A. *Telomeres, Crisis and Cancer*; 2005; Vol. 5.

(18) Leão, R.; Apolónio, J. D.; Lee, D.; Figueiredo, A.; Tabori, U.; Castelo-Branco, P. Mechanisms of Human Telomerase Reverse Transcriptase (HTERT) Regulation: Clinical Impacts in Cancer. *Journal of Biomedical Science* **2018**, *25* (1), 22. https://doi.org/10.1186/s12929-018-0422-8.

(19) Cesare, A. J.; Reddel, R. R. Alternative Lengthening of Telomeres in Mammalian Cells. In: Madame Curie Bioscience Database https://www.ncbi.nlm.nih.gov/books/NBK6486/ (accessed Apr 6, 2020).

(20) Pagès, G.; Pouysségur, J. Transcriptional Regulation of the Vascular Endothelial Growth Factor Gene–a Concert of Activating Factors*. *Cardiovascular Research* **2005**, *65* (3), 564–573. https://doi.org/10.1016/j.cardiores.2004.09.032.

(21) Beck, B.; Driessens, G.; Goossens, S.; Youssef, K. K.; Kuchnio, A.; Caauwe, A.; Sotiropoulou, P. A.; Loges, S.; Lapouge, G.; Candi, A.; Mascre, G.; Drogat, B.; Dekoninck, S.; Haigh, J. J.; Carmeliet, P.; Blanpain, C. A Vascular Niche and a VEGF–Nrp1 Loop Regulate the Initiation and Stemness of Skin Tumours. *Nature* **2011**, *478* (7369), 399–403. https://doi.org/10.1038/nature10525.

(22) Gonzalez-Perez, R. R.; Rueda, B. R. *Tumor Angiogenesis*, 1st ed.; CRC Press.

(23) Lee, S. Y.; Jeong, E. K.; Ju, M. K.; Jeon, H. M.; Kim, M. Y.; Kim, C. H.; Park, H. G.; Han, S. I.; Kang, H. S. Induction of Metastasis, Cancer Stem Cell Phenotype, and Oncogenic Metabolism in Cancer Cells by Ionizing Radiation. *Molecular Cancer*. BioMed Central Ltd. January 30, 2017. https://doi.org/10.1186/s12943-016-0577-4.

(24) Craene, B. de; Berx, G. Regulatory Networks Defining EMT during Cancer Initiation and Progression. *Nature Reviews Cancer* **2013**, *13* (2), 97–110. https://doi.org/10.1038/nrc3447.

(25) Kalluri, R. Basement Membranes: Structure, Assembly and Role in Tumour Angiogenesis. *Nature Reviews Cancer* **2003**, *3* (6), 422–433. https://doi.org/10.1038/nrc1094.

(26) Chaffer, C. L.; Weinberg, R. A. A Perspective on Cancer Cell Metastasis. *Science* **2011**, *331* (6024), 1559. https://doi.org/10.1126/science.1203543.

(27) Sugihara, E.; Saya, H. Complexity of Cancer Stem Cells. *International Journal of Cancer* **2013**, *132* (6), 1249–1259. https://doi.org/10.1002/ijc.27961.

(28) Fridman, W. H.; Zitvogel, L.; Sautès–Fridman, C.; Kroemer, G. The Immune Contexture in Cancer Prognosis and Treatment. *Nature Reviews Clinical Oncology* **2017**, *14* (12), 717–734. https://doi.org/10.1038/nrclinonc.2017.101.

(29) Virchow, R. Reizung Und Reizbarkeit. *Archiv für pathologische Anatomie und Physiologie und für klinische Medicin* **1858**, *14* (1), 1–63. https://doi.org/10.1007/BF01877355.

(30) Colotta, F.; Allavena, P.; Sica, A.; Garlanda, C.; Mantovani, A. Cancer-Related Inflammation, the Seventh Hallmark of Cancer: Links to Genetic Instability. *Carcinogenesis*. 2009, pp 1073–1081. https://doi.org/10.1093/carcin/bgp127.

(31) Shanmugam, M. K.; Lee, J. H.; Chai, E. Z. P.; Kanchi, M. M.; Kar, S.; Arfuso, F.; Dharmarajan, A.; Kumar, A. P.; Ramar, P. S.; Looi, C. Y.; Mustafa, M. R.; Tergaonkar, V.; Bishayee, A.; Ahn, K. S.;

Sethi, G. Cancer Prevention and Therapy through the Modulation of Transcription Factors by Bioactive Natural Compounds. *Seminars in Cancer Biology* **2016**, *40–41*, 35–47. https://doi.org/https://doi.org/10.1016/j.semcancer.2016.03.005.

(32) Vinay, D. S.; Ryan, E. P.; Pawelec, G.; Talib, W. H.; Stagg, J.; Elkord, E.; Lichtor, T.; Decker, W. K.; Whelan, R. L.; Kumara, H. M. C. S.; Signori, E.; Honoki, K.; Georgakilas, A. G.; Amin, A.; Helferich, W. G.; Boosani, C. S.; Guha, G.; Ciriolo, M. R.; Chen, S.; Mohammed, S. I.; Azmi, A. S.; Keith, W. N.; Bilsland, A.; Bhakta, D.; Halicka, D.; Fujii, H.; Aquilano, K.; Ashraf, S. S.; Nowsheen, S.; Yang, X.; Choi, B. K.; Kwon, B. S. Immune Evasion in Cancer: Mechanistic Basis and Therapeutic Strategies. *Seminars in Cancer Biology* **2015**, *35*, S185–S198. https://doi.org/https://doi.org/10.1016/j.semcancer.2015.03.004.

(33) Dunn, G. P.; Old, L. J.; Schreiber, R. D. The Three Es of Cancer Immunoediting. *Annual Review of Immunology* **2004**, *22* (1), 329–360. https://doi.org/10.1146/annurev.immunol.22.012703.104803.

(34) Gubin, M. M.; Artyomov, M. N.; Mardis, E. R.; Schreiber, R. D. Tumor Neoantigens: Building a Framework for Personalized Cancer Immunotherapy. *Journal of Clinical Investigation*. American Society for Clinical Investigation September 1, 2015, pp 3413–3421. https://doi.org/10.1172/JCI80008.

(35) Teng, M. W. L.; Swann, J. B.; Koebel, C. M.; Schreiber, R. D.; Smyth, M. J. Immune-Mediated Dormancy: An Equilibrium with Cancer. *Journal of Leukocyte Biology* **2008**, *84* (4), 988–993. https://doi.org/10.1189/jlb.1107774.

(36) Schmidt-Rohr, K. Oxygen Is the High-Energy Molecule Powering Complex Multicellular Life: Fundamental Corrections to Traditional Bioenergetics. *ACS Omega* **2020**, *5* (5), 2221–2233. https://doi.org/10.1021/acsomega.9b03352.

(37) Oronsky, B. T.; Oronsky, N.; Fanger, G. R.; Parker, C. W.; Caroen, S. Z.; Lybeck, M.; Scicinski, J. J. Follow the ATP: Tumor Energy Production: A Perspective. *Anti-Cancer Agents in Medicinal Chemistry* **2014**, *14* (9), 1187–1198. https://doi.org/10.2174/18715206146661408.

(38) Phan, L. M.; Yeung, S.-C. J.; Lee, M.-H. Cancer Metabolic Reprogramming: Importance, Main Features, and Potentials for Precise Targeted Anti-Cancer Therapies. *Cancer biology & medicine* **2014**, *11* (1), 1–19. https://doi.org/10.7497/j.issn.2095-3941.2014.01.001.

(39) Koppenol, W. H.; Bounds, P. L.; Dang, C. v. Otto Warburg's Contributions to Current Concepts of Cancer Metabolism. *Nature Reviews Cancer* **2011**, *11* (5), 325–337. https://doi.org/10.1038/nrc3038.

(40) Pikor, L.; Thu, K.; Vucic, E.; Lam, W. The Detection and Implication of Genome Instability in Cancer. *Cancer metastasis reviews* **2013**, *32* (3–4), 341–352. https://doi.org/10.1007/s10555-013-9429-5.

(41) National Cancer Institute. Surgery to Treat Cancer https://www.cancer.gov/about-cancer/treatment/types/surgery (accessed Apr 10, 2020).

(42) National Cancer Institute. Radiation Therapy to Treat Cancer https://www.cancer.gov/about-cancer/treatment/types/radiation-therapy (accessed Apr 10, 2020).

(43) National Cancer Institute. Radiation Therapy Side Effects https://www.cancer.gov/about-cancer/treatment/types/radiation-therapy/side-effects (accessed Apr 10, 2020).

(44) Meiliana, A.; Dewi, N.; Wijaya, A. Cancer Immunotherapy: A Review. *The Indonesian Biomedical Journal* **2016**, *8*, 1. https://doi.org/10.18585/inabj.v8i1.189.

(45) Chabner, B. A.; Roberts, T. G. Chemotherapy and the War on Cancer. *Nature Reviews Cancer* **2005**, *5* (1), 65–72. https://doi.org/10.1038/nrc1529.

(46) Oun, R.; Moussa, Y. E.; Wheate, N. J. The Side Effects of Platinum-Based Chemotherapy Drugs: A Review for Chemists. *Dalton Transactions* **2018**, *47* (19), 6645–6653. https://doi.org/10.1039/C8DT00838H.

(47) Kumar, R.; Chaudhary, K.; Gupta, S.; Singh, H.; Kumar, S.; Gautam, A.; Kapoor, P.; Raghava, G. P. S. CancerDR: Cancer Drug Resistance Database. *Scientific reports* **2013**, *3*, 1445. https://doi.org/10.1038/srep01445.

(48) Zahreddine, H.; Borden, K. L. B. Mechanisms and Insights into Drug Resistance in Cancer. *Frontiers in pharmacology* **2013**, *4*, 28. https://doi.org/10.3389/fphar.2013.00028.

(49) Weidmann, A. G.; Komor, A. C.; Barton, J. K. Targeted Chemotherapy with Metal Complexes. *Comments on modern chemistry. Part A, Comments on inorganic chemistry : a journal of critical discussion of the current literature* **2014**, *34* (3–4), 114–123. https://doi.org/10.1080/02603594.2014.890099.

(50) Galanski, M.; Keppler, B. K. Tumorhemmende Metallverbindungen. *Pharmazie in Unserer Zeit* **2006**, *35* (2), 118–123. https://doi.org/10.1002/pauz.200500160.

(51) Market Study Report LLC. Platinum based cancer drugs market size to reach US$1.8 billion by 2026 https://www.marketstudyreport.com/reports/global-platinum-based-cancer-drugs-market-share-size-trends-industry-analysis-report-by-drug-type-cisplatin-oxaliplatin-carboplatin-other-by-application-colorectal-cancer-ovarian-cancer-lung-cancer-other-by-region (accessed Apr 22, 2020).

(52) Crespo, M. Cyclometallated Platinum(IV) Compounds as Promising Antitumour Agents. *Journal of Organometallic Chemistry* **2019**, *879*, 15–26. https://doi.org/https://doi.org/10.1016/j.jorganchem.2018.10.008.

(53) Johnstone, T. C.; Suntharalingam, K.; Lippard, S. J. The Next Generation of Platinum Drugs: Targeted Pt(II) Agents, Nanoparticle Delivery, and Pt(IV) Prodrugs. *Chemical Reviews* **2016**, *116* (5), 3436–3486. https://doi.org/10.1021/acs.chemrev.5b00597.

(54) Cheff, D. M.; Hall, M. D. Correction to A Drug of Such Damned Nature. Challenges and Opportunities in Translational Platinum Drug Research. *Journal of Medicinal Chemistry* **2018**, *61* (19), 8944. https://doi.org/10.1021/acs.jmedchem.8b01420.

(55) Lentz, F.; Drescher, A.; Lindauer, A.; Henke, M.; Hilger, R. A.; Hartinger, C. G.; Scheulen, M. E.; Dittrich, C.; Keppler, B. K.; Jaehde, U.; Research-EWIV, in collaboration with C. E. S. for A. D. Pharmacokinetics of a Novel Anticancer Ruthenium Complex (KP1019, FFC14A) in a Phase I Dose-Escalation Study. *Anti-Cancer Drugs* **2009**, *20* (2).

(56) Massai, L.; Fernández-Gallardo, J.; Guerri, A.; Arcangeli, A.; Pillozzi, S.; Contel, M.; Messori, L. Design, Synthesis and Characterisation of New Chimeric Ruthenium(Ii)–Gold(i) Complexes as Improved Cytotoxic Agents. *Dalton Transactions* **2015**, *44* (24), 11067–11076. https://doi.org/10.1039/C5DT01614B.

(57) Szczepaniak, A.; Fichna, J. Organometallic Compounds and Metal Complexes in Current and Future Treatments of Inflammatory Bowel Disease and Colorectal Cancer-a Critical Review. *Biomolecules* **2019**, *9* (9), 398. https://doi.org/10.3390/biom9090398.

(58) Pongratz, M.; Schluga, P.; Jakupec, M. A.; Arion, V. B.; Hartinger, C. G.; Allmaier, G.; Keppler, B. K. Transferrin Binding and Transferrin-Mediated Cellular Uptake of the Ruthenium Coordination Compound KP1019, Studied by Means of AAS, ESI-MS and CD Spectroscopy. *Journal of Analytical Atomic Spectrometry* **2004**, *19* (1), 46–51. https://doi.org/10.1039/b309160k.

(59) el Hout, M.; dos Santos, L.; Hamaï, A.; Mehrpour, M. A Promising New Approach to Cancer Therapy: Targeting Iron Metabolism in Cancer Stem Cells. *Seminars in Cancer Biology* **2018**, *53*, 125–138. https://doi.org/https://doi.org/10.1016/j.semcancer.2018.07.009.

(60) Torti, S. v; Torti, F. M. Iron and Cancer: More Ore to Be Mined. *Nature reviews. Cancer* **2013**, *13* (5), 342–355. https://doi.org/10.1038/nrc3495.

(61) Jaouen, G.; Vessières, A.; Top, S. Ferrocifen Type Anti Cancer Drugs. *Chemical Society Reviews*. Royal Society of Chemistry December 21, 2015, pp 8802–8817. https://doi.org/10.1039/c5cs00486a.

(62) Simpson, P. v.; Desai, N. M.; Casari, I.; Massi, M.; Falasca, M. Metal-Based Antitumor Compounds: Beyond Cisplatin. *Future Medicinal Chemistry*. Future Medicine Ltd. January 1, 2019, pp 119–135. https://doi.org/10.4155/fmc-2018-0248.

(63) Pigeon, P.; Wang, Y.; Top, S.; Najlaoui, F.; Garcia Alvarez, M. C.; Bignon, J.; McGlinchey, M. J.; Jaouen, G. A New Series of Succinimido-Ferrociphenols and Related Heterocyclic Species Induce Strong Antiproliferative Effects, Especially against Ovarian Cancer Cells Resistant to Cisplatin. *Journal of Medicinal Chemistry* **2017**, *60* (20), 8358–8368. https://doi.org/10.1021/acs.jmedchem.7b00743.

(64) Chakrapani, H.; Wilde, T. C.; Citro, M. L.; Goodblatt, M. M.; Keefer, L. K.; Saavedra, J. E. Synthesis, Nitric Oxide Release, and Anti-Leukemic Activity of Glutathione-Activated Nitric Oxide Prodrugs: Structural Analogues of PABA/NO, an Anti-Cancer Lead Compound. *Bioorganic & medicinal chemistry* **2008**, *16* (5), 2657–2664. https://doi.org/10.1016/j.bmc.2007.11.035.

(65) Zeng, L.; Gupta, P.; Chen, Y.; Wang, E.; Ji, L.; Chao, H.; Chen, Z. S. The Development of Anticancer Ruthenium(II) Complexes: From Single Molecule Compounds to Nanomaterials. *Chemical Society Reviews*. Royal Society of Chemistry October 7, 2017, pp 5771–5804. https://doi.org/10.1039/c7cs00195a.

(66) Meier-Menches, S. M.; Gerner, C.; Berger, W.; Hartinger, C. G.; Keppler, B. K. Structure-Activity Relationships for Ruthenium and Osmium Anticancer Agents-towards Clinical Development. *Chemical Society Reviews*. Royal Society of Chemistry February 7, 2018, pp 909–928. https://doi.org/10.1039/c7cs00332c.

(67) Kretsinger, R. H.; Uversky, V. N.; Permyakov, E. A. *Encyclopedia of Metalloproteins*.

(68) Hanif, M.; Babak, M. v.; Hartinger, C. G. Development of Anticancer Agents: Wizardry with Osmium. *Drug Discovery Today*. Elsevier Ltd 2014, pp 1640–1648. https://doi.org/10.1016/j.drudis.2014.06.016.

(69) Berger, G.; Grauwet, K.; Zhang, H.; Hussey, A. M.; Nowicki, M. O.; Wang, D. I.; Chiocca, E. A.; Lawler, S. E.; Lippard, S. J. Anticancer Activity of Osmium(VI) Nitrido Complexes in Patient-Derived Glioblastoma Initiating Cells and in Vivo Mouse Models. *Cancer Letters* **2018**, *416*, 138–148. https://doi.org/https://doi.org/10.1016/j.canlet.2017.11.041.

(70) Santini, C.; Pellei, M.; Gandin, V.; Porchia, M.; Tisato, F.; Marzano, C. Advances in Copper Complexes as Anticancer Agents. *Chemical Reviews*. January 8, 2014, pp 815–862. https://doi.org/10.1021/cr400135x.

(71) McGivern, T. J. P.; Afsharpour, S.; Marmion, C. J. Copper Complexes as Artificial DNA Metallonucleases: From Sigman's Reagent to next Generation Anti-Cancer Agent? *Inorganica Chimica Acta*. Elsevier S.A. March 1, 2018, pp 12–39. https://doi.org/10.1016/j.ica.2017.08.043.

(72) Hormann, J.; Malina, J.; Lemke, O.; Hülsey, M. J.; Wedepohl, S.; Potthoff, J.; Schmidt, C.; Ott, I.; Keller, B. G.; Brabec, V.; Kulak, N. Multiply Intercalator-Substituted Cu(II) Cyclen Complexes as DNA Condensers and DNA/RNA Synthesis Inhibitors. *Inorganic Chemistry* **2018**, *57* (9), 5004–5012. https://doi.org/10.1021/acs.inorgchem.8b00027.

(73) Huang, J.; Chaudhary, R.; Cohen, A. L.; Fink, K.; Goldlust, S.; Boockvar, J.; Chinnaiyan, P.; Wan, L.; Marcus, S.; Campian, J. L. A Multicenter Phase II Study of Temozolomide plus Disulfiram and Copper for Recurrent Temozolomide-Resistant Glioblastoma. *Journal of Neuro-Oncology* **2019**, *142* (3), 537–544. https://doi.org/10.1007/s11060-019-03125-y.

(74) Schatzschneider, U. Metallointercalators and Metalloinsertos: Structural Requirements for DNA Recognition and Anticancer Activity. In *Metallo-Drugs: Development and Action of Anticancer Agents*; De Gruyter: Berlin, Boston, 2018; pp 387–436. https://doi.org/https://doi.org/10.1515/9783110470734-014.

(75) Brana, M. F.; Cacho, M.; Gradillas, A.; de Pascual-Teresa, B.; Ramos, A. Intercalators as Anticancer Drugs. *Current Pharmaceutical Design* **2005**, *7* (17). https://doi.org/10.2174/1381612013397113.

(76) Deo, K. M.; Pages, B. J.; Ang, D. L.; Gordon, C. P.; Aldrich-Wright, J. R. Transition Metal Intercalators as Anticancer Agents-Recent Advances. *International journal of molecular sciences* **2016**, *17* (11). https://doi.org/10.3390/ijms17111818.

(77) Riechert-Krause, F.; Weisz, K. Indoloquinolines as DNA Binding Ligands. *Heterocyclic Communications*. June 2013, pp 145–166. https://doi.org/10.1515/hc-2013-0034.

(78) Pommier, Y.; Leo, E.; Zhang, H.; Marchand, C. DNA Topoisomerases and Their Poisoning by Anticancer and Antibacterial Drugs. *Chemistry & Biology* **2010**, *17* (5), 421–433. https://doi.org/https://doi.org/10.1016/j.chembiol.2010.04.012.

(79) Hevener, K.; Verstak, T. A.; Lutat, K. E.; Riggsbee, D. L.; Mooney, J. W. Recent Developments in Topoisomerase-Targeted Cancer Chemotherapy. *Acta pharmaceutica Sinica. B* **2018**, *8* (6), 844–861. https://doi.org/10.1016/j.apsb.2018.07.008.

(80) Collins, T.; Hammes, G.; Hsieh, T.-S. Analysis of the Eukaryotic Topoisomerase II DNA Gate: A Single-Molecule FRET and Structural Perspective. *Nucleic acids research* **2009**, *37*, 712–720. https://doi.org/10.1093/nar/gkn1059.

(81) Murphy, M. B.; Mercer, S. L.; Deweese, J. E. Inhibitors and Poisons of Mammalian Type II Topoisomerases. In *Advances in Molecular Toxicology*; Fishbein, J. C., Heilman, J. M., Eds.;

Elsevier, 2017; Vol. 11, pp 203–240. https://doi.org/https://doi.org/10.1016/B978-0-12-812522-9.00005-1.

(82) Méndez, M. v.; Bracca, A. B. J.; Kaufman, T. S. Isolation, Synthesis, and Biological Activity of Quindoline, a Valuable Indoloquinoline Natural Product and Useful Key Intermediate. *Synthesis (Germany)*. Georg Thieme Verlag April 3, 2018, pp 1417–1429. https://doi.org/10.1055/s-0036-1591947.

(83) National Center for Biotechnology Information. PubChem Database. Cryptolepine https://pubchem.ncbi.nlm.nih.gov/compound/Cryptolepine (accessed May 11, 2020).

(84) Parvatkar, P. T.; Parameswaran, P. S. *Indoloquinolines: Possible Biogenesis from Common Indole Precursors and Their Synthesis Using Domino Strategies*; 2016; Vol. 13. https://doi.org/10.2174/1570179412666150511224648.

(85) Parvatkar, P. T.; Parameswaran, P. S.; Tilve, S. G. *Isolation, Biological Activities and Synthesis of Indoloquinoline Alkaloids: Cryptole-Pine, Isocryptolepine and Neocryptolepine*; 2011; Vol. 15.

(86) Peczynska-Czoch, W.; Pognan, F.; Kaczmarek, L.; Boratynski, J. Synthesis and Structure-Activity Relationship of Methyl-Substituted Indolo[2,3-b]Quinolines: Novel Cytotoxic, DNA Topoisomerase II Inhibitors. *Journal of Medicinal Chemistry* **1994**, *37* (21), 3503–3510. https://doi.org/10.1021/jm00047a008.

(87) Filak, L. K.; Göschl, S.; Heffeter, P.; Ghannadzadeh Samper, K.; Egger, A. E.; Jakupec, M. A.; Keppler, B. K.; Berger, W.; Arion, V. B. Metal-Arene Complexes with Indolo[3,2-c]-Quinolines: Effects of Ruthenium vs Osmium and Modifications of the Lactam Unit on Intermolecular Interactions, Anticancer Activity, Cell Cycle, and Cellular Accumulation. *Organometallics* **2013**, *32* (3), 903–914. https://doi.org/10.1021/om3012272.

(88) Nadein, O. N.; Aksenov, D. A.; Abakarov, G. M.; Aksenov, N. A.; Voskressensky, L. G.; Aksenov, A. v. Methods of Synthesis of Natural Indoloquinolines Isolated from Cryptolepis Sanguinolenta. *Chemistry of Heterocyclic Compounds* **2019**, *55* (10), 905–932. https://doi.org/10.1007/s10593-019-02557-8.

(89) Ansah, C.; Mensah, K. B. A Review of the Anticancer Potential of the Antimalarial Herbal Cryptolepis Sanguinolenta and Its Major Alkaloid Cryptolepine. *Ghana medical journal* **2013**, *47* (3), 137–147.

(90) Filak, L. K.; Mühlgassner, G.; Jakupec, M. A.; Heffeter, P.; Berger, W.; Arion, V. B.; Keppler, B. K. Organometallic Indolo[3,2-c]Quinolines versus Indolo[3,2-d]Benzazepines: Synthesis, Structural and Spectroscopic Characterization, and Biological Efficacy. *Journal of Biological Inorganic Chemistry* **2010**, *15* (6), 903–918. https://doi.org/10.1007/s00775-010-0653-y.

(91) Petersen, J. B.; Lakowitz, K. H. New Methods for the Preparation of 1,4-Benzodiazepinones, Carbostyrils and Indolo[2,3-c]Quinolones.

(92) Filak, L. K.; Mühlgassner, G.; Jakupec, M. A.; Heffeter, P.; Berger, W.; Arion, V. B.; Keppler, B. K. Organometallic Indolo[3,2-c]Quinolines versus Indolo[3,2-d]Benzazepines: Synthesis, Structural and Spectroscopic Characterization, and Biological Efficacy. *Journal of Biological Inorganic Chemistry* **2010**, *15* (6), 903–918. https://doi.org/10.1007/s00775-010-0653-y.

(93) Primik, M. F.; Göschl, S.; Meier, S. M.; Eberherr, N.; Jakupec, M. A.; Enyedy, É. A.; Novitchi, G.; Arion, V. B. Dicopper(II) and Dizinc(II) Complexes with Nonsymmetric Dinucleating Ligands

Based on Indolo[3,2-c]Quinolines: Synthesis, Structure, Cytotoxicity, and Intracellular Distribution. *Inorganic Chemistry* **2013**, *52* (17), 10137–10146. https://doi.org/10.1021/ic401573d.

(94) Primik, M. F.; Mühlgassner, G.; Jakupec, M. A.; Zava, O.; Dyson, P. J.; Arion, V. B.; Keppler, B. K. Highly Cytotoxic Copper(II) Complexes with Modified Paullone Ligands. *Inorganic Chemistry* **2010**, *49* (1), 302–311. https://doi.org/10.1021/ic902042a.

(95) Primik, M. F.; Göschl, S.; Jakupec, M. A.; Roller, A.; Keppler, B. K.; Arion, V. B. Structure-Activity Relationships of Highly Cytotoxic Copper(II) Complexes with Modified Indolo[3,2- c]Quinoline Ligands. *Inorganic Chemistry* **2010**, *49* (23), 11084–11095. https://doi.org/10.1021/ic101633z.

(96) Szabó, F.; Daru, J.; Simkó, D.; Nagy, T. Zs.; Stirling, A.; Novák, Z. Mild Palladium-Catalyzed Oxidative Direct Ortho-C□H Acylation of Anilides under Aqueous Conditions. *Advanced Synthesis & Catalysis* **2013**, *355* (4), 685–691. https://doi.org/https://doi.org/10.1002/adsc.201200948.

(97) Han, J.; Aceña, J. L.; Yasuda, N.; Uekusa, H.; Ono, T.; Soloshonok, V. A.; Klika, K. D. Carbonyl Group Coordination Preferences in Square-Planar NiII and PdII Complexes of Pentadentate Ligands by Electron-Withdrawing/Donating Substituents. *Inorganica Chimica Acta* **2015**, *433*, 3–12. https://doi.org/https://doi.org/10.1016/j.ica.2015.04.029.